




2020

## INVOLVEMENT OF THE RENIN ANGIOTENSIN SYSTEM IN MARFAN SYNDROME ASSOCIATED THORACIC AORTIC ANEURYSMS

Jeff Zheyang Chen

University of Kentucky, zheyang.chen@gmail.com

Author ORCID Identifier:

 <https://orcid.org/0000-0002-2893-1523>

Digital Object Identifier: <https://doi.org/10.13023/etd.2020.352>

[Right click to open a feedback form in a new tab to let us know how this document benefits you.](#)

### Recommended Citation

Chen, Jeff Zheyang, "INVOLVEMENT OF THE RENIN ANGIOTENSIN SYSTEM IN MARFAN SYNDROME ASSOCIATED THORACIC AORTIC ANEURYSMS" (2020). *Theses and Dissertations--Physiology*. 47. [https://uknowledge.uky.edu/physiology\\_etds/47](https://uknowledge.uky.edu/physiology_etds/47)

This Doctoral Dissertation is brought to you for free and open access by the Physiology at UKnowledge. It has been accepted for inclusion in Theses and Dissertations--Physiology by an authorized administrator of UKnowledge. For more information, please contact [UKnowledge@lsv.uky.edu](mailto:UKnowledge@lsv.uky.edu).

## **STUDENT AGREEMENT:**

I represent that my thesis or dissertation and abstract are my original work. Proper attribution has been given to all outside sources. I understand that I am solely responsible for obtaining any needed copyright permissions. I have obtained needed written permission statement(s) from the owner(s) of each third-party copyrighted matter to be included in my work, allowing electronic distribution (if such use is not permitted by the fair use doctrine) which will be submitted to UKnowledge as Additional File.

I hereby grant to The University of Kentucky and its agents the irrevocable, non-exclusive, and royalty-free license to archive and make accessible my work in whole or in part in all forms of media, now or hereafter known. I agree that the document mentioned above may be made available immediately for worldwide access unless an embargo applies.

I retain all other ownership rights to the copyright of my work. I also retain the right to use in future works (such as articles or books) all or part of my work. I understand that I am free to register the copyright to my work.

## **REVIEW, APPROVAL AND ACCEPTANCE**

The document mentioned above has been reviewed and accepted by the student's advisor, on behalf of the advisory committee, and by the Director of Graduate Studies (DGS), on behalf of the program; we verify that this is the final, approved version of the student's thesis including all changes required by the advisory committee. The undersigned agree to abide by the statements above.

Jeff Zheyang Chen, Student

Dr. Alan Daugherty, Major Professor

Dr. Kenneth S. Campbell, Director of Graduate Studies

INVOLVEMENT OF THE RENIN ANGIOTENSIN SYSTEM IN MARFAN  
SYNDROME ASSOCIATED THORACIC AORTIC ANEURYSMS

---

DISSERTATION

---

A dissertation submitted in partial fulfillment of the  
requirements for the degree of Doctor of Philosophy in the  
College of Medicine  
at the University of Kentucky

By  
Jeff Zheyang Chen  
Lexington, Kentucky  
Director: Dr. Alan Daugherty, Professor of Physiology  
Lexington, Kentucky  
2020

Copyright © Jeff Zheyang Chen 2020  
<https://orcid.org/0000-0002-2893-1523>

## ABSTRACT OF DISSERTATION

### INVOLVEMENT OF THE RENIN ANGIOTENSIN SYSTEM IN MARFAN SYNDROME ASSOCIATED THORACIC AORTIC ANEURYSMS

Thoracic aortic aneurysms (TAAs) are clinically-silent dilations of the aorta which greatly increase the risk of aortic rupture, a condition with 50-90% mortality. Marfan syndrome (MFS) is caused by mutations in fibrillin-1 (FBN1) and is associated with TAAs. Due to an absence of validated and effective pharmacologic therapies to prevent or reverse TAA, most MFS patients require surgical aortic repair. Understanding MFS associated TAA pathogenesis would direct development of new pharmacologic therapies. Previous research has implicated the renin angiotensin system in TAA. In both males and females, angiotensinogen (AGT) is cleaved serially to generate the main effector peptide angiotensin II (AngII). AngII is the main ligand of AngII receptor type 1a (AT1aR). However, the role of angiotensin II (AngII) receptor type 1a (AT1aR) in MFS associated TAA formation is unclear. Here, we test the hypothesis that AngII-dependent AT1aR stimulation is responsible for Marfan syndrome associated TAA.

To study the contribution of the renin angiotensin system on MFS associated TAA, we used the fibrillin-1 haploinsufficient (Fbn1C1041G/+) and fibrillin-1 hypomorphic (Fbn1mgR/mgR) mouse models. TAA in MFS mice demonstrated sexual dimorphism. Compared to male Fbn1C1041G/+ mice, female Fbn1C1041G/+ mice exhibited less ascending aortic dilation. To study AT1aR in MFS associated TAA, we bred male and female AT1aR deficient (AT1aR<sup>-/-</sup>) x Fbn1C1041G/+ mice. We measured the ascending aorta up to 12 months of age by high frequency ultrasound sequentially. We evaluated aortic medial structure at study termination. Compared to male AT1aR<sup>+/+</sup> x Fbn1C1041G/+ mice, male AT1aR<sup>-/-</sup> x Fbn1C1041G/+ mice exhibited less ascending aortic dilation and reduced elastin fragmentation. Ascending aortic dilation was not significant between female AT1aR<sup>-/-</sup> x Fbn1C1041G/+ mice and female AT1aR<sup>+/+</sup> x Fbn1C1041G/+ mice. To study the contribution of angiotensin peptides, we administered angiotensinogen antisense oligonucleotides (AGT ASO) to male Fbn1C1041G/+ mice. Compared to male Fbn1C1041G/+ mice

administered control ASO, mice administered AGT ASO exhibited less ascending aortic dilation and reduced elastin fragmentation.

TAA in the mouse models of MFS is sexually dimorphic. Inhibition of the renin angiotensin system via either AT1aR deletion or AGT ASO is sufficient to attenuate ascending aortic dilation in male Fbn1C1041G/+ mice. However, the effect of AT1aR deletion was not detectable in female Fbn1C1041G/+ mice. Depletion of angiotensin ligands was efficacious in attenuating MFS associated TAA in male Fbn1C1041G/+ mice. However, factors that impact TAA of other etiologies have minimal impact on MFS associated TAA. These studies indicate that modulating the renin angiotensin system is highly effective to attenuate MFS associated TAA in males.

KEYWORDS: Marfan syndrome, Thoracic Aortic Aneurysm, Renin Angiotensin System, Angiotensin II

---

Jeff Zheyang Chen  
(Name of Student)

---

04/20/2020

Date

INVOLVEMENT OF THE RENIN ANGIOTENSIN SYSTEM IN MARFAN  
SYNDROME ASSOCIATED THORACIC AORTIC ANEURYSMS

By  
Jeff Zheyang Chen

Alan Daugherty PhD Dsc  
\_\_\_\_\_  
Director of Dissertation

Kenneth S Campbell PhD  
\_\_\_\_\_  
Director of Graduate Studies

04/20/2020  
\_\_\_\_\_  
Date

## DEDICATION

To: The mice, who enabled these studies.

## ACKNOWLEDGMENTS

This work was supported by my advisors, colleagues, friends, and family at the University of Kentucky and beyond. It was done in hopes that the knowledge and ideas described here can - one day - be leveraged to improve the lives of people and their families living with Marfan syndrome.

Thank you, my advisor – Dr. Alan Daugherty – for his mentorship, support, and patience; for teaching me not only how to do good science but also how to be a good scientist; for giving a lifetime worth of lessons over the last four years.

Thank you, my PhD advisory committee members – Drs. Kenneth Campbell, Ming Gong, Nancy Webb – who encouraged, and challenged, me to reach past my potential; especially when I needed it.

Thank you, Dr. Mary Sheppard, who guided me in both the lab and clinic – constantly reminding me of the higher purpose for this work – and is the physician-scientist I one day hope to be.

Thank you, members of the Daugherty Lab past and present. Drs. Hong Lu and Hisashi Sawada, who entertained my ideas and shared both victories and setbacks. Deborah Howatt, Jessica Moorleghen, Debra Rateri, and Micheal Franklin, whose expertise and support enabled it all. Colleagues in the Department of Physiology, Saha Cardiovascular Research Center, and the UK-BCM Aortic Research Center. Countless members who briefly overlapped but left lasting impressions.



Thank you, Therese Stearns, for her friendship through the years and the University of Kentucky MDPHD program for giving me the chance to prove myself. This work was enabled through the support of the National Institutes of Health and American Heart Association as well as through Dr. Susan Smyth and the University of Kentucky Center for Clinical and Translational Science.

Thank you to my family, who grew roots in this country so that they could tirelessly support me, even if they may not understand all the details of what I do.

Finally, thank you Dr. Eileen Hu. From the time we met, almost a decade ago, you have been my best friend, partner in crime, cheerleader, critic, and rival. You inspire me to be my best. Without you, I would not be where I am today. I can't wait to see where we go from here.

## TABLE OF CONTENTS

<b>ACKNOWLEDGMENTS .....</b>	<b>iii</b>
<b>LIST OF TABLES .....</b>	<b>vii</b>
<b>LIST OF FIGURES.....</b>	<b>Error! Bookmark not defined.</b>
<b>CHAPTER 1.Introduction .....</b>	<b>10</b>
1.1 <i>Marfan syndrome .....</i>	<i>10</i>
1.2 <i>Structure of the Thoracic Aortic Media .....</i>	<i>11</i>
1.3 <i>Thoracic Aortic Aneurysms .....</i>	<i>12</i>
1.4 <i>Etiologies of Thoracic Aortic Aneurysms.....</i>	<i>13</i>
1.5 <i>Current Therapies for Thoracic Aortic Aneurysms .....</i>	<i>14</i>
1.6 <i>The Renin Angiotensin System in TAA .....</i>	<i>15</i>
1.7 <i>Gaps in knowledge, hypotheses tested, and points discussed .....</i>	<i>17</i>
<b>CHAPTER 2.Major methods of measuring TAA.....</b>	<b>23</b>
2.1 <i>Synopsis.....</i>	<i>23</i>
2.2 <i>Introduction .....</i>	<i>23</i>
2.3 <i>Methods .....</i>	<i>24</i>
2.4 <i>Results .....</i>	<i>26</i>
2.5 <i>Discussion.....</i>	<i>27</i>
<b>CHAPTER 3.Inhibition of Angiotensin II-Dependent AT1a Receptor Stimulation Attenuates Thoracic Aortic Dilatation in Fibrillin-1<sup>C1041G/+</sup> Mice</b>	<b>40</b>
3.1 <i>Synopsis.....</i>	<i>40</i>
3.2 <i>Introduction .....</i>	<i>41</i>
3.3 <i>Methods .....</i>	<i>42</i>
3.4 <i>Results .....</i>	<i>44</i>
3.5 <i>Discussion.....</i>	<i>47</i>
<b>CHAPTER 4.Endogenous Sex Hormone Removal Attenuates Acquired Thoracic Aortic Aneurysms.....</b>	<b>63</b>
4.1 <i>Synopsis.....</i>	<i>63</i>

4.2	<i>Introduction</i> .....	63
4.3	<i>Methods</i> .....	65
4.4	<i>Results</i> .....	66
4.5	<i>Discussion</i> .....	69
<b>CHAPTER 5.S100A4-Cre Mediated Excision of AT1a Receptors Attenuates Spontaneous but not Syndromic Aortic Aneurysms in Mice</b> .....		<b>82</b>
5.1	<i>Synopsis</i> .....	82
5.2	<i>Introduction</i> .....	82
5.3	<i>Methods</i> .....	83
5.4	<i>Results</i> .....	85
5.5	<i>Discussion</i> .....	86
<b>CHAPTER 6.Discussion and Future Directions</b> .....		<b>92</b>
6.1	<i>Key Methods</i> .....	92
6.2	<i>Role of AngII-AT1aR axis in Marfan syndrome</i> .....	93
6.3	<i>Role of endogenous sex hormones in aortopathy</i> .....	94
6.4	<i>Role of AT1aR on fibroblasts in aortopathy</i> .....	95
6.5	<i>Future directions</i> .....	96
<b>REFERENCES</b> .....		<b>99</b>
<b>VITA</b> .....		<b>118</b>

## LIST OF TABLES

<b>Table 1.1 Conserved domains in fibrillin-1.....</b>	<b>20</b>
<b>Table 1.2 Mutant microfibril mouse models and phenotypes.....</b>	<b>21</b>
<b>Table 1.3 Mouse Models Where AT1aR Inhibition Attenuates TAA .....</b>	<b>22</b>
<b>Table 2.1 Characteristics of wild type and FBN1<sup>mgR/mgR</sup> mice.....</b>	<b>30</b>

## LIST OF FIGURES

Figure 2.1 Probe positions used to measure aortic diameter.....	31
Figure 2.2 Modified right parasternal long axis view and measurement protocol of the ascending aorta.....	33
Figure 2.3 Effect of cardiac cycle on ascending aortic diameters.....	34
Figure 2.4 Circumferential Green-Lagrange strain of the aorta during cardiac cycle in wild type and FBN1 <sup>mgR/mgR</sup> mice.....	35
Figure 2.5 Elastin fragmentation of WT and FBN1 <sup>mgR/mgR</sup> correlated with ascending aortic diameter.....	36
Figure 2.6 Ultrasonographic measurements of aortic diameter in diastole closely reflected ex vivo aortic diameter measurements.....	38
Figure 2.7 Bland-Altman analyses comparing measurements obtained by two independent observers that were blinded to the experimental design.....	39
Figure 3.1 Regional heterogeneity of TAA in Fbn1 <sup>C1041G/+</sup> mice.....	50
Figure 3.2 TAA in Fbn1 <sup>C1041G/+</sup> mice is sexually dimorphic.....	51
Figure 3.3 AT1aR deletion attenuated ascending aortic dilation in male Fbn1 <sup>C1041G/+</sup> mice.....	52
Figure 3.4 Aortic dimensions at 1 month of age and aortic growth in male mice.....	53
Figure 3.5 Growth from 1 month of age in male AT1aR deficient, Fbn1 <sup>C1041G/+</sup> mice.....	54
Figure 3.6 Confounding factors did not contribute to TAA phenotype in male Fbn1 <sup>C1041G/+</sup> mice.....	55
Figure 3.7 AT1aR deletion had no effect on aortic measurements in female Fbn1 <sup>C1041G/+</sup> mice.....	56
Figure 3.8 Aortic dimensions at 1 month of age and aortic growth in female mice.....	57
Figure 3.9 Generation of ascending aortic sections to measure elastin fragmentation and medial thickening.....	58
Figure 3.10 AT1aR deletion attenuated medial remodeling in male Fbn1 <sup>C1041G/+</sup> mice.....	59
Figure 3.11 AGT ASOs depleted AGT and attenuated TAA in male Fbn1 <sup>C1041G/+</sup> mice.....	60
Figure 3.12 AGT ASOs have low toxicity and effectively reduce circulating AGT.....	61
Figure 3.13 AGT ASOs attenuated medial remodeling in male Fbn1 <sup>C1041G/+</sup> mice.....	62
Figure 4.1 Sexual dimorphism occurs in both acquired and syndromic mouse models of thoracic aortic aneurysms.....	71
Figure 4.2 Gonadectomy modulated ascending aortic and aortic root dimensions in AngII-infused female and male mice.....	73

<b>Figure 4.3 Atrophy of sex responsive organs after gonadectomy of female and male AngII-infused mice .....</b>	<b>74</b>
<b>Figure 4.4 Systolic blood pressure was not altered by gonadectomy and did not correlate with aortic diameter .....</b>	<b>75</b>
<b>Figure 4.5 Body weight of mice was not altered by gonadectomy .....</b>	<b>76</b>
<b>Figure 4.6 Gonadectomy did not alter aortic dilation after 4 weeks in FBN1<sup>mgR/mgR</sup> mice.....</b>	<b>77</b>
<b>Figure 4.7 Gonadectomy modulated elastin fragmentation in ascending aorta of male and female mice .....</b>	<b>78</b>
<b>Figure 4.8 Controls for <math>\alpha</math>-smooth muscle actin immunostaining.....</b>	<b>80</b>
<b>Figure 4.9 Gonadectomy modulates aortic medial expression of contractile smooth muscle markers in ascending aorta of AngII-infused male mice ...</b>	<b>81</b>
<b>Figure 5.1 S100A4-Cre traced cells were preferentially enriched in fibroblast rich tissues.....</b>	<b>88</b>
<b>Figure 5.2 AT1a receptor deletion attenuated AngII-induced TAA and AAA but not AngII-exacerbated atherosclerosis .....</b>	<b>89</b>
<b>Figure 5.3 Fibroblast specific AT1aR deletion failed to modulate TAA in Fbn1<sup>C1041G/+</sup> mice .....</b>	<b>91</b>

## CHAPTER 1. INTRODUCTION

### 1.1 Marfan syndrome

Marfan syndrome (MFS) is an autosomal dominant genetic disease caused by mutations in a large extracellular matrix protein, fibrillin-1 (FBN1). (1) It has an incidence of approximately 1:3000 live births and is associated with increased morbidity and mortality for a significant number of affected patients. As a syndromic disorder, Marfan syndrome is characterized by a constellation of features that forms the basis of diagnosis. Thoracic aortic aneurysms (TAAs) are a key feature in Marfan syndrome that drives both diagnosis and prognosis. This section will review the common clinical features seen in Marfan syndrome, the fibrillin-1 gene and protein, and Marfan syndrome mouse models.

Clinical features of Marfan syndrome include dysmorphic features, ectopia lentis, and thoracic aortic aneurysms. Alongside genetic testing for pathologic mutations in the FBN1 gene and family history of Marfan syndrome, these form the basis of the 2010 Revised Ghent Nosology. (2) Dysmorphic features are tabulated as a systemic score. Characteristic features include hypermobility, skeletal deformations, skin features, and specific cardiopulmonary conditions. Another key phenotype is the presence of detached lenses in the eye or ectopia lentis. Evaluation of this feature requires an ophthalmologist. However, the most important criteria is the presence of aortic root dilation. Specifically, if the aortic z-score (aortic root diameter normalized to body surface area) is greater than 2, only one additional of the above criteria is needed to make a definitive diagnosis of Marfan syndrome in patients without a family history. In patients with a positive family history of Marfan syndrome or known pathologic FBN1 mutation, aortic dilation alone is enough to make the diagnosis of Marfan syndrome. Male patients with Marfan syndrome develop more severe aortic dilation compared to female counterparts. (3-5) Because Marfan syndrome is inherited in an autosomal dominant fashion, it is unclear why this sexual dimorphism exists. Thoracic aortic aneurysm by itself is clinically silent and often asymptomatic. However, it is associated with an increased risk of aortic rupture and dissection due to loss of aortic wall integrity. This topic will be reviewed in a later section. Although Marfan syndrome is a systemic disease that affects multiple organ systems, TAA remains the leading cause of morbidity and mortality in patients with Marfan syndrome.

Fibrillin-1 mutations form the basis of Marfan syndrome, a disorder characterized by connective tissue abnormalities and thoracic aortic aneurysms.(6) Aortic tissues from patients with Marfan syndrome display extensive elastin fragmentation (7) and strikingly decreased mature elastin - as detected by desmosine extraction - without changes in collagen content.(8) Fibrillin-1 is one of the most well characterized microfibrillar proteins in the context of aortic elastin stability. Members of the fibrillin protein family are found in elastic connective tissue where they serve as a critical component of the microfibrillar scaffold. In general, fibrillins are comprised of an identifying N-terminal domain that distinguishes FBN1 from FBN2, structural calcium binding

epidermal growth factor domains and proline/glycine domains that provide flexibility and rigidity, and tumor growth factor  $\beta$  (TGF $\beta$ ) binding domains that anchor cell-signaling elements. Other notable binding partners include growth factors, structure proteins (elastin and fibulins), as well as cells through integrin binding. (9, 10) (**Table 1.1**) Mutations in fibrillin-1 affect elastic tissue integrity by disrupting these interactions.

Based on mutations in FBN1, several mouse models of Marfan syndrome have been developed to mimic the human disease. These mouse models display progressive aortic dilation of varying severity. The fibrillin-1 haploinsufficient ( $Fbn1^{C1041G/+}$ ) mouse model is based on a single nucleotide substitution that causes a missense mutation. This mouse model mimics the human FBN1<sup>C1039Y</sup> mutation, which impacts a calcium binding epidermal growth factor-like domain of fibrillin-1. (11)  $Fbn1^{C1041G/+}$  mice develop TAA over the course of 6 months. Our data indicates that aortic dilation can be detected as early as 1 month of age. The fibrillin-1 hypomorphic ( $Fbn1^{mgR/mgR}$ ) mouse model is a severe model of Marfan syndrome. (12) This mutation incorporates a targeting vector between exon 18 and 19. While native fibrillin-1 is expressed, protein levels are greatly diminished. These mice develop aggressive TAA and often die of aortic rupture. Our observations in this mouse model confirm that the median lifespan is approximately 3 months of age. Additionally, these mice develop dilated cardiomyopathy. The FBN1<sup>GT-8</sup> mouse model expresses a green fluorescence protein tagged, truncated fibrillin-1. (13) These mice also develop TAA and extensive elastin fragmentation. Deletion of FBN1 is embryonic lethal while deletion of one copy induces TAA. (14) In summary disruption of either the structure or normal abundance of fibrillin-1 results in TAA of varying severity.

Marfan syndrome was first described in 1896 and FBN1 was first linked to Marfan syndrome over 30 years ago, yet current therapies have not been shown to reverse TAA. Therefore, there is great need to investigate not only pathophysiology of Marfan syndrome associated TAA but also new therapies for this disease.

## 1.2 Structure of the Thoracic Aortic Media

The aorta is composed of three discrete layers: the intima, the media, and the adventitia. Of these, the aortic media occupies the majority of the aortic wall and is composed of vascular smooth muscle cells and elastin. In this section, we will outline the key characteristics of the major cellular and extracellular components in the aortic media.

Vascular smooth muscle cells found in the aortic media provide structural stability to the thoracic aorta. These cells are derived from the second heart field and cardiac neural crest. Second heart field derived cells traced with the Mef2c promoter driven cre were found closer to the aortic root. Cardiac neural crest cells traced with the Wnt1 promoter driven cre were found up to the ligamentum arteriosum. (15, 16) Within the ascending aorta, second heart field derived cells occupy the outer aortic media and cardiac neural crest traced cells occupy the inner media. (16) While the functional importance of these embryologic origins is



unknown, lineage traced cells correlate closely with pathological remodeling in aortopathy. Aortopathies often involve remodeling of the outer aortic media. This includes elastin fragmentation and medial hemorrhage. (17) Smooth muscle cells are also the source of aortic extracellular matrix proteins. In fact, genetic depletion of the gene encoding tropoelastin in vascular smooth muscle cells results in extensive loss of elastin. (18) Interestingly, loss of elastin results in pathologic proliferation of smooth muscle cells and obstructive aortic disease (19-22) Thus vascular smooth muscle cells influence and are influenced by extracellular matrix of the aortic media.

Within the media, elastic fibers approximately 0.1 $\mu$ m thick are organized into discrete lamellar layers. The process of elastin fiber synthesis is highly orchestrated and requires multiple players. Elastin fiber synthesis requires formation of a microfibrillar complex composed of tropoelastin, fibrillins, fibulins, and EMILINs. Mutations and deficiencies of these components generally result in aortopathy. (**Table 1.2**) Elastin is more abundant in the ascending aorta and aortic arch compared to the descending and abdominal aorta. (23, 24). In humans, the thoracic aorta is comprised of up to 60 elastin layers, whereas the descending and abdominal aorta consists of about 30 or less discrete elastin lamina -- with a corresponding decrease in aortic wall thickness.(24-26) The decrease in layers and thickness is also associated with a decrease in the amount of elastin from the proximal to the distal aorta.(27) This feature is also seen in smaller animals. In mice, the ascending and arch regions consists of about 8-12 lamellar units, while the abdominal aorta consists of 3-5 lamellar units. (28) Likewise, comparative physiology studies revealed the number of aortic elastic lamella are directly and linearly proportional to aortic diameters. (25) Recent studies have indicated that the origins of elastic lamina are heterogenous. While smooth muscle cells generate the majority of elastin in the media, endothelial cells contribute to elastin in the internal elastic lamina. (18) Within the aorta, elastic lamina resist the cyclic force of blood throughout the cardiac cycle. The aorta slightly expands during systole, and this expansion is necessary to maintain perfusion pressure during diastole through the Windkessel effect. (29) By providing elasticity, elastin is a critical component to the structure and function of the aorta. When elastin is disrupted, vascular malformations occur. This suggests that the number of elastin lamina are adapted to cope with stress and strain on aortic tissue but does not explain why aneurysmal disease impacts the ascending and abdominal segments – the regions with the most and the least number of elastin lamina – while sparing the intervening descending segment.

The aortic media is made of a complex network of vascular smooth muscle cells and extracellular matrix proteins. In Marfan syndrome, mutations in fibrillin-1 are thought to disrupt these interactions. Disruption of these interactions weakens the structural integrity of the aortic wall and results in aortopathy.

### 1.3 Thoracic Aortic Aneurysms

Thoracic aortic aneurysms are expansions of the aortic lumen that weaken the aortic wall and increase the risk of catastrophic failure. Tools and mouse models developed to study and measure TAA must assay these disease features and replicate common etiologies in order to develop effective medical therapies. Aortic dilation and medial remodeling are two hallmarks of TAA. Thoracic aortic aneurysms are clinically defined as greater than 150% expansion of the normal aorta. This criterion is often not used in murine studies of the thoracic aorta because there is no evidence of a bimodal distribution of responders/non-responders unlike in the abdominal aorta. TAA is characterized by expansion of the aortic lumen without separating layers of the aortic wall. Interestingly, TAA can affect both the aortic root and ascending aorta by separate, distinct mechanisms. (30, 31) TAAs of different etiologies give rise to a distinct pattern of aneurysms involving regions of the thoracic aorta. Due to this regional heterogeneity, standardization of measurements is important in order to make equivalent comparisons. Although there is currently no published recommendation in aortopathies, we may extrapolate suggestions from atherosclerosis studies. Specifically, both the sex of mouse and region of aorta analyzed should be similar across all groups. (32, 33) Thus standardization of measurement is important, and will be covered in a later chapter. We have developed and validated a protocol for the measurement of ascending aorta in mice by ultrasound. This standardized protocol states that measurements should be consistently imaged in diastole from the left parasternal view.(34) Additionally, we have correlated these measurements with other indicators of TAA such as elastin fragmentation. (35) Elastin fragmentation is a common feature of TAA. (17) It is defined as breaks in the elastic lamina as detected by histology. Normal aortic medial architecture displays continuous, concentric elastin layers. Concentric lamina are fragmented in TAA. Although its etiology is unknown, it may be caused by either malformation of elastic lamina or degradation of mature elastic lamina. Both aortic dilation and loss of aortic integrity weaken the aortic wall and increase risk of rupture or dissection. Ultimately, loss of normal aortic architecture increases risk of dissection and rupture. Thus, it is important to measure both the degree of aortic dilation and elastin fragmentation to determine the overall severity of TAA.

#### 1.4 Etiologies of Thoracic Aortic Aneurysms

TAA can occur spontaneously or in context of syndromic disease, both of these etiologies are replicated in TAA mouse models. In humans, risk factors such as smoking and hypertension increase the risk of spontaneous TAA. (36) However, mouse models of spontaneous TAA, such as the AngII-infused,  $\beta$ -Aminopropionitrile induced, and deoxycorticosterone acetate and salt induced TAA do not entirely mimic human disease. (37-39) While hypertension is seen in the AngII and DOCA-salt models, TAA occurs independently of hypertension. In fact, norepinephrine administered mice that develop increased systolic blood pressure equivalent to AngII-infusion do not develop TAA. (17) Thus, the mechanism by which spontaneous TAAs develop in both humans and mice is

unclear. TAA can also occur in context of syndromic disease. Fibrillin-1 mutations form the basis of Marfan syndrome, a disorder also characterized by connective tissue abnormalities and thoracic aortic aneurysms.(6) (6, 40) However, mutations in genes that encode proteins which interact with fibrillin-1, such as *LOX* and *LTBP3*, are also associated with syndromic TAA. (41, 42) Mutations in the TGF $\beta$  pathway also lead to syndromic TAA and specific mutations are defined as subtypes of Loeys-Dietz syndrome. (43, 44) Vascular Ehlers-Danlos Syndrome is caused by mutations in *COL3A1*. (45) Finally, next generation sequencing has elucidated several genes, such as *FOXE3*, *ACTA2*, and *MYLK*, involved in familial TAA and dissection. (46-49) Several mouse models have been developed to mimic human TAA. Although there are nuanced differences between TAA mouse models, the majority display some degree of luminal dilation and elastin fragmentation in the aortic media. (50) The Marfan syndrome mouse models, specifically the fibrillin-1 haploinsufficiency (*Fbn1*<sup>C1041G/+</sup>) and hypomorphic (*Fbn1*<sup>mgR/mgR</sup>) mouse models, display progressive aortic dilation of varying severity. (11, 12, 51, 52) Mice with loss of function mutations affecting TGF $\beta$  signaling develop TAA and dissections. (53-55) Ehlers-Danlos model mice display aortic defects. (45) This area of research is rapidly expanding with the ability to rapidly replicate human mutations in mice. Interestingly, most research has used male mice only or have only studied sex differences in these models in the context of pregnancy and nursing. (45, 56) Only one study in the *Fbn1*<sup>GT8/+</sup> model of Marfan syndrome has shown sexual dimorphism in this context. (56) Thus mouse models of both spontaneous and syndromic TAA are valuable tools to study the pathogenesis of this disease.

## 1.5 Current Therapies for Thoracic Aortic Aneurysms

Currently, there is no proven medical therapy that reverses TAA. In Marfan syndrome, both beta- adrenergic blockers and renin angiotensin system inhibitors are used clinically. (57, 58) Despite widespread usage, evidence for the efficacy of beta-blockers in attenuating or reversing TAA is lacking. (59) Similarly, randomized control trials of losartan, an angiotensin receptor blocker, have shown mixed results. Losartan is a short acting, surmountable AT1aR antagonist, and may not be adequate to suppress the renin angiotensin system. Of the three largest trials of losartan, COMPARE demonstrated that losartan was superior to no additional treatment, the Pediatric Heart Network trial demonstrated no difference between losartan and atenolol, and MARFAN SARTAN demonstrated losartan added-on was not superior to placebo. (60-62) Conversely, the AIMS trial demonstrated that use of an insurmountable AT1aR antagonist, irbesartan, resulted in a reduction of the rate of aortic dilation.(63) These studies were based on the observation that losartan attenuated TAA in a Marfan syndrome mouse model. (64) The efficacy of irbesartan, an insurmountable agonist, holds further promise that adequate and sustained inhibition of renin angiotensin system may be efficacious. The mechanism by which these pharmacologic agents attenuate TAA is not known. We will review the evidence for the involvement of the renin

angiotensin system in TAA in the next section. Conversely, several pharmacologic agents have been shown to exacerbate TAA. One observational study demonstrated that calcium channel blockers were associated with worse outcomes in patients with Marfan syndrome. (65) Additionally, patients exposed to fluoroquinolones, a common antibiotic, had increased risk for aortic rupture. (66) The mechanism for these observations is unclear. Due to a lack of understanding of TAA pathogenesis, there is a lack of effective medical therapies to reverse TAA. In this dissertation, we will focus on syndromic TAA by investigating the contribution of the renin angiotensin system to aortopathy in a mouse model of Marfan syndrome. We not only describe validation of key measurements that assay thoracic luminal dilation and elastin fragmentation but also test the efficacy of a novel modality of renin angiotensin system inhibition in attenuating Marfan syndrome associated TAA.

## 1.6 The Renin Angiotensin System in TAA

The renin angiotensin system is a key mediator of aortic homeostasis that can be pharmacologically and genetically manipulated. These manipulations can be leveraged to impact TAA, but the mechanism by which this occurs is unknown. In this section, we will outline the ligand and receptor portions of the renin angiotensin system, genetic and pharmacologic modulators of the renin angiotensin system, and evidence for the involvement of the renin angiotensin system in TAA.

The renin angiotensin system can be separated into a ligand portion and a receptor portion. To generate angiotensin ligands, a series of enzymatic cleavages process angiotensinogen into its main effector peptide, angiotensin II (AngII). Angiotensinogen is the sole endogenous precursor to all angiotensin peptides. It contains 452 amino acids that is mainly synthesized by the liver. (67) Action of renin cleaves the 10 N-terminal residues to liberate the decapeptide angiotensin I from the parent AGT. Although the parent AGT molecule was historically thought to have few biologic functions independent of AngI and AngII, this concept has been recently challenged. (68) AngI is then processed by angiotensin converting enzyme into the main effector peptide of the renin angiotensin system, angiotensin II. AngII can be further processed into Ang(1-7) by angiotensin converting enzyme 2, but AngII is responsible for the majority of vascular effects. In humans, angiotensin peptides, and specifically AngII, acts on angiotensinII receptor type 1 (AT1R) and type 2 (AT2R). (69) Mice have two isoforms of AT1 receptors separated into AT1aR and AT1bR. AT1aR, AT1bR, and AT2R are seven transmembrane G-protein coupled receptors. While each isoform has specific functions, previous research indicates that AT1aR drives pathogenesis in the thoracic aorta. Specifically, deletion of either AT1bR or AT2R did not alter AngII induced atherosclerosis and aneurysms in either the thoracic or abdominal aortas. (70, 71) Genetic deletion of AT1aR attenuated AngII induced aortopathies. (72) Therefore, the main effector peptide of the renin angiotensin system in the aorta is derived from AGT and the main receptor isoform responsible for aortopathies is the AT1aR.

Modulation of the renin angiotensin system, through manipulations of angiotensin peptides and AT1aR, impacts TAAs. (**Table 1.3**) In general, activation of the renin angiotensin system exacerbates TAAs. Exogenous infusion of AngII induces TAA in C57BL/6J wild type mice and exacerbates TAA in FBN1<sup>C1041G/+</sup> mouse model of Marfan syndrome. (37, 73) Conversely, inhibition of the renin angiotensin system attenuates TAAs. Losartan, an AT1 receptor blocker, attenuates TAA in two different mouse models of Marfan syndrome. (64, 74) Endothelial specific deletion of AT1aR attenuated TAA and death by aortic rupture in the severe FBN1<sup>mgR/mgR</sup> mouse model of Marfan syndrome. (75) This effect is highly reproducible. (76-78) Additionally, this phenomenon is generalizable to other syndromic TAA mouse models, including fibulin-4 deficiency, TGFβ receptor 1 and 2 mutants. (79-81) Therefore, inhibition of RAS by pharmacologic and genetic means is a promising avenue for ameliorating TAAs of multiple etiologies.

However, recently published studies indicate that the involvement of the renin angiotensin system in Marfan syndrome associated TAA may be more nuanced than previously believed. One key controversy is the involvement of AT1aR in pathogenesis of Marfan syndrome associated TAA. While the site of action of AT1aR is still unknown, AT1aR deletion attenuated spontaneous, AngII-induced TAA. Losartan was shown to be effective in attenuating TAA in a mouse model of Marfan syndrome. However, losartan is a surmountable prodrug that may have effects beyond AT1R inhibition. (82) One study claimed that pharmacologic inhibition of AT1aR using losartan attenuated TAA in a mouse model of Marfan syndrome through hyperstimulation of AT2R. (83) However, direct stimulation of AT2R, using a specific agonist compound 21, failed to attenuate Marfan syndrome associated TAA. (84, 85) This is consistent with research in spontaneous TAA outlined above and indicates that losartan's primary protective effect may not be through AT2R hyperstimulation. Another study claimed that AT1aR deletion was unable to attenuate TAA in the FBN1<sup>C1041G/+</sup> mouse model of Marfan syndrome. However, losartan was able to attenuate TAA in AT1aR deficient mice at 6 months of age. (86) This study was limited by non-standard use of ultrasound and impact was reduced by a failure to state the sex of mice studied. Small changes in measurement protocols such as use of different viewing angles in ultrasound can greatly affect reliability of TAA measurements. Based on studies in the Fbn1<sup>GT8/+</sup> model, (56) male and non-parous female have different thoracic aortic dimensions. If treatment groups included unequal distributions of female and male animals, sexual dimorphism would hinder comparisons between groups. Directly contradicting this study, AT1aR deletion in FBN1<sup>mgR/mgR</sup> mice attenuated both TAA and death by aortic rupture. (75) Therefore it is unclear whether inhibition of AT1aR alone is sufficient to attenuate Marfan syndrome associated TAA.

Another controversy is the involvement of angiotensin peptides in pathogenesis of Marfan syndrome associated TAA. Inhibition of AngII production by angiotensin converting enzyme inhibitor enalapril attenuates AngII-induced aneurysms and atherosclerosis. (87) (88) However, AT1aR can be activated in a cell-stretch activated manner. This can occur by direct stimulation of the AT1

receptor and can be attenuated by an insurmountable AT1 receptor antagonist. (89) Activation of the AT1 receptor in this manner is completely independent of AngII. Cell stretch can also induce autocrine/paracrine release of AngII, thus activating the AT1 receptor. (90, 91) Evidence for ligand independent activation of AT1 receptors in Marfan syndrome revolve around the observation that deletion of AGT does not attenuate dilated cardiomyopathy in  $FBN1^{mgR/mgR}$  mice. (92) Additionally, ACE inhibitors minimally inhibited TAA in  $FBN1^{C1041G/+}$  mice. (83) Interestingly, clinical data on the efficacy of ACE inhibitors in human aneurysmal disease is mixed. (93-96) It is unclear whether angiotensin ligands are critical for the development of Marfan syndrome associated TAA. Ultimately, it is difficult to separate out ligand-dependent and ligand-independent effects of AT1aR using ACE inhibitors. ACE, also known as kininase II, can cleave numerous ligands in addition to AngI. (97) The kinin-kallikrein system plays a role in inflammation and can counteract the renin-angiotensin system. (98, 99) Thus, to deplete AngII alone, a novel modality targeting upstream of ACE is needed.

The renin angiotensin system is a complex hormonal system with numerous players. The paradoxical observations of the benefits in modulating the renin angiotensin system in Marfan syndrome merit investigation. Specifically, it is unclear whether AT1aR is involved in development of Marfan syndrome associated TAA. If AT1aR is involved, it is unclear whether that occurs in an AngII-dependent or AngII-independent manner.

## 1.7 Gaps in knowledge, hypotheses tested, and points discussed

Due to lack of understanding in the pathogenesis of Marfan syndrome associated thoracic aortic aneurysms, there is no effective medical therapy to reverse aortic dilation. One promising area of investigation is the contribution of the renin angiotensin system through the action of AngII on AT1aR to development of Marfan syndrome associated TAAs. However, the gaps in knowledge include whether and how AT1aR activation is responsible for TAA. These gaps have remained unfilled due to inadequate standardization of measurement techniques assaying the ascending aorta. Previous studies have also been biased due to either exclusive use of male animals or failure to specify the sex of animals studied. To address these gaps in knowledge this dissertation tests the overarching hypothesis that deletion of endogenous AngII attenuates Marfan syndrome associated thoracic aortic aneurysm through inhibition of ligand-dependent AT1aR activity. We tested this hypothesis by developing standardized measurements of TAA, investigating the role of the AngII-AT1aR axis in Marfan syndrome associated TAA, and exploring factors outside the renin angiotensin system that modulate TAA.

First, we developed and validated standardized methods to assay thoracic aortic aneurysms. In Chapter 2, we outline the effect of the cardiac cycle on measurements of the ascending aorta, demonstrating that the expansion of the aorta during systole is not equivalent between normal and aneurysmal aortas. Two-dimensional ultrasound is an accurate and precise modality to measure in vivo aortic diameters. We quantified the degree of expansion, showing that the

effect of cardiac cycle on aortic measurements can be a significant confounder in studies with small effect sizes. Additionally, we verify that assessment of elastin fragmentation by human observers blinded to group allocation is a reliable and reproducible method not subject to observer bias. Finally, we correlated these measurements to demonstrate that both luminal dilation and elastin fragmentation are complementary and consistent measurements of the severity of thoracic aortic aneurysms. Our subsequent studies benefitted from this development of standardized protocols for assaying TAAs.

Next, we studied the differential effects of inhibiting ligand-dependent and ligand-independent AT1aR activity of TAA in FBN1<sup>C1041G/+</sup> mice. Our hypothesis was that inhibition of the AngII-AT1aR axis is sufficient to attenuate TAA in FBN1<sup>C1041G/+</sup> mice. These studies are outlined in Chapter 3. Interestingly, we noticed striking sexual dimorphism in FBN1<sup>C1041G/+</sup> mice, causing us to pursue studies in male mice to maximize study power. Next, we generated FBN1<sup>C1041G/+</sup> mice with AT1aR deficiency alongside AT1aR intact mice to investigate the contribution of AT1aR. Using our validated methods of assaying TAA, we measured aortic diameters up to 12 months and elastin fragmentation in the ascending aorta at study termination. We found that ablation of both ligand-dependent and ligand-independent attenuated TAA in male FBN1<sup>C1041G/+</sup> mice. To distinguish between ligand-dependent and ligand-independent effects of AT1aR, we used a novel antisense oligonucleotide targeted against angiotensinogen to deplete plasma AGT. Depletion of AGT in male FBN1<sup>C1041G/+</sup> mice was sufficient to attenuate TAA, indicating that angiotensin ligands play a critical role in TAA pathogenesis.

Finally, we explored and discussed modulating factors of TAA. Although the renin angiotensin system is a major mediator of vascular homeostasis, other systemic and cell-specific factors may increase or decrease severity of Marfan syndrome associated TAA. One hypothesis is that estrogens were protective and androgens exacerbated TAA. Sex hormone removal impacted sexual dimorphism in TAA mouse models. Gonadectomy reduces endogenous sex hormones and causes atrophy of sex responsive organs. Ovariectomy of female mice exacerbated AngII-induced TAA. Orchiectomy of male mice attenuated AngII-induced TAA. However, gonadectomy was unable to alter existing TAA in juvenile FBN1<sup>mgR/mgR</sup> mice due to the model's aggressive TAA development. Another hypothesis is that AngII acts on AT1aR within the vascular wall, and specifically on adventitial fibroblasts to induce TAA. Previous research indicates that deletion of AT1aR on smooth muscle cells has no effect on TAA. (17, 75, 100) Additionally, endothelial specific deletion of AT1aR had marginal attenuation of Marfan syndrome associated TAA. Our evidence indicates that fibroblast specific deletion of AT1aR (driven by s100a4-cre) attenuates AngII induced aortopathies but not Marfan syndrome associated TAA. Thus, the cell type responsible for TAA in Marfan syndrome is still elusive and may differ from TAA of other etiologies. Altogether, these modulating factors, both the impact of sex hormones and the contribution of cell specific AT1aRs, represent interesting associations that need further exploration.

The studies outlined in this dissertation reveal novel insights into factors that modulate TAA. In discussing the conclusions of these findings, we will critically inspect these studies for limitations as well as propose future directions that can be taken given these revelations. Possible future studies may include use of AGT ASOs in human trials, determining the source of increased AngII in Marfan syndrome aortas, and determining the cell type responsible for AT1aR stimulation in Marfan syndrome. These findings are significant not only for increasing our understanding of the pathogenesis of Marfan syndrome associated thoracic aortic aneurysms but also for outlining novel treatment modalities that we hope to ultimately blunt the progression of this disease.



**Table 1.1 Conserved domains in fibrillin-1**

<b>Conserved Domain</b>	<b>Function</b>	<b>Refs</b>
Fibrillin unique N-terminus domain	Binding to fibrillin family C-terminus	(101) (102)
	Binding site for heparin sulfate proteoglycans	
	Fibronectin dependent microfibrillar assembly	(103)
EGF/cbEGF domains	Calcium dependent structural rigidity under tension	(102, 104)
TGF $\beta$ binding-like domain	Integrins $\alpha 5\beta 1$ , $\alpha v\beta 3$ , and $\alpha v\beta 6$ binding site	(102, 105)
	Weak calcium binding, structural rigidity	
Hybrid domains	Calcium binding, structural rigidity	
Proline/glycine rich domains	Unique identifiers between fibrillin family members	(102)
	tropoelastin binding	(103)
C-terminal and Aprosins	Furin cleaved endocrine regulator of glucose homeostasis	(102)
	Latent TGF $\beta$ binding protein interaction site	
	ADAMTS interaction site	
	BMP family binding site	

**Table 1.2 Mutant microfibril mouse models and phenotypes**

<b>Protein</b>	<b>Mouse Models</b>	<b>Mutation</b>	<b>Aortic Phenotype</b>	<b>Reference</b>
<b>Elastin</b>				
Tropoelastin	ELN -/-	Null	Aortic occlusion and tortuosity	(106)
	ELN +/-	Null	Aortic occlusion and tortuosity	(107)
	SM22-ELN-/-	Cell specific deletion	Aortic occlusion and tortuosity	(18)
	Tie2-ELN-/-	Cell specific deletion	Disrupted IEL	(18)
	Cdh5-ELN-/-	Cell specific deletion	Disrupted IEL	(18)
<b>Fibrillins</b>				
Fibrillin-1	FBN1 mgR/mgR	Hypomorphic	Severe TAA	(12)
	FBN1 C1041G/+	Missense	TAA	(11)
	FBN1 GT8/+	Truncation	TAA	(52)
	FBN1 H1Δ	Exon 7 deletion	Unknown - perinatal lethal	(52)
	FBN1mgΔ	Exon 19-24 deletion	Unknown - perinatal lethal	(51)
	FBN1 -/-	Null	Perinatal systemic vascular compromise	(108)
Fibrillin-2	FBN2 -/-	Null	None	(108)
<b>Fibulins</b>				
Fibulin-1	FBLN1 -/-	Null	Aortic Rupture - perinatal lethal	(109)
Fibulin-2	FBLN2 -/-	Null	None	(110)
Fibulin-3	FBLN3 -/-	Null	None	(111)
Fibulin-4	FBLN4 -/-	Null	TAA, perinatal lethal	(112, 113)
Fibulin-5	FBLN5 -/-	Null	Tortuous Aorta	(114)
<b>EMILIN</b>				
EMILIN-1	EMILIN-1 -/-	Null	Elastin fragmentation	(115)
EMILIN -2	EMILIN-2 -/-	Null	Not characterized; not expressed in aorta	(116)
EMILIN -3	EMILIN-3 -/-	Null	Not characterized; not expressed in aorta	(117)

**Table 1.3 Mouse Models Where AT1aR Inhibition Attenuates TAA**

<b>TAA Model</b>	<b>AT1 Inhibition Modality</b>	<b>Reference</b>
FBN1 <sup>C1041G/+</sup>	Losartan	(64)
AngII-infused	AT1a receptor deletion	(118)
Transverse Aortic Constriction	Losartan	(119)
DOCA-Salt	Losartan	(39)
Tgfbr2 <sup>G357W/+</sup>	Losartan	(81)
Fibulin4 <sup>R/R</sup>	Losartan	(120)
FBN1 <sup>mgR/mgR</sup>	Losartan	(74)
FBN1 <sup>mgR/mgR</sup>	AT1a receptor deletion	(75)

## CHAPTER 2. MAJOR METHODS OF MEASURING TAA

This chapter is based on a previously published manuscript:  
Chen JZ, Sawada H, Moorleggen JJ, Weiland M, Daugherty A, Sheppard MB. Aortic strain correlates with elastin fragmentation in Fibrillin-1 hypomorphic mice. *Circ Rep.* 2019;1(5):199-205. doi: 10.1253/circrep.CR-18-0012. PubMed PMID: 31123721; PMCID: PMC6528667.

### 2.1 Synopsis

**Background:** High frequency ultrasound has facilitated in vivo measurements of murine ascending aortas, allowing aortic strains to be gleaned from two-dimensional images. Thoracic aortic aneurysms associated with mutations in fibrillin-1 (*FBN1*) display elastin fragmentation, which may impact aortic strain. In this study, we determined the relationship between elastin fragmentation and aortic circumferential strain in wild type and fibrillin-1 hypomorphic (*FBN1*<sup>mgR/mgR</sup>) mice.

**Methods and Results:** Luminal diameters of the ascending aorta from wild type and *FBN1* hypomorphic (*FBN1*<sup>mgR/mgR</sup>) mice were measured in systole and diastole. Expansion of the ascending aorta during systole in male and female wild type mice was 0.21±0.02 mm (16.3%) and 0.21±0.01 mm (17.0%) respectively, while expansion in male and female *FBN1*<sup>mgR/mgR</sup> mice was 0.11±0.04 mm (4.9%) and 0.07±0.02 mm (4.5%) respectively. Reduced circumferential strain was observed in *FBN1*<sup>mgR/mgR</sup> mice compared to wild type littermates. Elastin fragmentation was inversely correlated to circumferential strain ( $R^2 = 0.628$   $p = 0.004$ ) and significantly correlated with aortic diameter. ( $R^2 = 0.397$ ,  $p = 0.038$  in systole and  $R^2 = 0.515$ ,  $p = 0.013$  in diastole)

**Conclusions:** *FBN1*<sup>mgR/mgR</sup> mice had increased aortic diameters, reduced circumferential strain, and increased elastin fragmentation. Elastin fragmentation in *FBN1*<sup>mgR/mgR</sup> and their wild type littermates was correlated with reduced circumferential strain.

### 2.2 Introduction

Thoracic aortic aneurysms (TAAs) are abnormal dilations of the aorta associated with increased risk of life-threatening aortic dissection and rupture.(36) While the majority of TAAs have not yet been associated with a specific mutation, TAAs often occur in the context of inherited genetic disorders such as Marfan syndrome. TAA tissues from patients with Marfan syndrome display decreased aortic elasticity.(121) Measurement of aortic diameter is a critical prognostic indicator as larger diameters are associated with higher risk of rupture.(36)

Mouse models of spontaneous TAAs can be generated by systemic administration of chemicals such as angiotensin II (AngII) or  $\beta$ -

aminopropionitrile.(37, 38) Mouse models of heritable TAAs can be generated by manipulation of genes responsible for extracellular matrix integrity or smooth muscle cell function such as fibrillin-1, fibulin-4, and ACTA-2.(11, 12, 47, 113, 122) In this study we used the fibrillin-1 hypomorphic (*FBN1*<sup>mgR/mgR</sup>) mouse model, which aggressively develop TAA early in life. Previous studies in these mice have revealed decreased elastin expression and increased elastin fragmentation in aneurysmal tissue. (12, 77, 123-125) This elastin fragmentation may influence aortic circumferential strain. We hypothesized that vascular strain in the ascending aorta, measured by two-dimensional high frequency ultrasound, correlated with elastin fragmentation. To test this hypothesis, we compared circumferential aortic strains in the *FBN1*<sup>mgR/mgR</sup> mice, which naturally develop elastin fragmentation, versus sex-matched wild type littermates.

Aortic diameter measurements are the primary endpoint to quantify TAA severity in disease models. Previously, ascending aortic measurements in mice were limited to terminal endpoints.(126, 127) This included measurements of aortic elasticity and shear strain performed on ex vivo tissues. (77) Development of high frequency ultrasound, in the range of 40-50 MHz, has enabled resolution that distinguishes small changes of aortic dimension over sequential measurements.(17) This resolution allows measurements of circumferential strain from two-dimensional images captured in vivo and enables investigation of the impact of elastin fragmentation on aortic strain.

This study used two-dimensional, trans-thoracic ascending aortic ultrasound measurements of the ascending aorta in wild type mice and their *FBN1*<sup>mgR/mgR</sup> littermates to measure circumferential strain in vivo. When standardized, two-dimensional, trans-thoracic ascending aortic ultrasound measurements correlate closely with traditional ex vivo measurements and have low interobserver variability. (34) Finally, we determined the correlation of these findings to elastin fragmentation.

## 2.3 Methods

### Mice

Male and female wild type (WT) C57BL/6J and *FBN1*<sup>mgR/mgR</sup> littermates were generated at The Jackson Laboratory (Bar Harbor, ME) from stock # 005704. Heterozygous *FBN1*<sup>mgR/+</sup> males were bred with *FBN1*<sup>mgR/+</sup> females to generate mice of desired genotypes. Mice were fed standard laboratory diet and water *ad libitum* and maintained on a 14:10 hour light:dark cycle. Mice were transferred to a barrier facility at the University of Kentucky. All protocols were approved by the University of Kentucky IACUC.

### Non-invasive blood pressure measurements

Systolic blood pressure was measured by tail cuff using a Kent Scientific Coda 8 as described previously.(128) All measurements were performed at the beginning of the light cycle. Briefly, mice were restrained and placed on a warming platform. Twenty cycles of blood pressure measurements were obtained for each mouse. Measurements <50 mmHg and >220 mmHg were excluded.

Pulse rates <400 bpm were excluded from calculation. Blood pressures were measured on 3 consecutive days at the same time of day. Measurements represented means over 3 days.

#### Ultrasound measurements

Ultrasound images were acquired in wild type and *FBN1*<sup>mgR/mgR</sup> mice at 11 weeks of age. Mice were anesthetized using isoflurane; dose was titrated between 2-3% wt/vol isoflurane with 2 L/min O<sub>2</sub> to maintain a heart rate of 400 - 500 beats per minute as monitored by concurrent three lead electrocardiogram (ECG). Ultrasound cine-loops were captured using a Vevo 2100 system with a MicroScan MS550 40 MHz transducer (VisualSonics, Toronto, ON). Frame rate was at least 300 frames per second and 300 frames were stored per cine-loop. Aortic images were acquired from a modified right parasternal long axis view (1 – 2 ribs caudal to the right parasternal long axis view, **Figure 2.1**). The probe was angled 45 degrees relative to the chest to avoid sternum artefacts. Images were standardized to include visualization of two anatomical landmarks: the innominate artery and aortic valve (**Figure 2.2A**). The ascending aorta was defined as the region between the sinotubular junction and the innominate artery. The largest ascending aortic diameter was measured in both systole and diastole of 3 separate cardiac cycles for each mouse. To facilitate measurements, a center line was drawn on the acquired image at the midpoint between the aortic walls. Aortic diameters (AoD) were measured at the largest diameter perpendicular to the center line of the aorta (**Figure 2.2B**). AoD in systole (AoD;s) was measured at physiologic systole: when aorta was maximally dilated. AoD in diastole (AoD;d) was measured at the end of diastole: defined as during the R wave (**Figure 2.2C**). Aortic images were analyzed by two independent observers that were blinded to the experimental groups. Circumferential strain was calculated as previously described using Equation 1.(129)

$$0.5 \left[ \left( \frac{AoD;s}{AoD;d} \right)^2 - 1 \right] * 100\% \quad (1)$$

#### Ex vivo aortic measurements

Mice were terminated by overdose of ketamine:xylazine at 11 weeks of age followed by exsanguination via cardiac puncture and saline perfusion. Aortas were dissected away from surrounding tissue and Optimal Cutting Temperature Compound (Sakura Finetek, Torrance, CA) was slowly introduced via the left ventricle to maintain aortic patency. A black plastic sheet was inserted behind the aorta and heart to increase contrast and facilitate visualization of aortic borders. Aortas were immediately imaged using a Nikon SMZ800 stereoscope and measurements were recorded using NIS-Elements AR 4.51 software (Nikon Instruments Inc., Melville, NY). Fluid OCT maintained aortic patency to facilitate ex vivo and histologic analyses. Ascending aortic diameters were measured at the largest width perpendicular to the vessel.

#### Quantification of elastin fragmentation

Three proximal thoracic aortas per group were selected randomly and at least nine tissue sections per aorta were generated using a cryostat. Tissue

sections (10  $\mu\text{m}$ ) were generated from the aortic root to the aortic arch at 100  $\mu\text{m}$  intervals. Three sections corresponding to the region of largest dilation between the sinotubular junction and the arch were analyzed. Briefly, elastin was visualized by auto-fluorescence by an excitation spectrum of 460 – 500 nm. Multiple high magnification images were acquired of each section that were subsequently aggregated to a single image of the entire section using ImageJ.(130) Fragmentation was defined as the presence of discernable breaks of continuous elastin fiber. The number of elastin breaks was counted by two independent investigators who were blinded to the sample identification. Individual data were represented as the mean number of elastin breaks per aortic section calculated by two independent investigators.

### Statistics

Data are reported as mean  $\pm$  standard error. Statistical analyses were performed using SigmaPlot (Systat Software Inc; San Jose, CA). For two-group comparisons, all data passed normality and equal variance tests. Paired Student's t-tests were used to compare systole and diastole from the same mouse and unpaired Student's t-tests were used between groups.  $P < 0.05$  was considered statistically significant. Regression was calculated via Pearson's Coefficient of Correlation. Bland-Altman analysis was performed by plotting the mean of aortic diameter measured ex vivo and by ultrasound versus the difference of aortic diameter measured ex vivo and by ultrasound with negative values indicated that ex vivo measurements are smaller than ultrasound measurements. (Equation 2) Bias and limits of agreement calculated for Bland-Altman analyses compared measurements of the same biological variable that had been obtained using two different measurement methods.

$$\text{Difference Aortic Diameter} = \text{ex vivo diameter} - \text{ultrasound diameter} \quad (2)$$

## 2.4 Results

Wild type and  $FBN1^{\text{mgR/mgR}}$  mice exhibited similar body weight and systolic blood pressure at 11 weeks of age.

Systolic and diastolic blood pressures were measured by tail-cuff at 11 weeks of age in mice for 3 consecutive days before termination at similar times of the day. Blood pressure was not significantly different in wild type and  $FBN1^{\text{mgR/mgR}}$  sex-matched littermates. In addition, body weights were not different between wild type and  $FBN1^{\text{mgR/mgR}}$  sex-matched littermates (**Table 2.1**). During ultrasonography, anesthesia was titrated to maintain a heart rate of 400-500 beats per minute. Therefore, heart rate was not significantly different between groups during ultrasonography (Heart rate wild type =  $453 \pm 27$  bpm;  $FBN1^{\text{mgR/mgR}}$  =  $439 \pm 26$  bpm;  $p = 0.86$ ). Heart rates during ultrasound were lower than normal due to anesthesia effect. Heart rates were also not different between groups during non-invasive blood pressure measurements (**Table 2.1**). Two-dimensional ultrasound measurements of the ascending aorta in  $FBN1^{\text{mgR/mgR}}$  mice.

Ultrasound measurements of ascending aortas of 11 week old male and female wild type mice and their *FBN1*<sup>mgR/mgR</sup> littermates in systole and diastole were measured via a standardized protocol described above (**Figure 2.3, A – D**). Ascending aortic diameters measured in systole were significantly greater than those measured in diastole (**Figure 2.3, E and F**) in both male and female mice. (**Table 2.1**) The difference between systole and diastole in wild type mice was larger than in *FBN1*<sup>mgR/mgR</sup> sex-matched littermates. Ascending aortas from *FBN1*<sup>mgR/mgR</sup> mice demonstrated less circumferential strain during systole.

Fibrillin-1 hypomorphic mice exhibited significantly less circumferential expansion during systole compared to their wild type littermates. Green-Lagrange strain was calculated using equation 1 from aortic diameters obtained from B-mode images of systole and diastole from each individual mouse. Increased circumferential strain was observed in WT ascending aortas compared to aortas from *FBN1*<sup>mgR/mgR</sup> mice (**Figure 2.4, A and B**). This effect was seen in both male and female mice. In male mice: mean percent strain wild type =  $18.2 \pm 1.8\%$ ; *FBN1*<sup>mgR/mgR</sup> =  $5.9 \pm 2.4\%$ ;  $p = 0.001$ . In female mice: mean percent strain wild type =  $17.4 \pm 1.9\%$ ; *FBN1*<sup>mgR/mgR</sup> =  $5.4 \pm 1.8\%$ ;  $p = 0.001$ . Elastin fragmentation correlates inversely with circumferential strain and positively with aortic diameter.

As expected, aortic sections from *FBN1*<sup>mgR/mgR</sup> mice displayed significantly greater elastin fragmentation compared to their wild type counterparts. (**Figure 2.5, A – C**). Elastin fragmentation was also significantly inversely correlated to in vivo circumferential strain ( $R^2 = 0.628$   $p = 0.004$ ) and positively correlated to both systolic and diastolic aortic diameters ( $R^2 = 0.397$ ,  $p = 0.038$  in systole and  $R^2 = 0.515$ ,  $p = 0.013$  in diastole) (**Figure 2.5, D – F**). By fitting a multiple linear regression model, we also determined that the *FBN1* genotype contributed significantly to differences in elastin fragmentation ( $p = 0.001$ ) and that elastin fragmentation did not correlate with sex ( $p = 0.414$ ).

## 2.5 Discussion

Previously, our group reported aortic diameters in aneurysm studies without specifying the cardiac phase during which these in vivo measurements were taken.(17, 70, 131, 132) In this study, we demonstrated that in vivo two dimensional ultrasound measurements are accurate and correlate with in situ measurements of exposed aortas. (**Figure 2.6**) Furthermore, we quantified the difference between measurements taken in systole and diastole in the thoracic aorta. (**Figure 2.3**) This suggested that two-dimensional trans-thoracic ultrasound can be used to calculate circumferential aortic strain, despite the fact that the thoracic aorta experiences increased longitudinal displacement due to its proximity to the beating heart.(129, 133) Using a mouse model of elastin fragmentation, we further investigated whether differences in aortic strain between *FBN1*<sup>mgR/mgR</sup> mice and their wild type littermates correlated with elastin fragmentation.



Previously, circumferential strain has been characterized in the AngII-induced mouse model of aortic aneurysms.(134) However, these analyses have not been performed for mouse models of heritable thoracic aortic aneurysms, such as *FBN1*<sup>mgR/mgR</sup> mice. *FBN1*<sup>mgR/mgR</sup> mice were used in this study because of the rapid development of pronounced thoracic aneurysms. (12, 51) Mouse models with mutations in *FBN1* exhibit decreased aortic elastin expression, elastin fragmentation, and TAAs.(77) Aortas from wild type mice experienced greater circumferential strain during systole compared to aortas from *FBN1*<sup>mgR/mgR</sup> mice. In this study, systolic blood pressure was acquired using a standardized protocol on a system that measures the variance in tail volume in conjunction with a pressure cuff.(128) We have demonstrated previously that there is good correlation between blood pressure measurements obtained by this process compared to those obtained by telemetry.(135) Although absolute blood pressure measurements can differ between instruments, there were no differences detected in systolic blood pressure between wild type and *FBN1*<sup>mgR/mgR</sup> mice. There was also no statistical significant difference in heart rate measured while conscious or under anesthesia. The correlation between blood pressure and circumferential strain was not significant. However, blood pressures were not measured during ultrasound. We cannot assume that blood pressure in the awake state is equal to blood pressures during ultrasound in the anesthetized state. While this suggests that the increase in aortic stiffness is a function of intrinsic aortic tissue mechanics, this point merits further study. Indeed, this increase in aortic stiffness has been measured in other mouse models of spontaneous thoracic and abdominal aortic aneurysm and dissection. In fact, circumferential aortic strain in the AngII-induced mouse model of abdominal aortic aneurysms is approximately 15% in control mice and 5% in AngII infused mice.(134) These strains are consistent when measured by speckle tracking technology.(136) Interestingly, AngII-induced thoracic aortic aneurysms also had reduced circumferential strain. Circumferential strains in this model decrease from 20% before infusion to 10% after AngII infusion.(137) Data from AngII-induced aortic aneurysms are in agreement with our results in a heritable model of thoracic aortic aneurysm.

Strains have been measured ex vivo in the *FBN1*<sup>mgR/mgR</sup> mouse model. Previously, Lee et al.(77) demonstrated that compressive forces, measured by atomic force microscopy acting on aortas from *FBN1*<sup>mgR/mgR</sup> mice, produced greater deformation under stress.(77) This was attributed to the loss of elasticity in *FBN1*<sup>mgR/mgR</sup> aortas as evidenced by reduced area fraction of elastic fibers. We quantified elastin fragmentation as a proxy of aortic elastic behavior. While elastin fragmentation was correlated with reduced circumferential strain in response to circumferential tensile forces in vivo, this analysis is limited by the assumption that loss of continuous elastin layers leads to loss of elasticity. Paradoxically, loss of elasticity can explain both the loss of resistance to compressive forces outlined by Lee et al.(77) and the increased resistance to circumferential tensile forces shown in this study via the Poisson effect. Together, these observations imply that increased elastin fragmentation in

*FBN1*<sup>mgR/mgR</sup> aortic tissue may be responsible for reduced aortic strain observed during systole in *FBN1*<sup>mgR/mgR</sup> mouse.

The primary purpose of this study was to determine the relationship between circumferential aortic strain measured in vivo and elastin fragmentation. We additionally quantified aortic diameter increases during systole compared to diastole in both wild type and *FBN1*<sup>mgR/mgR</sup> mice. The significant size differences indicate that cardiac cycle influences interpretation of murine studies that report thoracic aortic diameters. Based on our data, the excursion of the aorta in systole can be as great as 0.2 mm in wild type aortas and 0.1 mm in aneurysmal aortas. This difference is larger than error attributable to interobserver variability in our dataset, where bias between observers was  $0.08 \pm 0.08$  mm in systole and  $-0.07 \pm 0.06$  mm in diastole (**Figure 2.7**). Thus, specifying whether ascending aortic diameter were measured in either systole or diastole is especially important in studies in order to detect small differences, ensure accuracy, and increase study power. Accounting for this phenomenon is important when ascending aortic diameter measured across different studies. This discrepancy occurs because studies have reported aortic diameters in systole, diastole, both, or omit reporting cardiac cycle. (17, 137-140) In lieu of these data, a correction factor of approximately 17% in C57BL/6J wild type aortas and 5% in *FBN1*<sup>mgR/mgR</sup> aneurysmal aortas may be taken to approximate measurements taken in systole compared to diastole.

This study used mice that spontaneously develop elastin fragmentation to demonstrate that reduced circumferential strain is correlated with increased elastin fragmentation and that two-dimensional ultrasound data can be used to measure circumferential strain in vivo.

**Table 2.1 Characteristics of wild type and  $FBN1^{mgR/mgR}$  mice**

Sex	Genotype	N	Age at Ultrasound (d)	Body Weight (g)	Systolic Blood Pressure (mmHg)	Pulse Rate (bpm)	Aortic Diameter; Systole (mm)	Aortic Diameter; Diastole (mm)	AoD;s – AoD;d (mm)
Male	WT	8	74.8 ± 1.0	25.7 ± 0.5	147 ± 7	506 ± 23	1.50 ± 0.05	1.29 ± 0.05***	0.21 ± 0.02
	$FBN1^{mgR/mgR}$	8	74.8 ± 1.0	26.2 ± 0.8	139 ± 18	524 ± 31	2.35 ± 0.13	2.24 ± 0.15**	0.11 ± 0.04*
Female	WT	5	74.7 ± 1.3	20.5 ± 0.7	137 ± 9	547 ± 58	1.42 ± 0.03	1.23 ± 0.04***	0.21 ± 0.01
	$FBN1^{mgR/mgR}$	7	75.2 ± 1.2	20.8 ± 0.8	125 ± 13	443 ± 23	1.64 ± 0.07	1.57 ± 0.08**	0.07 ± 0.02*

Male and female *FBN1* wild type (WT) and *FBN1*<sup>mgR/mgR</sup> mice were aged to 11 weeks. Body weight was measured before performing ultrasonography. SBP and pulse rate were measured for 3 consecutive days using a tail cuff-based technique. No measurements were significantly different between wild type and *FBN1*<sup>mgR/mgR</sup> within sex. Aortic diameters in systole and diastole were measured as described above. Male mice: wild type  $p < 0.001$ ; *FBN1*<sup>mgR/mgR</sup>  $p = 0.004$ . Female mice: wild type  $p < 0.001$ ; *FBN1*<sup>mgR/mgR</sup>  $p = 0.009$ . \*\*\* $p < 0.001$ , \*\*  $p < 0.01$  AoD;s vs AoD;d. AoD difference was calculated by AoD;s – AoD;d. In male mice: AoD difference between wild type and *FBN1*<sup>mgR/mgR</sup>,  $p = 0.03$ . Female mice,  $p = 0.01$ . \*  $p < 0.05$  WT vs *FBN1*<sup>mgR/mgR</sup>. Measures are represented as mean ± SEM.  $p > 0.05$  between groups via Student's t-test.

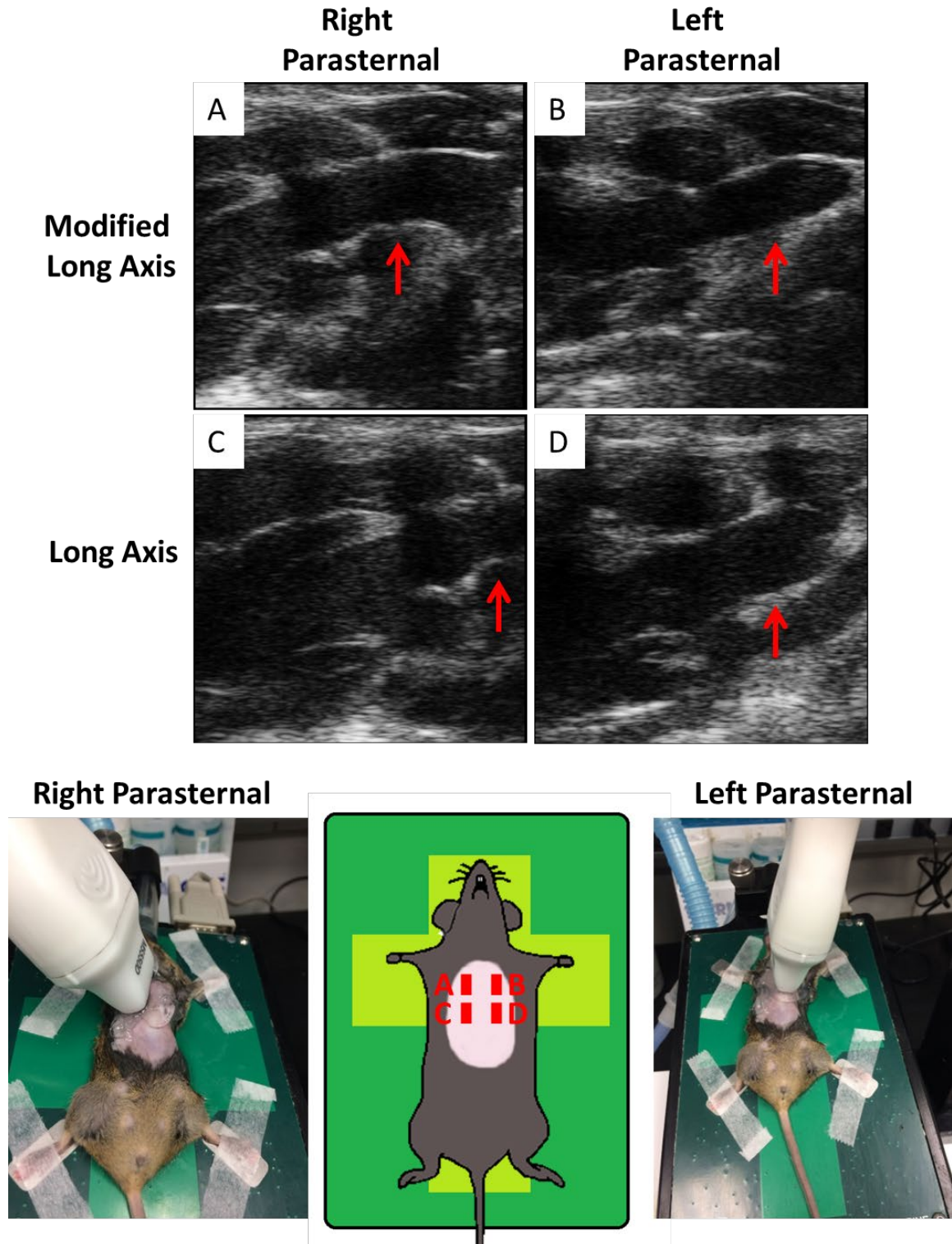


**Figure 2.1 Probe positions used to measure aortic diameter.** Aortas from a 12 week old wild type (WT) mouse was imaged in **A, C**) right parasternal long axis and **B, D**) left parasternal long axis views. Modified long axis views were taken from a location that was one to two ribs above the long

axis view to optimize visualization of the ascending aorta. Red arrows point to the ascending aorta.

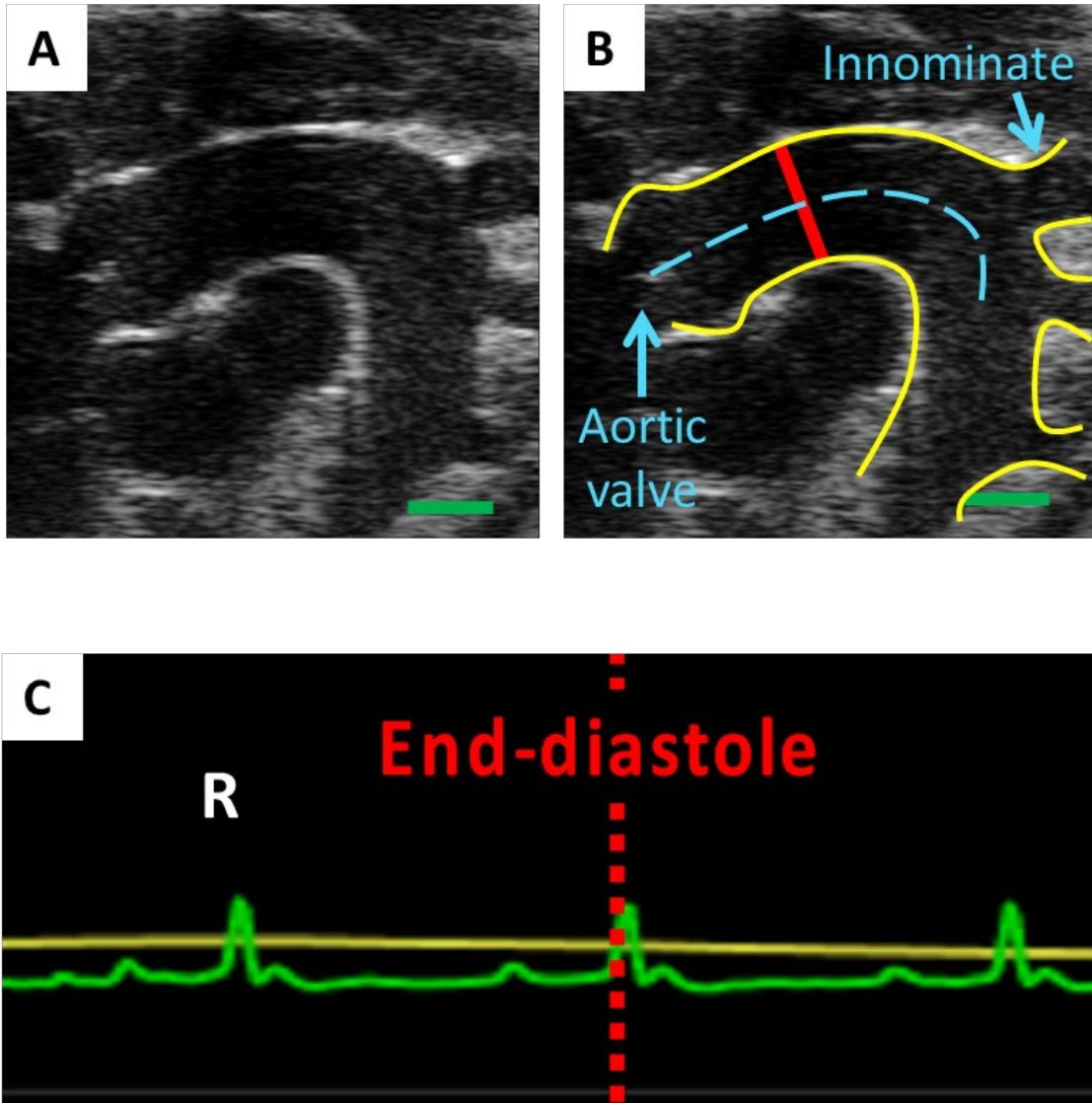


**Figure 2.2 Modified right parasternal long axis view and measurement protocol of the ascending aorta.**

**A)** B-mode images were standardized to include visualization of two distinct anatomical landmarks in the same field: the aortic valves and the innominate artery. **B)** Center line was defined as the midpoint between aortic walls (blue line). Measurements were taken inner-edge to inner-edge at the largest diameter (red line) perpendicular to the center line between the aortic root and innominate artery. Yellow lines depicting the aortic vessel wall were included for clarity in this diagram, but were not used for measurement purposes. Green bar = 1 mm. **C)** Concurrent ECG monitoring allowed standardization of end-diastole (dashed red line one frame within the QRS complex) to facilitate imaging at a specific interval of the cardiac phase. Images at systole were taken at physiologic systole.

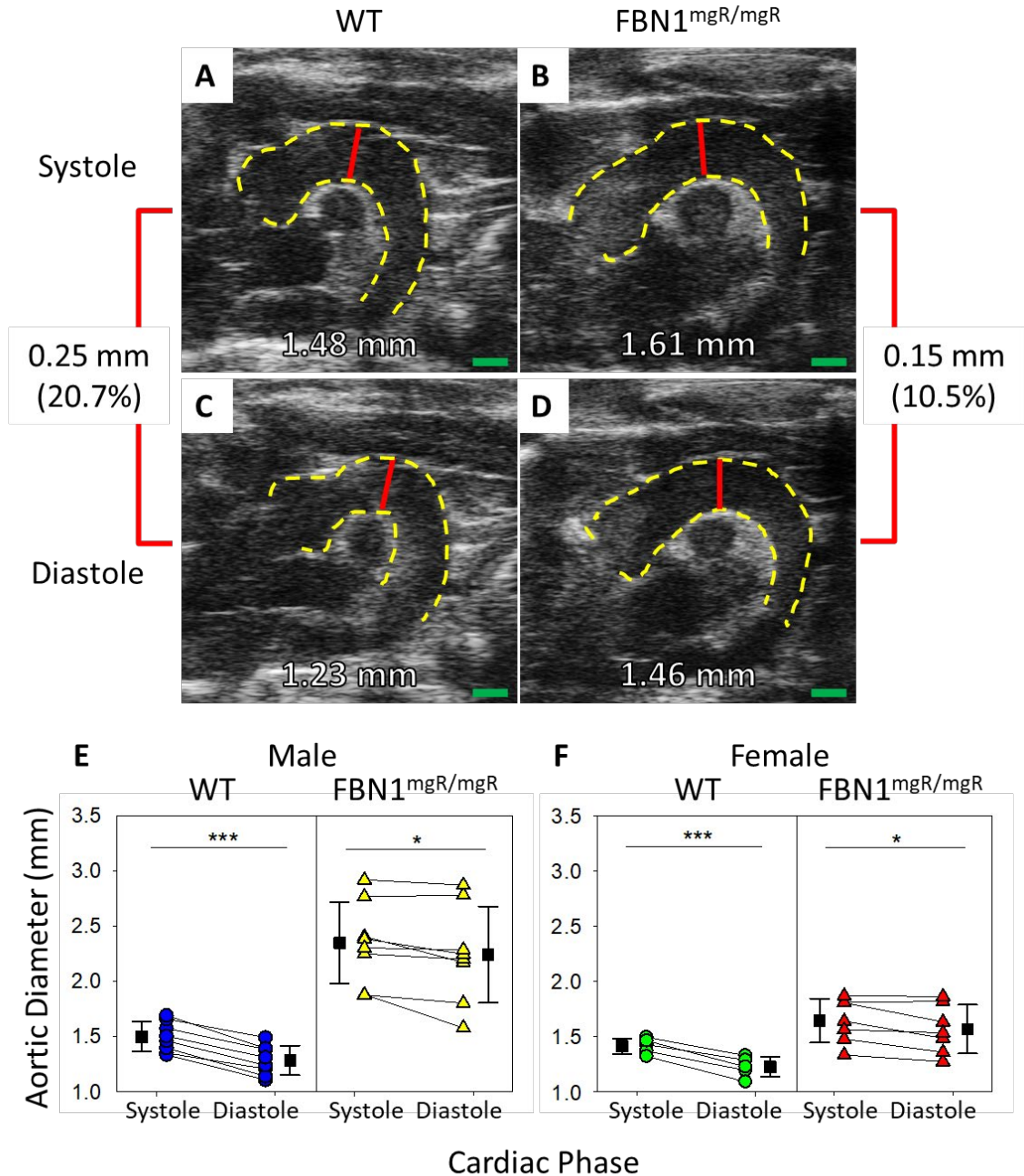


**Figure 2.3 Effect of cardiac cycle on ascending aortic diameters.**

**A – D)** Representative B-mode images of ascending aortas from 11 week old wild type (WT) and *FBN1*<sup>mgR/mgR</sup> mice. Quantification of aortic diameters in systole and diastole of **E)** male and **F)** female littermates. There were significant differences in aortic diameters between systole and diastole within both sex and genotype. Red line = region measured, green bar = 1 mm. Male: n = 8 WT and 8 *FBN1*<sup>mgR/mgR</sup>; Female: n = 5 WT and 7 *FBN1*<sup>mgR/mgR</sup>; \*\*\*p < 0.001, \*p < 0.05 between groups by paired Student's t-test.

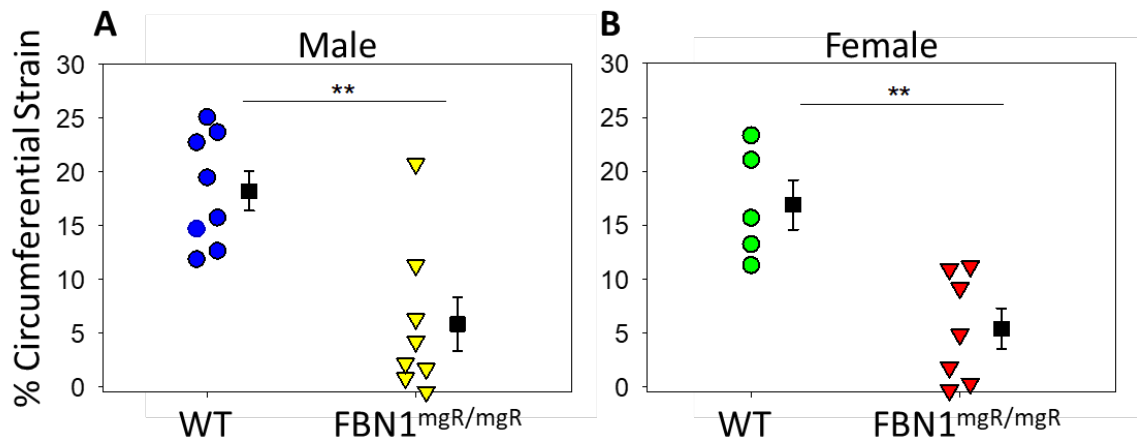


**Figure 2.4 Circumferential Green-Lagrange strain of the aorta during cardiac cycle in wild type and *FBN1*<sup>mgR/mgR</sup> mice.**

Percent expansion was calculated by comparing aortic measurements between systole and diastole within a cardiac cycle. **A)** Male and **B)** female wild type (WT) mice exhibited greater percent expansion during the cardiac cycle compared to their *FBN1*<sup>mgR/mgR</sup> littermates. Male: n = 8 WT and 8 *FBN1*<sup>mgR/mgR</sup>; Female: n = 5 WT and 7 *FBN1*<sup>mgR/mgR</sup>; \*\*p < 0.01 between groups by Student's t-test.



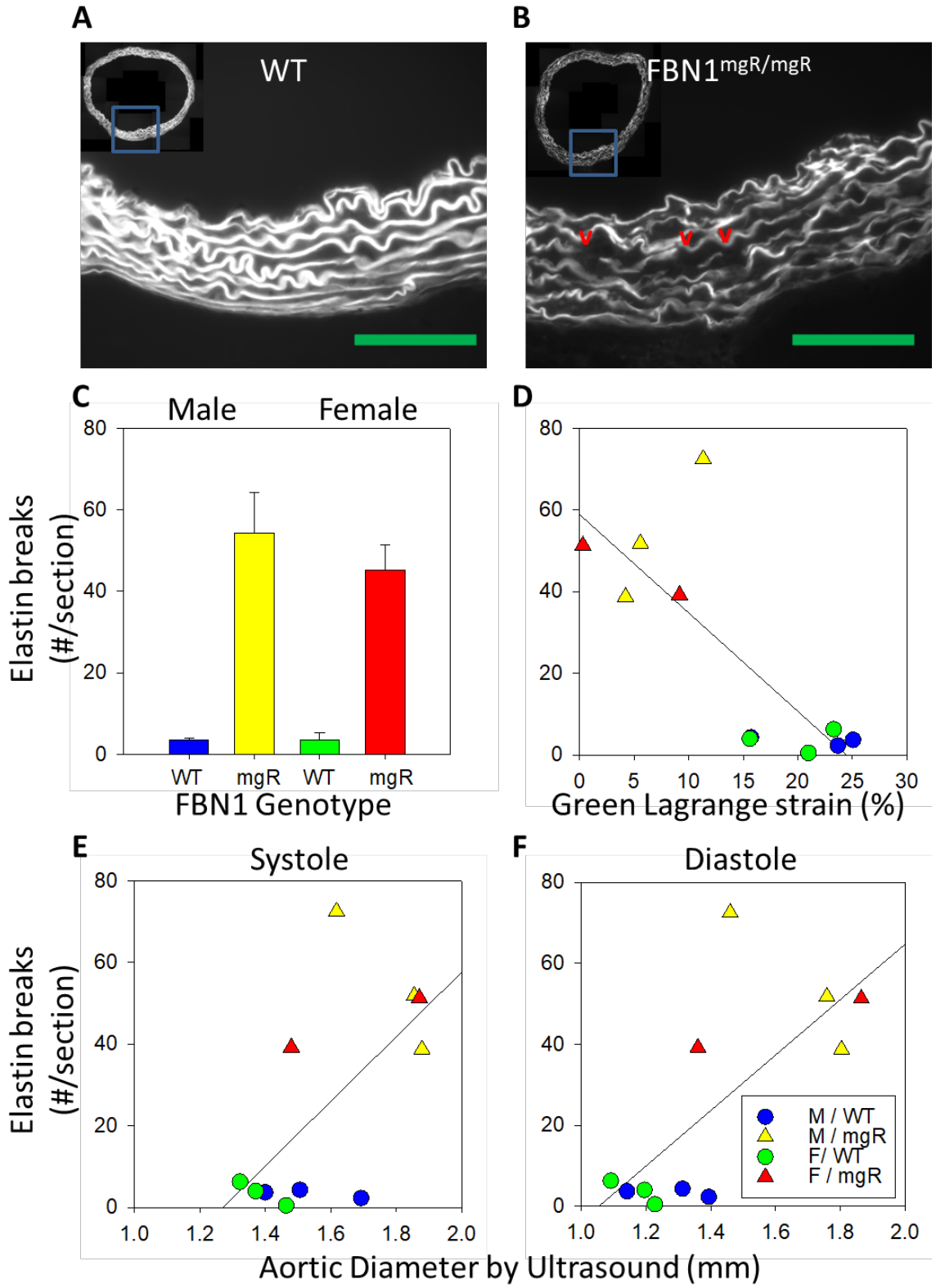


**Figure 2.5 Elastin fragmentation of WT and FBN1<sup>mgR/mgR</sup> correlated with ascending aortic diameter.**

**A, B)** Representative images of elastin fragmentation from WT and *FBN1*<sup>mgR/mgR</sup> mice acquired by elastin autofluorescence at the largest ascending aortic diameter. Green line = 100  $\mu$ m. **C)** Elastin fragmentation quantified **D)** Correlation analysis of elastin fragmentation versus circumferential strain revealed an inverse relationship. ( $R^2 = 0.628$ ,  $p = 0.004$ ). **E, F)** Correlation plots of elastin breaks compared to aortic diameter in systole and diastole.  $n = 3$  male WT, male mgR, and female WT.  $n = 2$  female mgR.  $R^2 = 0.397$ ,  $p = 0.038$  in systole and  $R^2 = 0.515$ ,  $p = 0.013$  in diastole. Male and female WT = blue and green circles. Male and female *FBN1*<sup>mgR/mgR</sup> = yellow and red triangles respectively.

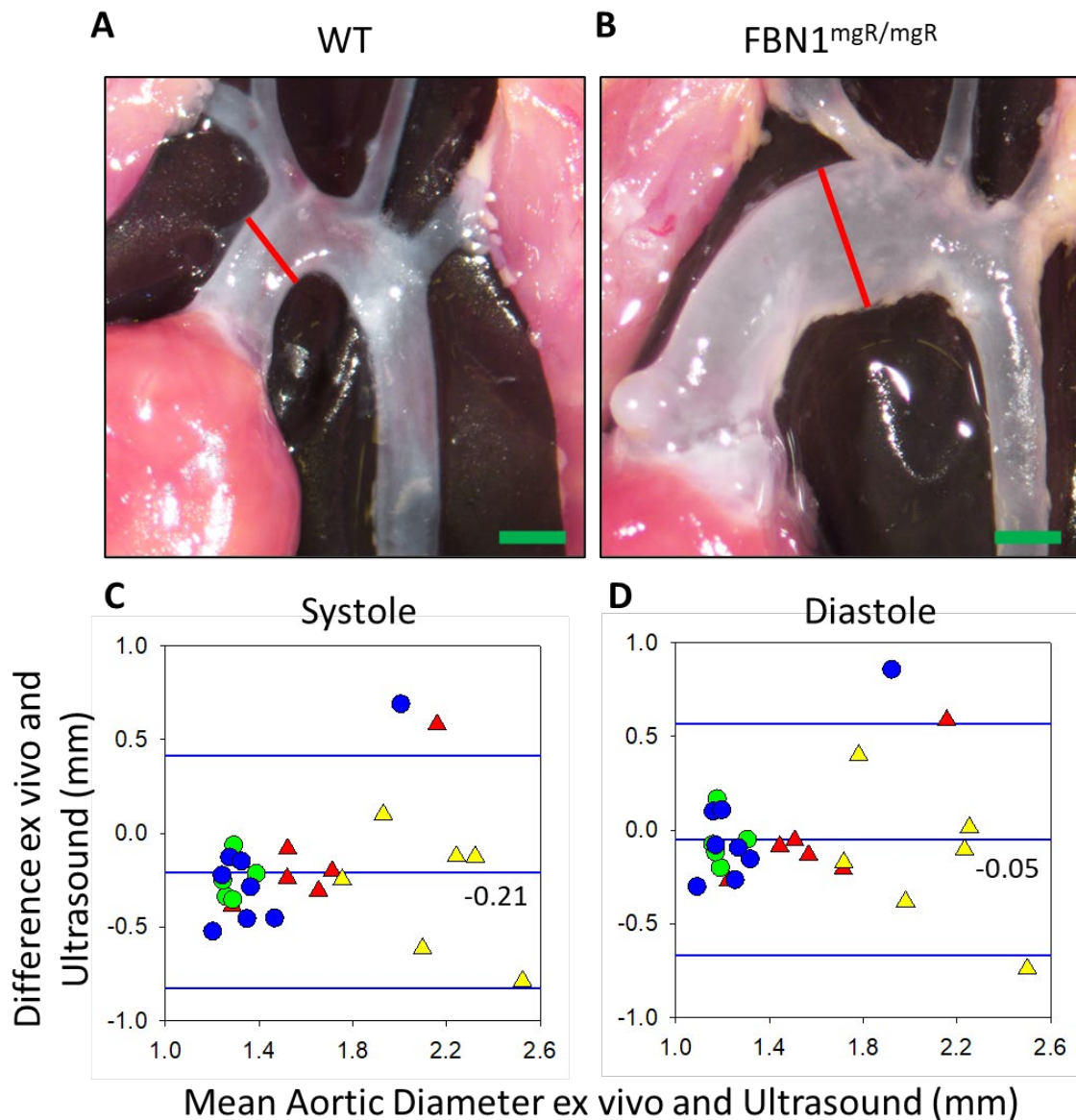


**Figure 2.6 Ultrasonographic measurements of aortic diameter in diastole closely reflected ex vivo aortic diameter measurements.**

Representative images of in situ aortas from **A**) WT and **B**)  $FBN1^{mgR/mgR}$  mice in which measurements were recorded at the largest ascending aortic diameter. Red line = region measured, green line = 1 mm. **C**, **D**) Bland-Altman analyses demonstrated that in situ diameters correlated more closely to ultrasonographic measurements in diastole than systole. (Bias in systole = -0.21 mm; in diastole = -0.05 mm). Measurements were less reliable at larger aortic diameters as shown by the divergence from bias in the Bland-Altman plot in ascending aortic diameters greater than 1.8 mm. Center blue line represents bias and outer blue lines represents the 95% limits of agreement. Male and female WT = blue and green circles. Male and female  $FBN1^{mgR/mgR}$  = yellow and red triangles respectively.

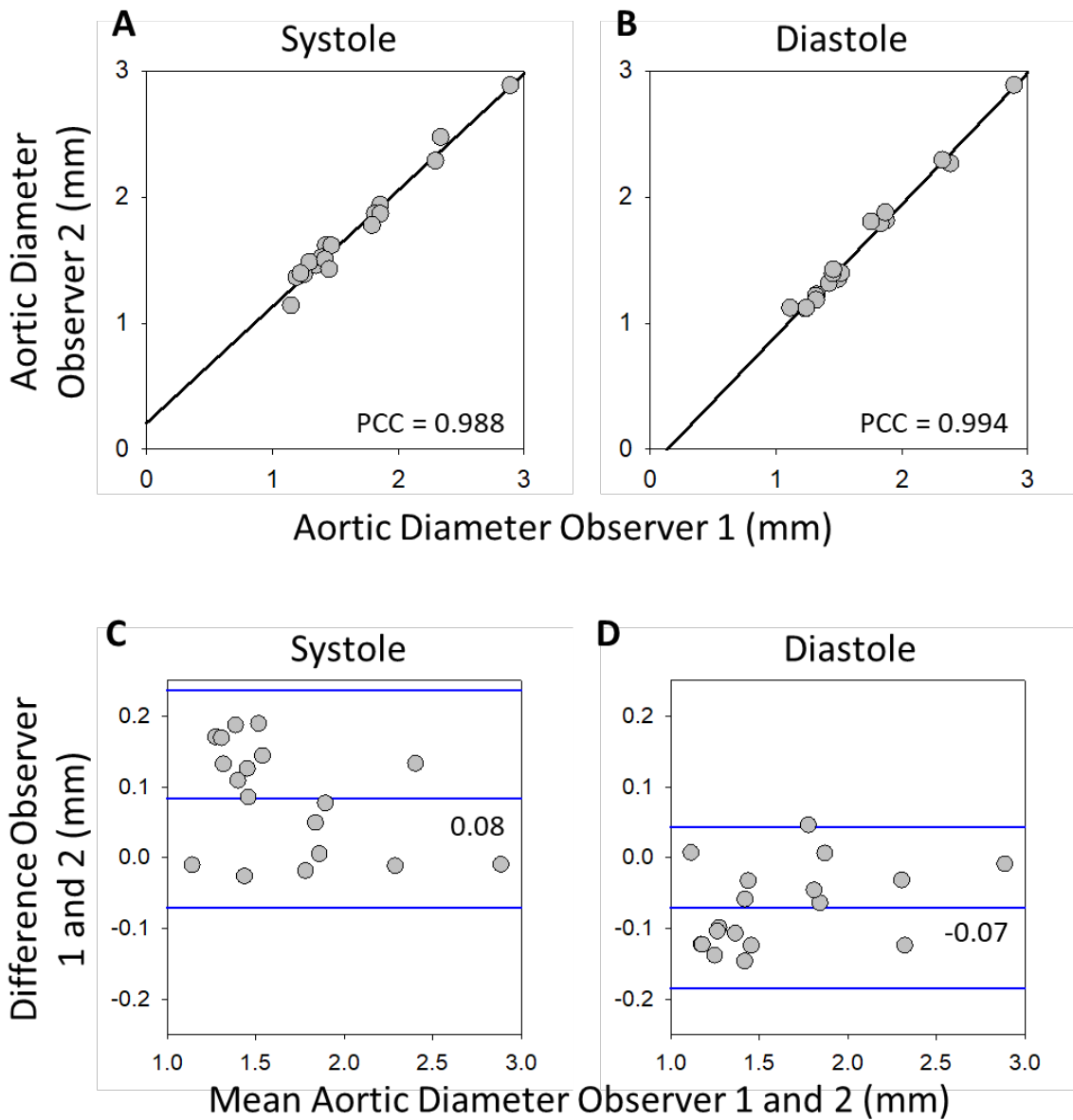


**Figure 2.7 Bland-Altman analyses comparing measurements obtained by two independent observers that were blinded to the experimental design. A, B) Measurements between observers in both systole and diastole were highly correlated. Systole  $R^2 = 0.976$ ; Diastole  $R^2 = 0.988$ ;  $p < 0.001$  C, D) Bland-Altman analyses of ascending aortic B-mode image measurements acquired by two independent, observers, who were blinded to the image identification, demonstrated negligible bias in systole and diastole. Bias in systole =  $0.08 \pm 0.08$  mm ; diastole =  $-0.07 \pm 0.06$  mm. Limit of agreement 95% CI  $[-0.70, 0.26]$  mm in systole and  $[-0.19, 0.04]$  mm in diastole)  $n =$  Aggregate measurements from 28 mice. The center blue line represents bias and outer blue lines represents the 95% limits of agreement.**

## CHAPTER 3. INHIBITION OF ANGIOTENSIN II-DEPENDENT AT1A RECEPTOR STIMULATION ATTENUATES THORACIC AORTIC DILATATION IN FIBRILLIN-1<sup>C1041G/+</sup> MICE

This chapter contains information adapted from a provisional patent application titled “TREATMENT USING ANGIOTENSINOGEN ANTISENSE OLIGONUCLEOTIDE” to Alan Daugherty, Mary Sheppard, Hong Lu, and Jeff Chen for describing use of a pharmacologic agent in Marfan syndrome associated thoracic aortic aneurysms.

This chapter is also based on a publication in process titled “Inhibition of Angiotensin II Dependent AT1a Receptor Stimulation Attenuates Thoracic Aortic Pathology in Fibrillin-1<sup>C1041G/+</sup> Mice” detailing the central finding that inhibition of the AngII- AT1a receptor axis attenuates Marfan syndrome associated thoracic aortic aneurysms.

### 3.1 Synopsis

#### Objective:

A cardinal feature of Marfan syndrome is thoracic aortic aneurysm (TAA). The contribution of ligand-dependent stimulation of angiotensin II receptor type 1a (AT1aR) to TAA progression remains controversial because the beneficial effects of angiotensin receptor blockers have been ascribed to off-target effects. This study used genetic and pharmacologic modes of attenuating angiotensin receptor and ligand, respectively, to determine their roles on TAA in mice with fibrillin-1 haploinsufficiency (Fbn1<sup>C1041G/+</sup>).

#### Approach and Results:

TAA in Fbn1<sup>C1041G/+</sup> mice were determined in both sexes and found to be strikingly sexually dimorphic. Males displayed progressive dilation over 12 months while ascending aortic dilation in Fbn1<sup>C1041G/+</sup> females did not differ significantly from wild type mice. To determine the role of AT1aR, Fbn1<sup>C1041G/+</sup> mice that were either +/+ or -/- for AT1aR were generated. AT1aR deletion reduced progressive expansion of ascending aorta and aortic root diameter from 1 to 12 months of age in males. Medial thickening and elastin fragmentation were attenuated. An antisense oligonucleotide against angiotensinogen (AGT-ASO) was administered to male Fbn1<sup>C1041G/+</sup> mice to determine the effects of angiotensin II depletion. AGT-ASO administration, at doses that markedly reduced plasma AGT concentrations, attenuated progressive dilation of the ascending aorta and aortic root. AGT-ASO also reduced medial thickening and elastin fragmentation.

#### Conclusions:

Genetic approaches to delete AT1aR and deplete AngII production exerted similar effects in attenuating pathology in the proximal thoracic aorta of

male  $Fbn1^{C1041G/+}$  mice. These data are consistent with ligand (AngII) dependent stimulation of AT1aR being responsible for aortic disease progression.

### 3.2 Introduction

Marfan syndrome is an autosomal dominant genetic disorder associated with thoracic aortic aneurysm (TAA) that enhance the risk for aortic rupture due to loss of aortic integrity.(141) The disease is caused by mutations in fibrillin-1; a protein incorporated into the microfibrils that decorate elastic fibers.(142) To gain insight into the mechanisms of the disease, mice have been developed with a heterozygous expression of the C1041G mutation of the mouse fibrillin-1 protein, which is analogous to the C1039Y mutation in humans.(11) These mice have a haploinsufficiency of fibrillin-1 and mimic some pathologies present in patients with Marfan syndrome including progressive expansion of the proximal thoracic aorta.

The renin angiotensin system has been invoked as a mediator of TAA in patients with Marfan syndrome.(143) Experimental evidence for the role of the renin angiotensin system has been based predominantly on the observation that losartan inhibits aortic pathology in mice. This was demonstrated initially in  $Fbn1^{C1041G/+}$  mice administered losartan starting at the prenatal phase of life.(64) Additionally, it has been consistently demonstrated that losartan reduces aortic expansion in many other mouse models of TAA. (74, 81, 83, 86, 119, 120) However, losartan's many well-characterized effects independent of AT1 receptor antagonism potentially hinder its use as a pharmacologic tool to specifically study AT1 receptors.(144) Indeed, the benefit of losartan in inhibiting aortic root dilation in  $Fbn1^{C1041G/+}$  mice has been attributed to effects such as TGF- $\beta$  antagonism or nitric oxide synthase stimulation.(64, 86) To overcome the limitations of pharmacological approaches, there is a critical need to determine the role of AT1aR using genetic deletion to specifically ascribe a function of AT1 receptors in general and AT1aR specifically.

Additionally, the mode by which AT1 receptors become activated in Marfan syndrome is uncertain. While activation of AT1 receptors is commonly due to engagement of the ligand, angiotensin II (AngII), the pathway can also be activated by conformational changes of the protein during cell stretch of myocytes and vascular smooth muscle cells.(145-147) This stretch activation of AT1 receptor is inhibited by pharmacological antagonists of the receptor. Based on studies in angiotensinogen deficient mice, dilated cardiomyopathy in the fibrillin-1 hypomorphic model of Marfan syndrome has been attributed to this AngII-independent activation of AT1aR.(92) The relative role of receptor activation of ligand versus stretch has not been evaluated in vascular disease.

The aim of the present study was to define the contribution of ligand-dependent activation of AT1aR to the progressive expansion of the proximal thoracic aorta in  $Fbn1^{C1041G/+}$  mice. Aortic diameters were measured for a 1 year interval using a standardized ultrasound protocol.(34, 35) In accord with current guidelines, the study was performed in both sexes of these mice. These studies demonstrated a strong sexual dimorphism with greater expansion in  $Fbn1^{C1041G/+}$

males and minimal progressive expansion in Fbn1<sup>C1041G/+</sup> females. Surprisingly, this disparity has not been reported previously. The role of AT1aR was determined subsequently using male mice with global AT1aR deletion. The role of the ligand was determined using an angiotensinogen antisense oligonucleotide (AGT-ASO) that depleted the unique precursor of AngII. This study demonstrated the importance of ligand-dependent activation of AT1aR to progression of aortic pathology.

### 3.3 Methods

#### *Mice*

Studies were performed in accordance with recommendations for design and reporting of animal aortopathy studies.(32, 33) Studies were performed using littermate controls. Mice and genealogy were tracked with Mosaic Vivarium Laboratory Animal Management Software (Virtual Chemistry). Male and female AT1aR deficient (AT1aR<sup>-/-</sup>) (stock #002682) and Fbn1<sup>C1041G/+</sup> (stock #012885) mice were obtained from The Jackson Laboratory. Male AT1aR heterozygous (AT1aR<sup>+/-</sup>) x Fbn1<sup>C1041G/+</sup> were bred with female AT1aR<sup>+/-</sup> x fibrillin-1 wild type (Fbn1<sup>+/+</sup>) mice to generate four experimental groups per sex: male and female AT1aR wild type (AT1aR<sup>+/+</sup>) x Fbn1<sup>+/+</sup>, AT1aR<sup>-/-</sup> x Fbn1<sup>+/+</sup>, AT1aR<sup>+/+</sup> x Fbn1<sup>C1041G/+</sup>, and AT1aR<sup>-/-</sup> x Fbn1<sup>C1041G/+</sup> mice. Littermates were separated by sex and genotypes and were randomized when housing mice after weaning. For AGT ASO experiments, 2-month-old male Fbn1<sup>C1041G/+</sup> mice were procured from The Jackson Laboratory and randomized into experimental groups using a random number generator. Mice were checked daily for health, and necropsy was performed to adjudicate cause of death. Mice were housed up to 5 per cage and maintained on a 14:10 hour light:dark cycle. Mice were fed Teklad Irradiated Global 18% Protein Rodent Diet # 2918 *ad libitum* and allowed *ad libitum* access to water via a Lixit system. Bedding was provided by P.J. Murphy (Coarse SaniChip) and changed weekly during the study. Cotton pads were provided as enrichment. The room temperature was maintained at 21°C and room humidity was maintained at 50%. All protocols were approved by University of Kentucky IACUC.

#### *Genotyping*

Mice were genotyped twice using tail tissue. Group allocation was based on genotyping performed after weaning at postnatal day 28 and again after study termination to verify genotypes. AT1aR deletion was assayed using forward primer 5'-AAATGGCCCTTA ACTCTTCTACTG-3' and reverse primer 5'-ATTAGGAAAGGGAACA GGAAGC-3' covering a neo cassette that disrupts AT1aR spanning bps 110-635. The neo cassette removed approximately 0.5 kb and inserted approximately 1 kb of neo gene. AT1aR<sup>+/+</sup> generated a 631 bp product. AT1aR<sup>-/-</sup> generated a ~1.1 kbp product. Fbn1<sup>C1041G/+</sup> was assayed using forward primer 5'-CTCATCATTTTTGGCCAGTTG-3' and reverse primer 5'-GCACTTGATGCACATTCACA-3' covering a single loxP intronic sequence within intron 24 which should not exist in wild type mice. The protocol used was as

described by The Jackson Laboratory. Fbn1<sup>+/+</sup> generates a 164 bp product. Fbn1<sup>C1041G/+</sup> generates a 212 bp product. Post-termination validation genotyping was performed by Transnetyx.

#### *Antisense Oligonucleotides*

Scrambled control ASO (#549149) and AGT ASO (#109547) were provided by Ionis Pharmaceuticals. Lyophilized ASOs were diluted in PBS as recommended by the manufacturer. Mice were randomized to study group using a random number generator. Two-month-old male Fbn1<sup>C1041G/+</sup> mice were administered control ASO or AGT ASO (80 mg/kg) subcutaneously at day 1 and 3 of study. Mice were maintained on subcutaneous control ASO or AGT ASO (40 mg/kg) every 7 days for the remainder of the study.

#### *Ultrasound Measurements*

Ultrasound was performed by standardized protocols that have been as described previously.(35, 148) Briefly, mice were anesthetized using inhaled isoflurane (2-3% vol/vol) and maintained at a heart rate of 450-550 beats per minute during image capture to reduce anesthesia exposure and maintain consistent heart rate between animals (Somnosuite, Kent Scientific). The order by which mice were subject to ultrasound was randomized. Ultrasound images were captured using a Vevo 3100 system with a 40 MHz transducer (Visualsonics). Images captured were standardized according to two anatomical landmarks: the innominate artery branch point and aortic valves. The largest luminal ascending aortic diameter between the sinotubular junction and the innominate artery were measured in end-diastole over three cardiac cycles by two independent observers.

#### *Measurement of in situ Aortic Diameters*

Mice were terminated by overdose of ketamine:xylazine followed by cardiac puncture and saline perfusion. The order in which mice were taken down was randomized. Aortas were dissected away from surrounding tissue and Optimal Cutting Temperature Compound (Sakura Finetek) was introduced into the left ventricle to maintain aortic patency. A black plastic sheet was inserted beneath the aorta and heart to increase contrast and facilitate visualization of aortic borders. Aortas were imaged using a Nikon SMZ800 stereoscope and measurements were recorded using NIS-Elements AR 4.51 software (Nikon Instruments Inc.). Ascending aortic diameters were measured at the largest width perpendicular to the vessel.

#### *Histology*

Mice were ranked according to their ascending aortic diameter by ultrasound, and the median five per group were selected for histology. Tissue sections (10 µm) were acquired from the aortic root to the aortic arch at 100 µm intervals using a cryostat. The section corresponding to a region of maximal dilation between the sinotubular junction and the arch was analyzed. Elastin fragmentation was visualized by Verhoeff elastin staining under 20x



magnification and images from three high powered fields per section were recorded for analysis. Individual data were represented as the mean of three high power fields. Fragmentation was defined as the presence of discernable breaks of continuous elastic lamina. Medial thickness was measured at the greatest thickness from inner to external elastic laminae in 3 images using NIS-Elements AR software. Measurements were verified by an independent investigator who was blinded to sample identification.

#### *AGT Western Blotting*

Reducing buffer (Bio-Rad 161-0737 and Sigma M7522) and plasma (0.3  $\mu$ L) from mice administered control or AGT ASO were heated to 95°C for 5 minutes. Samples were fractionated on an SDS-PAGE gel (10% wt/vol; Bio-Rad 456-8033). Proteins were transferred to a PVDF membrane via Trans-blot system (Bio-Rad 170-4256). Total proteins were detected by Ponceau S. Membranes were blocked by milk (5% wt/vol; Bio-Rad 170-6404) in TBS-T (0.1% wt/vol). Membranes were then incubated with antibodies against total AGT (0.1  $\mu$ g/mL; IBL 28101) for 1 hour at room temperature then with HRP-conjugated goat-antirabbit IgG (0.2  $\mu$ g/mL; Vector Pi-1000). Membranes were developed with Clarity Max ECL (Bio-Rad 1705064) on a ChemDoc MP system. Blots were quantified using Bio-Rad CFX software.

#### *Statistics*

All animals that met pre-specified inclusion criteria, and were not excluded due to death by humane endpoint unrelated to aortic disease (fighting, infection), had cause of death adjudicated by necropsy. Statistical analyses were performed using SigmaPlot 14.0. Equal variance and normality of data determined whether non-linear, logarithmic transformation was performed and whether parametric or non-parametric tests were used. Two-way ANOVA or Student's t-test was performed for parametric comparisons; Holm-Sidak was used for post-hoc tests. Kruskal-Wallis or Rank Sum was performed for non-parametric comparisons with Dunn's method for post hoc tests. Data are represented as individual data points, mean  $\pm$  SEM, or as box and whisker plots representing median and interquartile range where applicable.

### 3.4 Results

#### *Progression of Aortic Dimensions was Sexually Dimorphic in Fbn1<sup>C1041G/+</sup> Mice*

In initial studies, the progression of aortic diameters over a 12-month interval was determined in both male and female Fbn1<sup>+/+</sup> and Fbn1<sup>C1041G/+</sup> mice. Because TAA in Fbn1<sup>C1041G/+</sup> mice has variable pathology within the proximal thoracic aorta, several parameters were measured (**Figure 3.1**). This included the ascending aortic diameter, aortic root diameter, and ascending aortic length. In Fbn1<sup>+/+</sup> mice, there was no statistical difference in the ascending aorta diameter, aortic root diameter, or ascending aortic length between female and male at any interval up to 12 months of age (**Figure 3.2A, B, C**). At one month of age, aortic root diameters and ascending aortic lengths were increased in both

male and female  $Fbn1^{C1041G/+}$  mice compared to  $Fbn1^{+/+}$  mice. However, only male  $Fbn1^{C1041G/+}$  mice exhibited statistically significant ascending aortic dilation compared to sex-matched littermates at one month of age. Despite differences at 1 month of age in female mice, the subsequent increase in diameter of ascending aorta and aortic root, and length of the ascending region were not statistically different between  $Fbn1^{+/+}$  and  $Fbn1^{C1041G/+}$  mice (**Figure 3.2D, E, F**). In contrast, male  $Fbn1^{C1041G/+}$  mice had augmented increases in diameters of ascending aorta and aortic root and ascending aortic length, compared to male  $Fbn1^{+/+}$  littermates over the course of 12 months. Since female  $Fbn1^{C1041G/+}$  mice had no significant differences in the progression of aortic dimensions compared to their wild type littermates, subsequent experiments used predominantly male mice.

#### *AT1aR Deletion Attenuated Aortic Pathology in Male $Fbn1^{C1041G/+}$ Mice*

To study the effects of AT1aR on aortic dilation in  $Fbn1^{C1041G/+}$  mice,  $Fbn1^{C1041G/+}$  mice that were either  $AT1aR^{+/+}$  or  $AT1aR^{-/-}$  were generated.  $Fbn1^{C1041G/+}$  mice were also compared against  $Fbn1^{+/+}$  mice that were also either  $AT1aR^{+/+}$  or  $AT1aR^{-/-}$ . Aortic dimensions were measured using ultrasound images acquired from a right parasternal view at diastole (**Figure 3.3A**). Images were acquired from every mouse at the stated intervals up to 12 months of age, with no deaths of any cause occurring during the study.

Male  $Fbn1^{+/+}$  mice had modest increases in diameters of the ascending aorta (**Figure 3.3B**), aortic root (**Figure 3.3C**), and lengths of the ascending aorta (**Figure 3.3D**) during the course of the 12-month study. These increases were not significantly different from increases seen in  $Fbn1^{+/+}$  mice that were also  $AT1aR^{-/-}$ . These findings based on the ultrasound measurements were confirmed at the 12-month interval by direct measurements on in situ aortas (**Figure 3.3E, F**).

At 1 month of age, male  $Fbn1^{C1041G/+}$  mice had increased diameters of ascending aorta and aortic root and lengths of ascending aorta compared to  $Fbn1^{+/+}$  mice. At this early age, deletion of AT1aR had no effect on aortic dimensions (**Figure 3.4**). In  $Fbn1^{C1041G/+}$  mice that were  $AT1aR^{+/+}$ , there was a progressive increase in all 3 aorta dimensions acquired by ultrasound. In contrast, deletion of AT1aR markedly attenuated the progressive expansion of these dimensions to rates that were not statistically different from those in  $Fbn1^{+/+}$  mice (**Figure 3.5**). As with  $Fbn1^{+/+}$  mice, direct aortic measurements in situ at 12 months of age confirmed the data acquired by ultrasound. Consistent with previously published research,(17) body weight and systolic blood pressure were not correlated with ascending aortic dimensions in mice (**Figure 3.6**).

Female  $Fbn1^{+/+}$  and  $Fbn1^{C1041G/+}$  mice that were with either  $AT1aR^{+/+}$  or  $-/-$  were also generated and aortic dimensions measured up to 12 months of age. As noted above, beyond the initial differences at 1 month of age, progressive changes in aortic dimensions were not different between  $Fbn1^{+/+}$  and  $Fbn1^{C1041G/+}$  female mice. The deletion of AT1aR had no effect on the age-related changes in either group (**Figure 3.7, 3.8**).

To determine if AT1aR deletion impacted the structure of the aortic media, histological characteristics were determined in aortic tissues acquired at 12 months of age. Since the most dramatic differences in changes of dimensions described above were in the ascending aorta, this region was selected for tissue characterization using our validated and reproducible method (**Figure 3.9**). Ascending aortic tissues from Fbn1<sup>+/+</sup> mice had elastic fibers with minimal fragmentation (**Figure 3.10A**). Neither the extent of fragmentation nor medial thickness were altered by the absence of AT1aR in Fbn1<sup>+/+</sup> mice (**Figure 3.10B, C**). In contrast, Fbn1<sup>C1041G/+</sup> x AT1aR<sup>+/+</sup> mice had extensive fragmentation of elastic fibers and marked medial thickening. Deletion of AT1aR in these mice significantly reduced elastin fragmentation and medial thickening.

*Depletion of Plasma AGT Concentrations by AGT ASO Attenuated Aortic Pathology in Male Fbn1<sup>C1041G/+</sup> Mice*

We have demonstrated previously that administration of AGT ASO markedly reduces plasma concentration of AGT and attenuates AngII responses in mice.(68, 149) Using ASO against the same target as previous publications, male Fbn1<sup>C1041G/+</sup> mice received a loading dose (80 mg/kg) of either AGT or control ASO on day 1 and day 4 of the study. Starting on day 7, mice received a maintenance dose (40 mg/kg) every 7 days for 6 months. (**Figure 3.11A**). Mice tolerated the ASO well and displayed minimal hepatic and renal toxicity after administration of loading doses (**Figure 3.12**) AGT ASO effectively depleted AGT in plasma (**Figure 3.11B**).

Aortic dimensions were acquired starting at 2 months of age, and every month for a further 6 months using the same process described above (Figure 3.11C) with in situ aortic measurements at termination confirming the ultrasound measurement. (**Figure 3.11D**). AGT depletion achieved by the ASO administration led to statistically significant reductions in expansion of diameters of ascending aorta (**Figure 3.11E**) and aortic root (**Figure 3.11F**) and length of ascending aorta (**Figure 3.11G**) in male Fbn1<sup>C1041G/+</sup> mice.

To determine whether AGT ASO impacted aortic medial structure, histology was performed on ascending aortic tissue. Consistent with our previous observation, we detected aortic medial remodeling in 8-month-old male Fbn1<sup>C1041G/+</sup> mice administered control ASO (**Figure 3.13A**). Compared to male Fbn1<sup>C1041G/+</sup> mice administered control ASO, male Fbn1<sup>C1041G/+</sup> mice administered AGT ASO exhibited less elastin fragmentation and medial thickening (**Figure 3.13B, C**).

### 3.5 Discussion

Using pharmacological tools to manipulate the renin angiotensin system, there have been consistent demonstrations that losartan attenuates aortic pathology in mice with fibrillin-1 manipulations.(64, 74, 76, 83, 86, 150, 151) However, it has been proposed that losartan may exert these beneficial actions independent of AT1 receptor antagonism.(74, 83, 86) Additionally, it has been suggested that AngII may not be responsible for cardiovascular pathology in mice with genetically manipulated fibrillin-1.(92) However, the present study demonstrates that both genetic deletion of AT1aR and techniques to reduce AngII availability led to reduced aortic pathology in Fbn1<sup>C1041G/+</sup> mice. These findings are consistent with ligand activation of AT1aR being the basis for aortic expansion in fibrillin-1 haploinsufficient mice.

The sequential measurement of aortic dimensions over a protracted interval in multiple groups required development of a standardized ultrasound protocol for image acquisition. We have noted previously the variance imparted by the differences acquiring dimension at systole or diastole.(35) Given that this excursion can be as much as 0.2 mm, lack of consistency in acquiring data could have a profound effect on data interpretation. The approach used in this study also consistently imaged the aorta from the right parasternal view.(34) While this view is optimal for determining dimensions of the ascending aorta, we acknowledge that this reduces accuracy of aortic root measurements. In the present study, there was strenuous adherence to a standardized protocol. In addition, the measurements acquired from ultrasound images were validated at termination by direct measurement of aorta in situ. This degree of measurement validation allows us to not only produce reliable data but also reduces the variability between sequential measurements.

Since we were not aware of any previous study that defined the effects of sex on the aortic pathology in Fbn1<sup>C1041G/+</sup> mice, the initial studies used both males and females. The present study demonstrates a striking effect of sex on the aorta in these mice, with the female Fbn1<sup>C1041G/+</sup> mice exhibiting minimal progression of thoracic aortic expansion compared to sex-matched Fbn1<sup>+/+</sup> littermates. In mice with genetic manipulations of Fbn1, there had been only one study indicating that sexual dimorphism existed in the Fbn1<sup>GT8/+</sup> mouse model of Marfan syndrome.(56) However, sexual dimorphism of the Fbn1<sup>GT8/+</sup> mouse was only defined in the context of pregnancy. In addition to revealing that female Fbn1<sup>C1041G/+</sup> mice resist aortic dilation, we outlined the consequences of this sexual dimorphism on the role of AT1aR deletion. While the mechanism of this sexual dimorphism is beyond the scope of the present study, it illustrates the need for studies to report data on studies in these mice in a sex-specific manner.

Deletion of AT1aR markedly reduced progression of aortic pathology in male Fbn1<sup>C1041G/+</sup> mice. AT1 receptors in mice have two isoforms, AT1aR and AT1bR, that resulted from chromosomal duplication. While there is strong sequence homology between the two isoforms, they have different tissue distribution and different signaling mechanisms. Absence of AT1bR has modest

effects in vivo, although it is responsible for AngII induced contractions of the infrarenal mouse aorta.(70, 152) Absence of AT1bR has no effect on AngII-induced aortopathies.(70) AT1aR deficient mice were initially demonstrated to have lower blood pressure.(153) However, in agreement with the present study, there has also been several publications showing no difference in blood pressure between AT1aR<sup>+/+</sup> and <sup>-/-</sup> mice.(154) While the present study was ongoing, the genetic deletion of AT1aR was reported in Fbn1 hypomorphic mice. While global deletion of AT1aR in Fbn1 hypomorphic mice had no significant effect on the survival, there was decreased aortic expansion in mice that survived to 90 days.(75) This emphasizes the need for further study on the divergent roles of the renin angiotensin system in aneurysm versus rupture/dissection. The early acquisition of ultrasound data in this study also illustrated that there are changes in aortic dimension in the early postnatal interval. Despite the dramatic reduction of progression of aortic dimensions in AT1aR<sup>-/-</sup> mice following this postnatal interval, the absence of AT1aR failed to affect early changes. This is consistent with temporal-dependent mechanisms of the disease as have been demonstrated previously in Fbn1 hypomorphic mice.(75)

Others have noted that AT1aR deficiency had no effect on expansion of the aortic root at 3 and 6 months of age in Fbn1<sup>C1041G/+</sup> mice, whereas losartan had a divergent effect and was able to decrease aortic root expansion in these mice.(86) The beneficial effects of losartan were attributed to preservation of endothelial function in an AT1aR independent manner through an alternative VEGFR2/eNOS pathway. The basis for the disparity relative to the present study are not clear. Comparisons are hampered by the paucity of data on the protocol for ultrasound acquisition and on the sex of the mice in each group. Other studies suggested that losartan's protective effect may be due to tumor growth factor  $\beta$  inhibition or AngII receptor type 2 hyperstimulation.(64, 83) However, our data indicated that blockade of the AT1aR attenuates Marfan syndrome associated TAA. While the pleotropic effects of losartan may contribute to attenuating thoracic aortopathies, the present study is consistent with the postulate that its benefit is due to inhibition of AT1aR activation.

We used an ASO to decrease the synthesis of the unique precursor of all angiotensin peptides to determine whether AT1aR stimulation in aortopathies required AngII as a ligand. This approach is advantageous over the more common mode of reducing AngII production by inhibiting angiotensin-converting enzyme, which regulates other pathways including the kinin-kallikrein system. Additionally, the protracted half-life of ASO leads to persistent inhibition of AGT synthesis and profound reductions in plasma AGT concentrations. Use of this pharmacologic modality also avoids adverse consequences of genetic deletion of the renin angiotensin system components. Previous genetic approaches have included the use of mice with global deficiencies of AGT. However, these mice have several major developmental abnormalities include poor growth and cardiomyopathy.(155) Inhibition of AGT synthesis by an ASO reduces plasma concentrations by approximately 90% in the postnatal phase with no observable toxicity as demonstrated in the present study and other reports.(68, 156) Therefore, the use

of ASO to deplete AGT demonstrated the need for the presence of angiotensin ligands to augment aortic pathology in  $Fbn1^{C1041G/+}$  mice.

In humans, randomized control trials of angiotensin receptor blockers have yielded mixed results in Marfan syndrome associated TAA, in contrast to the consistent results that have been generated using mouse models of the disease.(64, 74, 76, 83, 86, 150, 151) Most of the mouse and human studies have been performed using losartan, which is characterized by a relatively short half-life and surmountable antagonism. The deficiencies of this drug were likely to have been ameliorated in mouse studies by consistent delivery, via osmotic pumps and diet, leading to a persistent inhibition. AT1 receptor antagonists with enhanced pharmacological profiles, such as irbesartan and candesartan, would be preferable to test the role of AT1 receptor inhibition in humans. Indeed, it has been demonstrated recently that irbesartan significantly attenuated aortic root expansion in individuals with Marfan syndrome.(63) Conversely, ASO affords chronic and persistent inhibition of AGT synthesis to effect long term depletion of angiotensin ligands. These durable effects of ASO enables inhibition of AGT synthesis to be tested as a possible approach to reduce thoracic aortic dilation in Marfan syndrome.

Our study provided strong evidence that both AT1aR deletion and AGT depletion resulted in significant attenuation of aortic dilation and lengthening. These data are consistent with AngII signaling through AT1aR being necessary for TAA progression in male  $Fbn1^{C1041G/+}$  mice and that profound and persistent depletion of either component is sufficient to attenuate TAA. This study enables future studies to focus on cell types(s) expressing AT1aR that are stimulated to promote the disease. These studies would give great insight into the role of AT1aR on key spatial and temporal events during TAA development but would require generation of cell-specific and lineage traced AT1aR knockouts in a Marfan mouse model. Collectively, these data indicate that renin angiotensin system blockade holds promise in treating Marfan syndrome associated TAA when durable inhibition is achieved. Durable inhibition would encompass use of angiotensin receptor blockers with long half-lives and unsurmountable modes of inhibition as well as ASO based approaches.

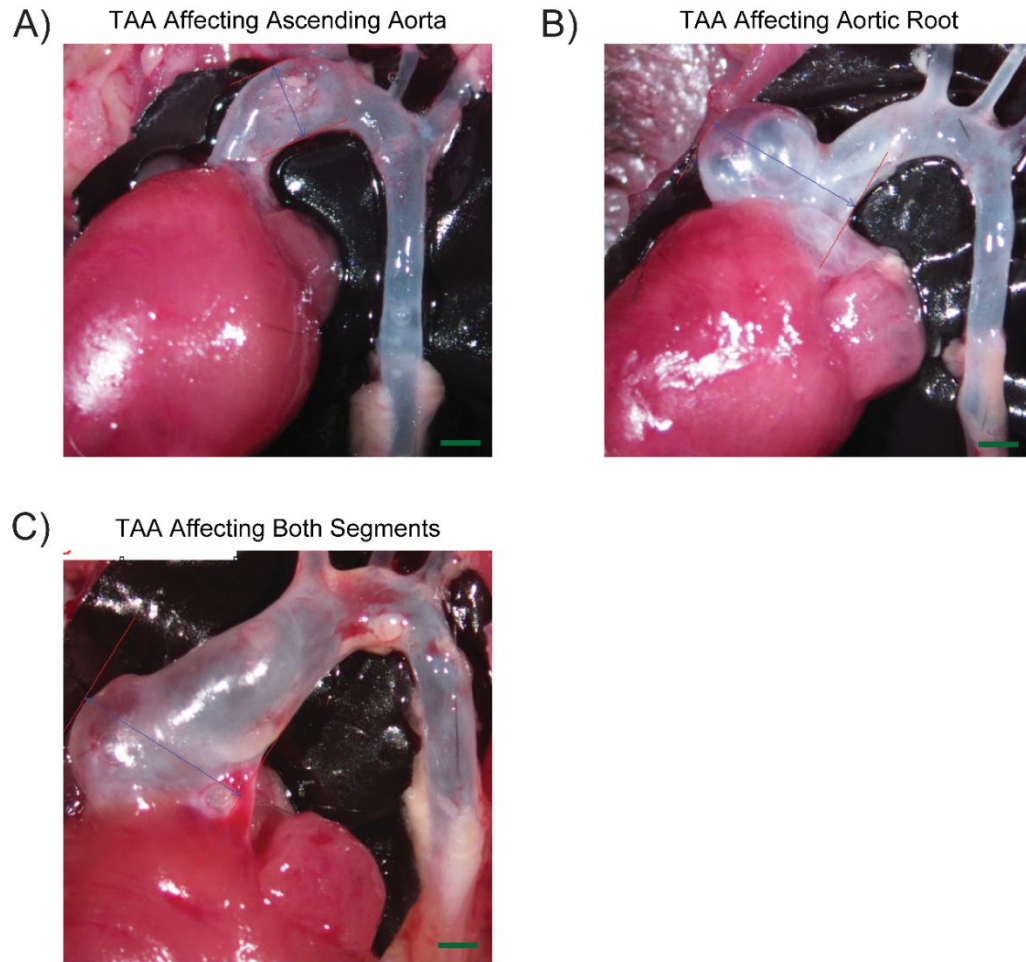


**Figure 3.1 Regional heterogeneity of TAA in  $Fbn1^{C1041G/+}$  mice**  
 TAAs in one year old  $Fbn1^{C1041G/+}$  mice have a variable phenotype of pathology location. Examples include aneurysmal presence in; **A)** ascending aorta only, **B)** aortic root only, or **C)** both segments. Green bar = 1 mm.

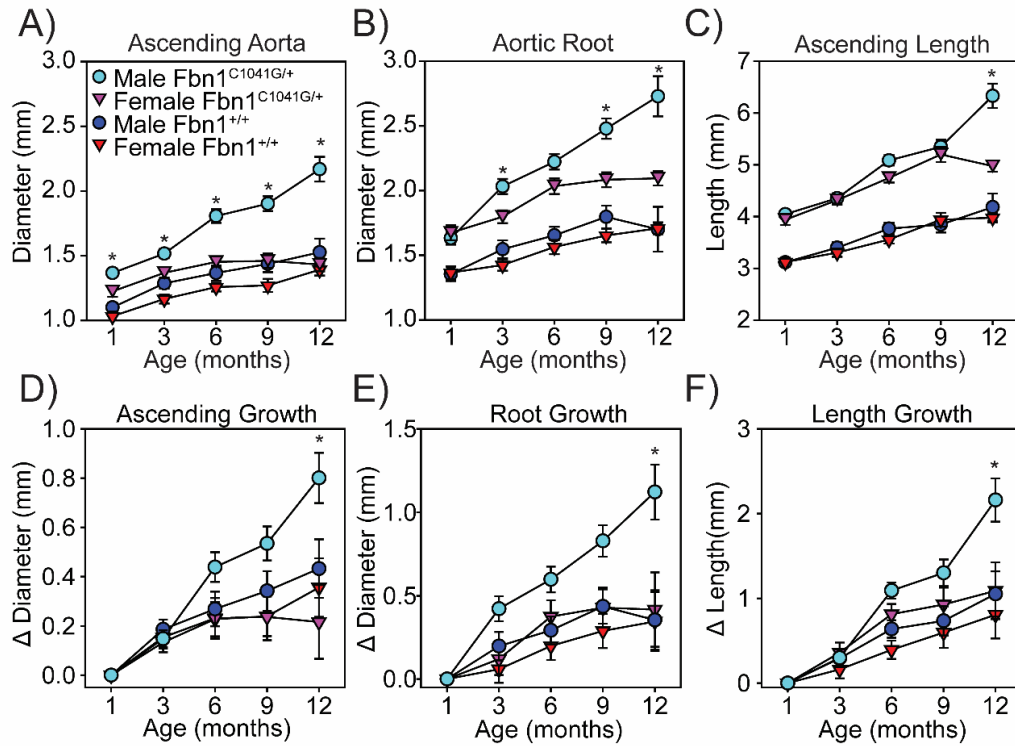


**Figure 3.2 TAA in  $Fbn1^{C1041G/+}$  mice is sexually dimorphic**

Sequential ultrasound measurements of the **A)** ascending aorta, **B)** aortic root, and **C)** aortic length in diastole from 1 month to 12 months of age of male and female  $Fbn1^{+/+}$  and  $Fbn1^{C1041G/+}$  mice. Data represented as change in dimensions over baseline at 1 month of age of the **D)** ascending aorta, **E)** aortic root, and **F)** aortic length. \*  $p < 0.05$  of male  $Fbn1^{C1041G/+}$  versus female  $Fbn1^{C1041G/+}$  mice;  $n = 9-15/\text{group}$ .



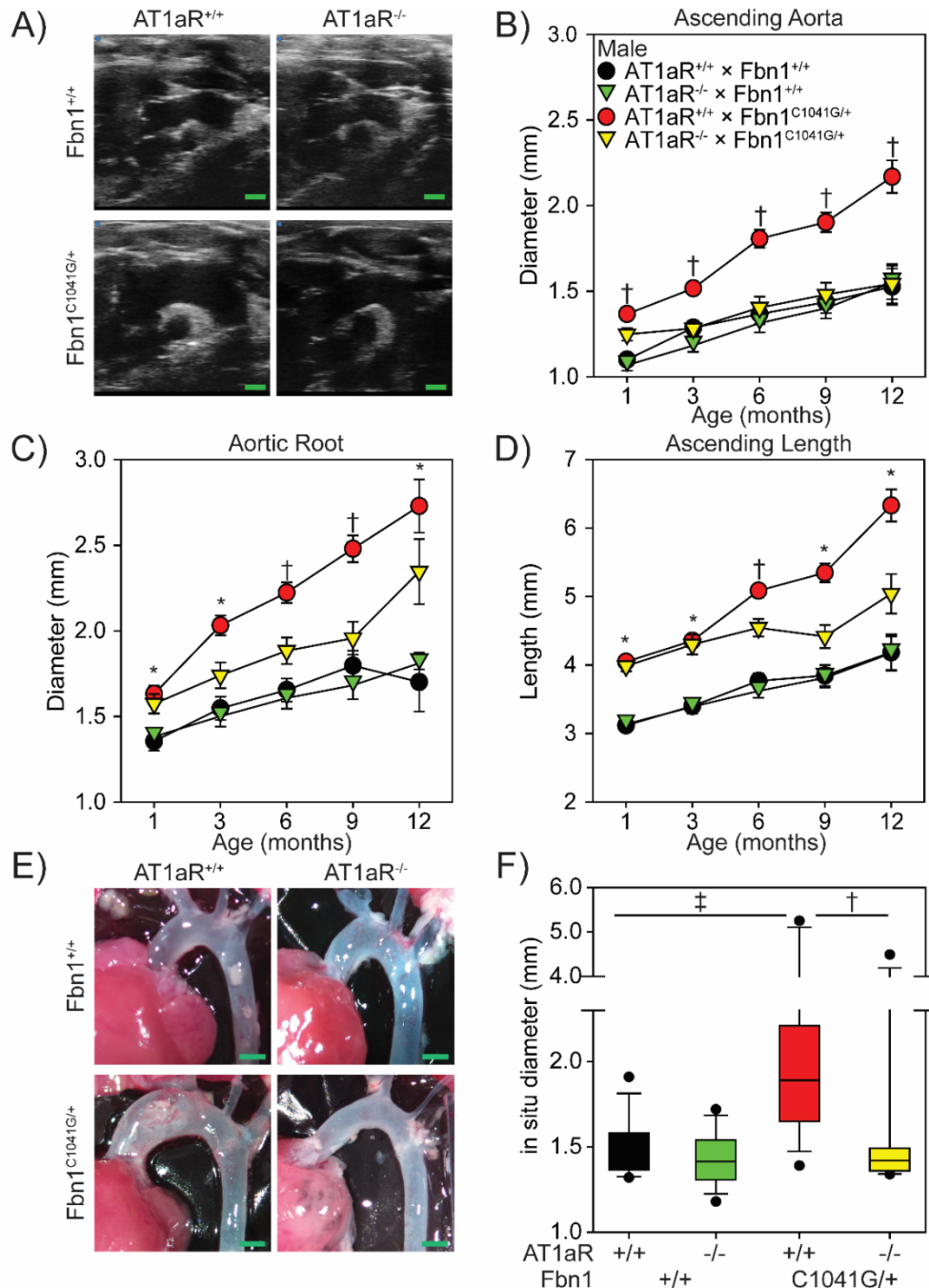


**Figure 3.3 AT1aR deletion attenuated ascending aortic dilation in male Fbn1<sup>C1041G/+</sup> mice**

**A)** Representative ultrasound images of the thoracic aorta in male AT1aR<sup>+/+</sup> x Fbn1<sup>+/+</sup>, AT1aR<sup>-/-</sup> x Fbn1<sup>+/+</sup>, AT1aR<sup>+/+</sup> x Fbn1<sup>C1041G/+</sup>, and AT1aR<sup>-/-</sup> x Fbn1<sup>C1041G/+</sup> mice. Green bar = 1 mm. Sequential ultrasound measurements of the **B)** ascending aorta **C)** aortic root and **D)** aortic length. \* p<0.05 of AT1aR<sup>+/+</sup> x Fbn1<sup>+/+</sup> versus AT1aR<sup>+/+</sup> x Fbn1<sup>C1041G/+</sup>; † p<0.05 of AT1aR<sup>+/+</sup> x Fbn1<sup>C1041G/+</sup> versus AT1aR<sup>-/-</sup> x Fbn1<sup>C1041G/+</sup>; n = 11-15/group. **E)** Representative *in situ* images of the thoracic aorta. **F)** Measurement of *in situ* aortic dimensions taken at the maximal aortic diameter. † p<0.01; ‡ p<0.001; n = 10-15 / group.

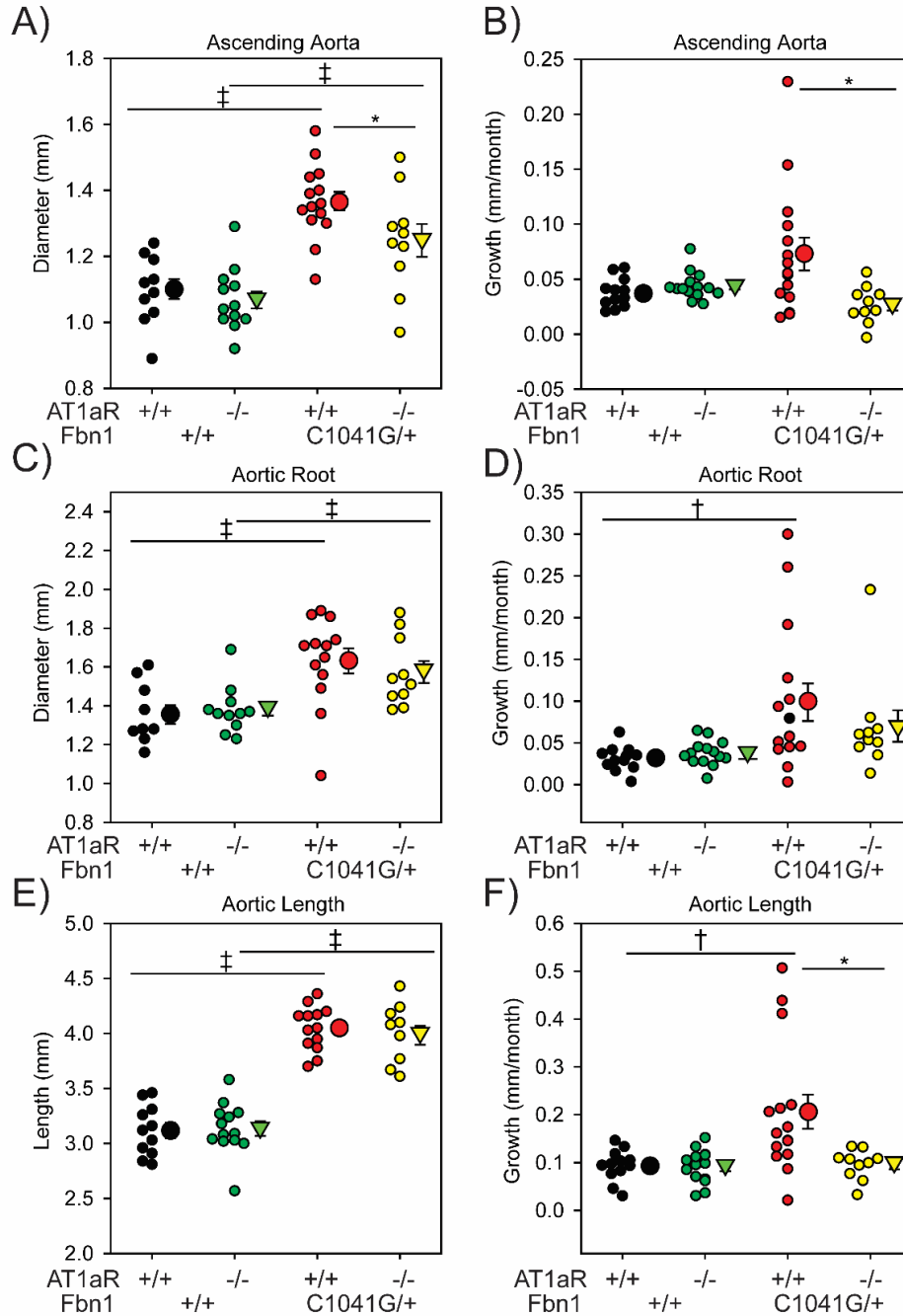


**Figure 3.4 Aortic dimensions at 1 month of age and aortic growth in male mice**

Ultrasound measurements of the **A)** ascending aorta, **C)** aortic root, and **E)** aortic length in diastole at 1 month of age from male AT1aR<sup>+/+</sup> x Fbn1<sup>+/+</sup>, AT1aR<sup>-/-</sup> x Fbn1<sup>+/+</sup>, AT1aR<sup>+/+</sup> x Fbn1<sup>C1041G/+</sup>, and AT1aR<sup>-/-</sup> x Fbn1<sup>C1041G/+</sup> mice. Mean monthly ascending **B)** ascending aorta growth, **D)** aortic root growth, and **F)** aortic length growth from 1 month to 12 months in male AT1aR<sup>+/+</sup> x Fbn1<sup>+/+</sup>, AT1aR<sup>-/-</sup> x Fbn1<sup>+/+</sup>, AT1aR<sup>+/+</sup> x Fbn1<sup>C1041G/+</sup>, and AT1aR<sup>-/-</sup> x Fbn1<sup>C1041G/+</sup> mice. \* p<0.05, † p<0.01, ‡ p<0.001; n = 11-15/group.

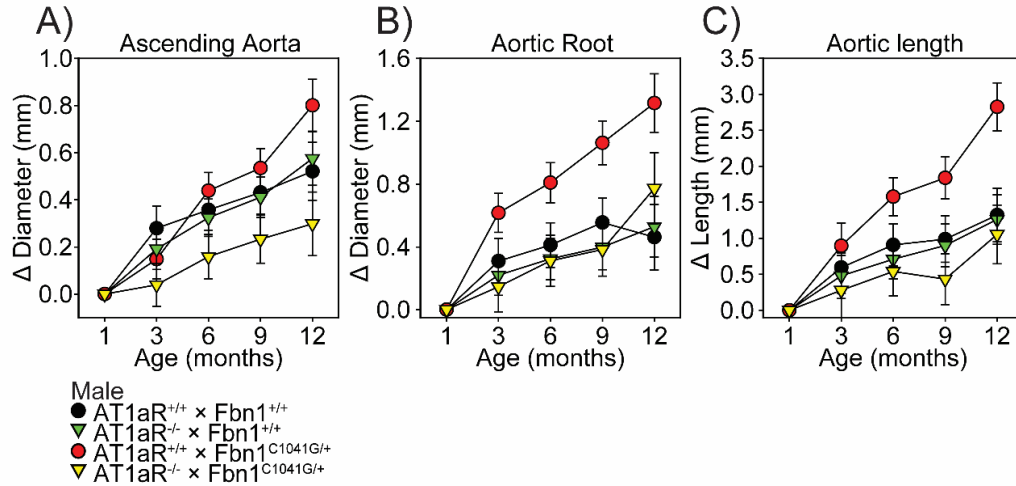


**Figure 3.5 Growth from 1 month of age in male AT1aR deficient, Fbn1<sup>C1041G/+</sup> mice**

Data are represented as change in dimensions over the measurement at 1 month of age of the **A)** ascending aorta, **B)** aortic root, and **C)** aortic length. \* p<0.05 of AT1aR<sup>+/+</sup> x Fbn1<sup>C1041G/+</sup> versus AT1aR<sup>-/-</sup> x Fbn1<sup>C1041G/+</sup>; n = 11-11/group.

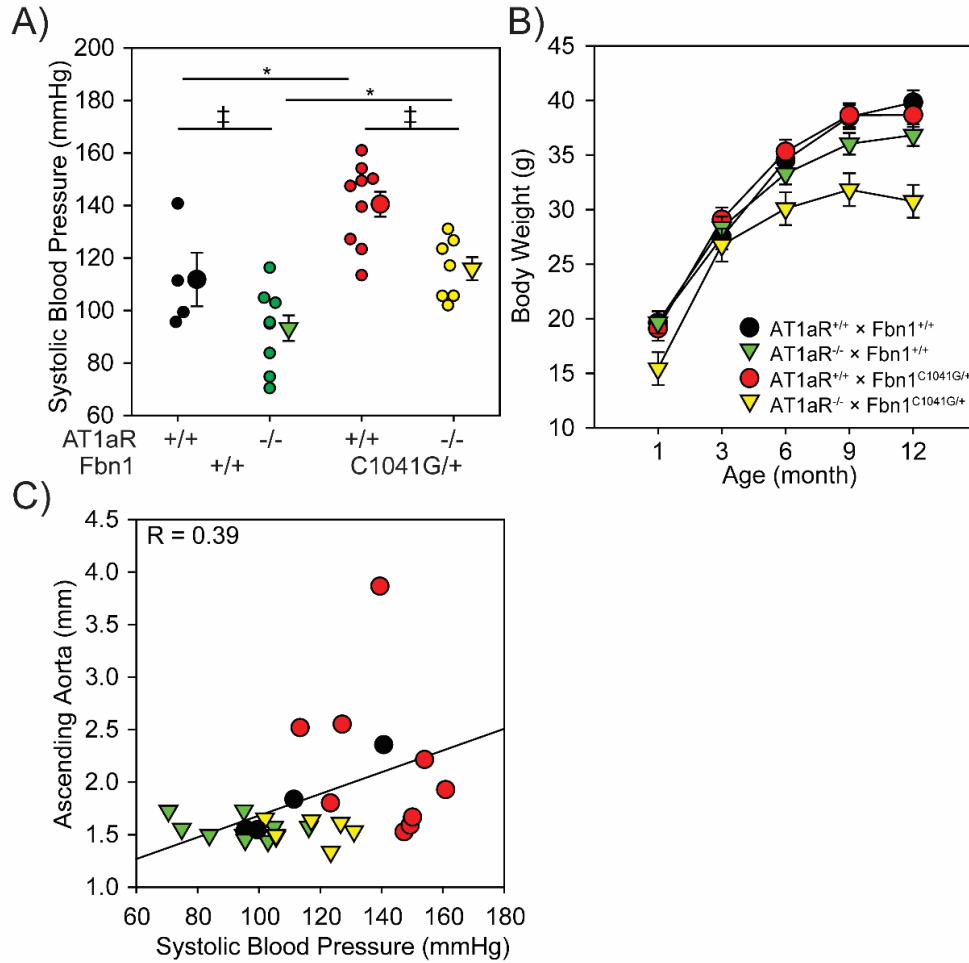


**Figure 3.6 Confounding factors did not contribute to TAA phenotype in male Fbn1<sup>C1041G/+</sup> mice**

**A)** Systolic blood pressure measured by a tail cuff based technique in 12 month old male mice. \* p < 0.05, † p < 0.01, ‡ p < 0.001; n = 5-10/group. **B)** Sequential body weight of male mice. **C)** Correlation between systolic blood pressure and aortic diameters at 12 months of age between male mice. n = 5-10/group. Black = AT1aR<sup>+/+</sup> × Fbn1<sup>+/+</sup>, green = AT1aR<sup>-/-</sup> × Fbn1<sup>+/+</sup>, red = AT1aR<sup>+/+</sup> × Fbn1<sup>C1041G/+</sup>, and yellow = AT1aR<sup>-/-</sup> × Fbn1<sup>C1041G/+</sup>.

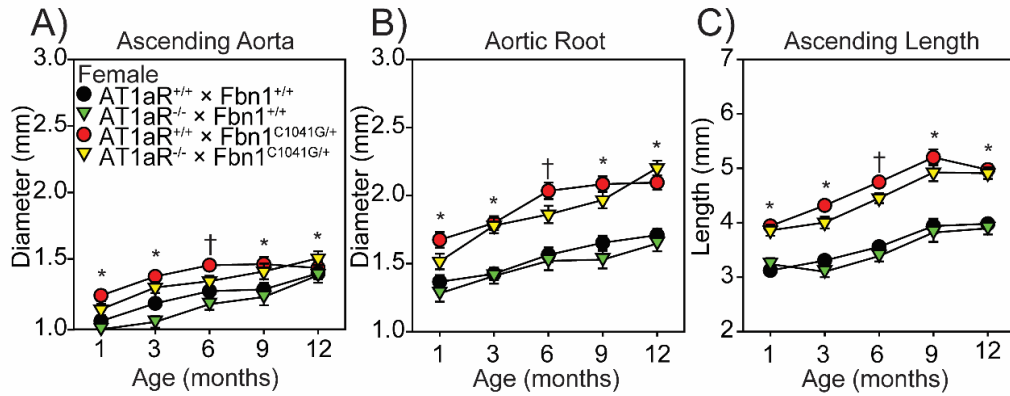


**Figure 3.7 AT1aR deletion had no effect on aortic measurements in female Fbn1<sup>C1041G/+</sup> mice**

Sequential ultrasound measurements of the; **A)** ascending aorta, **B)** aortic root, and **C)** aortic length in diastole from 1 month to 12 months of age of female AT1aR<sup>+/+</sup> x Fbn1<sup>+/+</sup>, AT1aR<sup>-/-</sup> x Fbn1<sup>+/+</sup>, AT1aR<sup>+/+</sup> x Fbn1<sup>C1041G/+</sup>, and AT1aR<sup>-/-</sup> x Fbn1<sup>C1041G/+</sup> mice. \* p<0.05 of AT1aR<sup>+/+</sup> x Fbn1<sup>+/+</sup> versus AT1aR<sup>+/+</sup> x Fbn1<sup>C1041G/+</sup>; † p<0.05 of AT1aR<sup>+/+</sup> x Fbn1<sup>C1041G/+</sup> versus AT1aR<sup>-/-</sup> x Fbn1<sup>C1041G/+</sup>; n = 7-11/group.

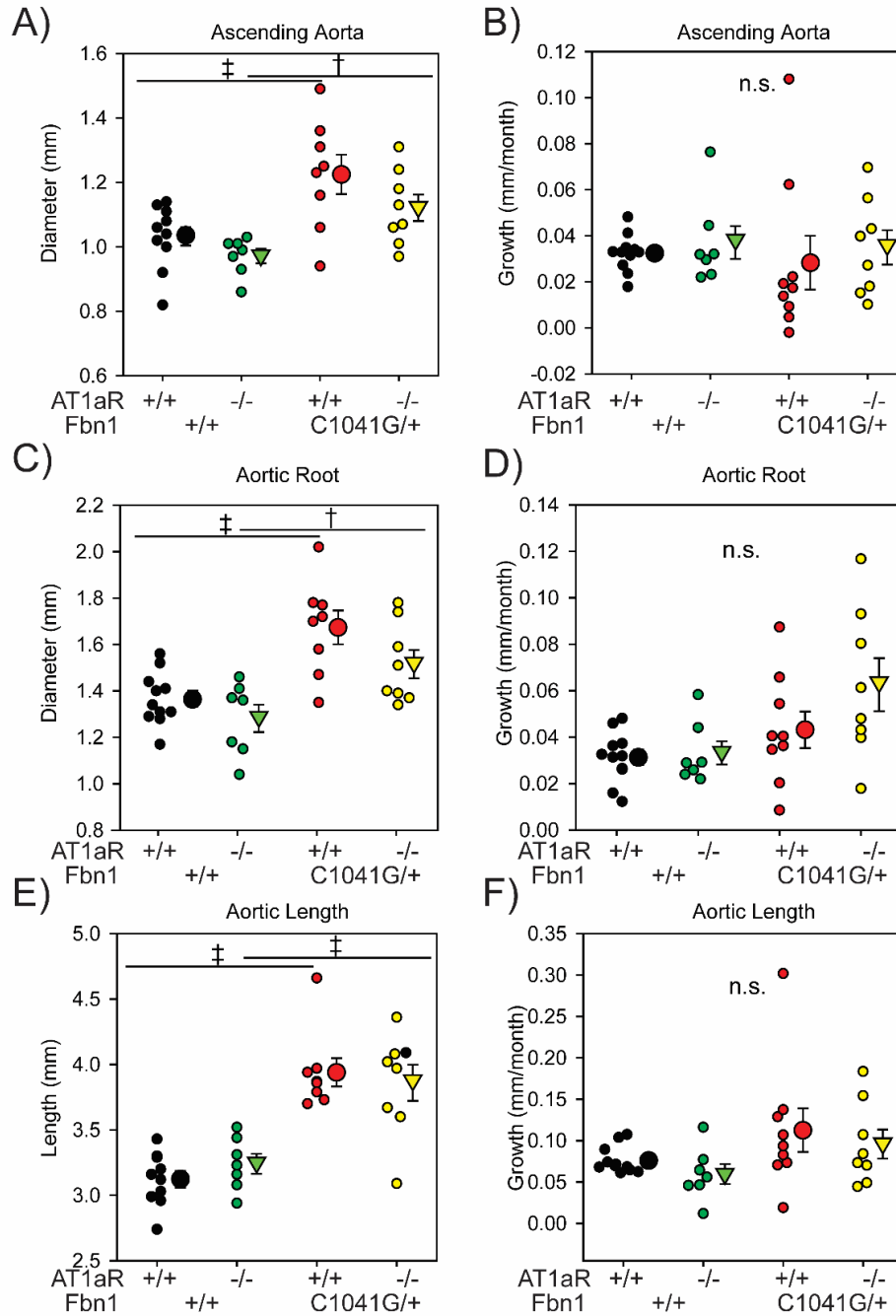


**Figure 3.8 Aortic dimensions at 1 month of age and aortic growth in female mice**

Ultrasound measurements of the; **A)** ascending aorta, **C)** aortic root, and **E)** aortic length in diastole at 1 month of age from female AT1aR<sup>+/+</sup> x Fbn1<sup>+/+</sup>, AT1aR<sup>-/-</sup> x Fbn1<sup>+/+</sup>, AT1aR<sup>+/+</sup> x Fbn1<sup>C1041G/+</sup>, and AT1aR<sup>-/-</sup> x Fbn1<sup>C1041G/+</sup> mice. Mean monthly ascending **B)** ascending aorta growth, **D)** aortic root growth, and **F)** aortic length growth from 1 month to 12 months in female AT1aR<sup>+/+</sup> x Fbn1<sup>+/+</sup>, AT1aR<sup>-/-</sup> x Fbn1<sup>+/+</sup>, AT1aR<sup>+/+</sup> x Fbn1<sup>C1041G/+</sup>, and AT1aR<sup>-/-</sup> x Fbn1<sup>C1041G/+</sup> mice. \* p < 0.05, † p < 0.01, ‡ p < 0.001; n = 7-11/group.

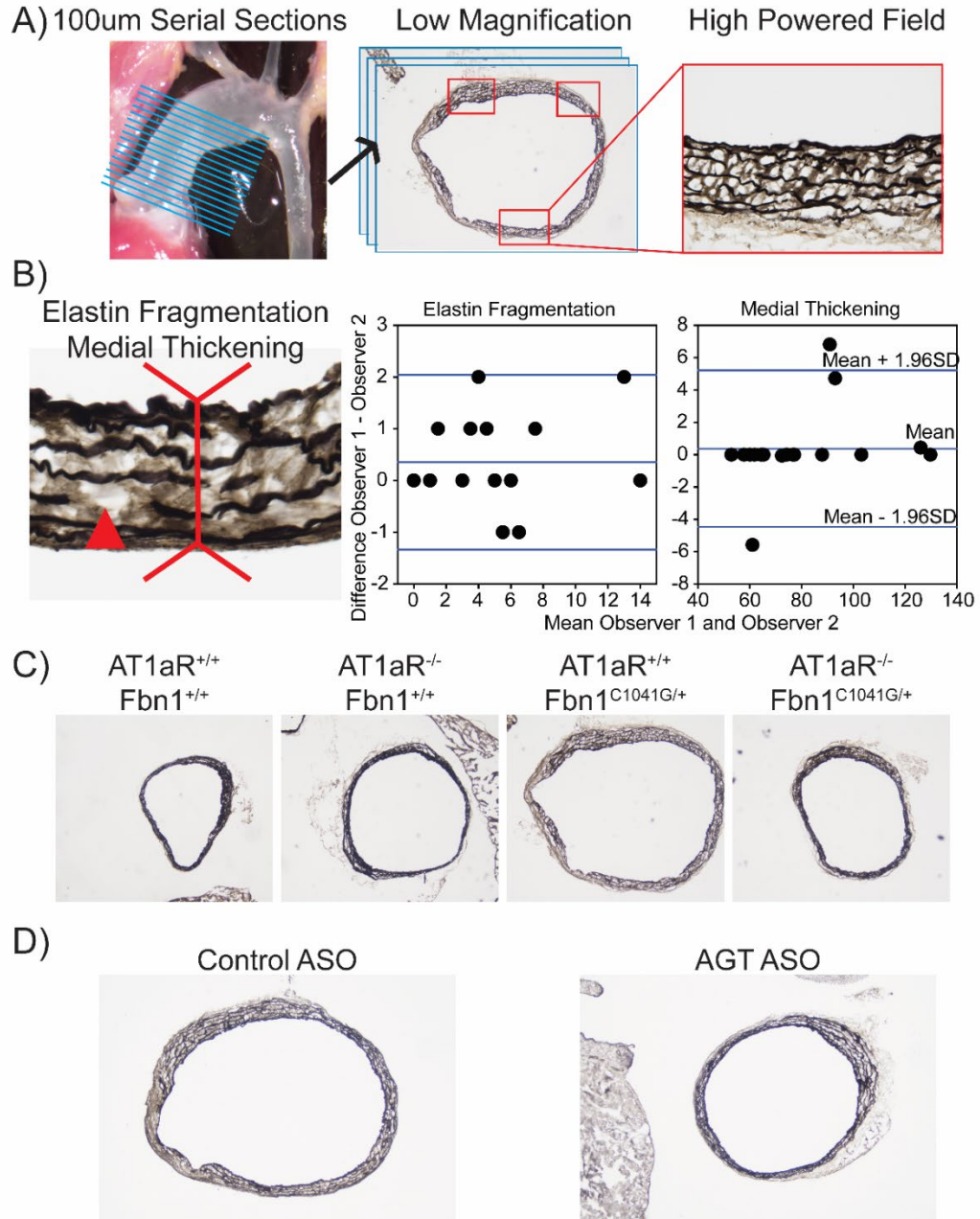


**Figure 3.9 Generation of ascending aortic sections to measure elastin fragmentation and medial thickening**

**A)** Generation of serial sections of ascending aortas used for histology. (blue lines) Three high powered fields / section were imaged and quantified per biological replicate. (red boxes) **B)** Quantification of elastin fragmentation (triangle) and medial thickening (inverted double arrow) by two independent observers demonstrated good agreement in both measures via Bland-Altman analysis. **C)** Low magnification images of aortic sections stained with Verhoeff elastin stain in 12 month old male AT1aR<sup>+/+</sup> x Fbn1<sup>+/+</sup>, AT1aR<sup>-/-</sup> x Fbn1<sup>+/+</sup>, AT1aR<sup>+/+</sup> x Fbn1<sup>C1041G/+</sup>, and AT1aR<sup>-/-</sup> x Fbn1<sup>C1041G/+</sup> mice. **D)** Low magnification images of aortic sections stained with Verhoeff elastin stain in 8 month old male Fbn1<sup>C1041G/+</sup> mice after 6 months of control ASO or AGT ASO.

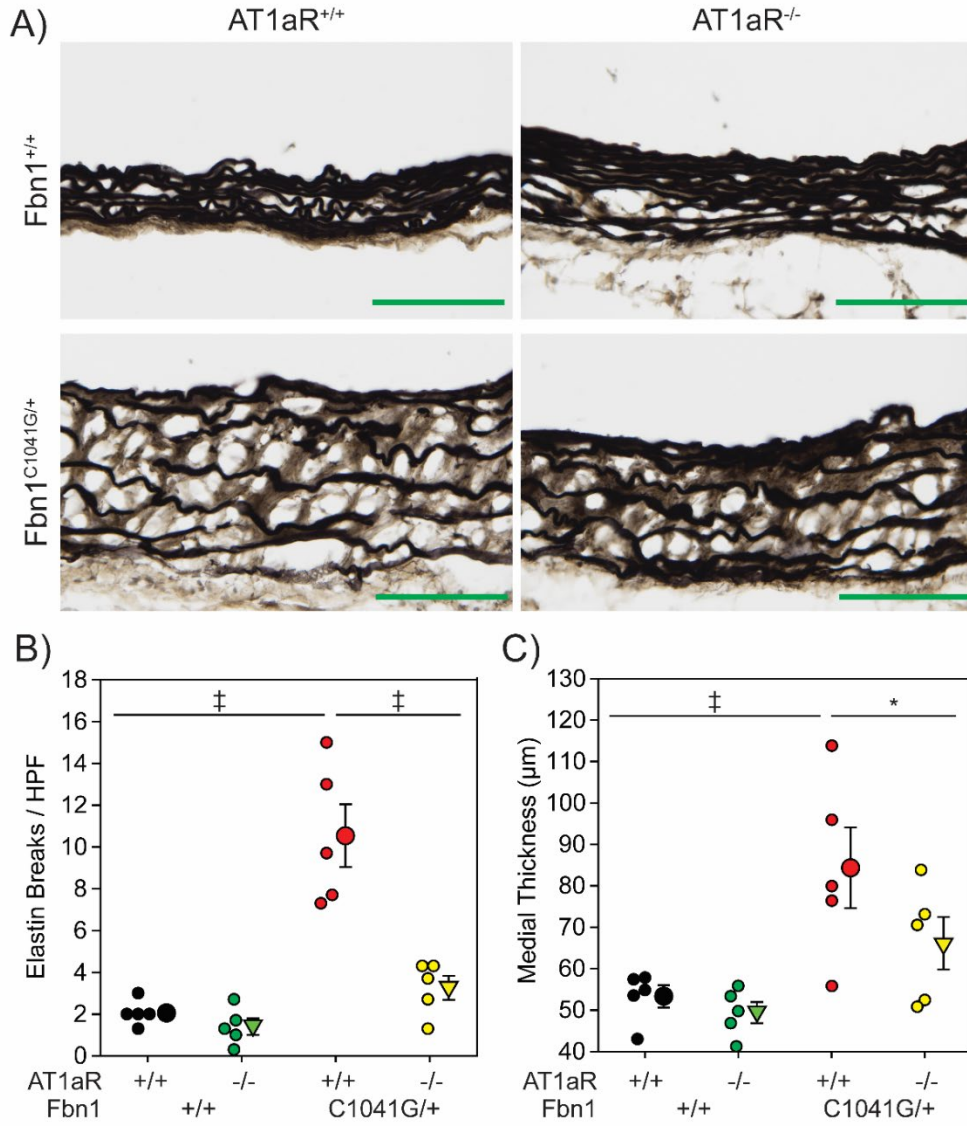


**Figure 3.10 AT1aR deletion attenuated medial remodeling in male Fbn1<sup>C1041G/+</sup> mice**

**A)** Representative images of Verhoeff's elastin staining in ascending aortic sections from male AT1aR<sup>+/+</sup> x Fbn1<sup>+/+</sup>, AT1aR<sup>-/-</sup> x Fbn1<sup>+/+</sup>, AT1aR<sup>+/+</sup> x Fbn1<sup>C1041G/+</sup>, and AT1aR<sup>-/-</sup> x Fbn1<sup>C1041G/+</sup> mice. Green bar = 100 μm. **B)** Number of breaks per high powered field detected in aortic sections. **C)** Medial thickness as measured by the distance between the inner elastic lamina and external elastic lamina in aortic sections. \* p<0.05, ‡ p<0.001; n = 5/group.



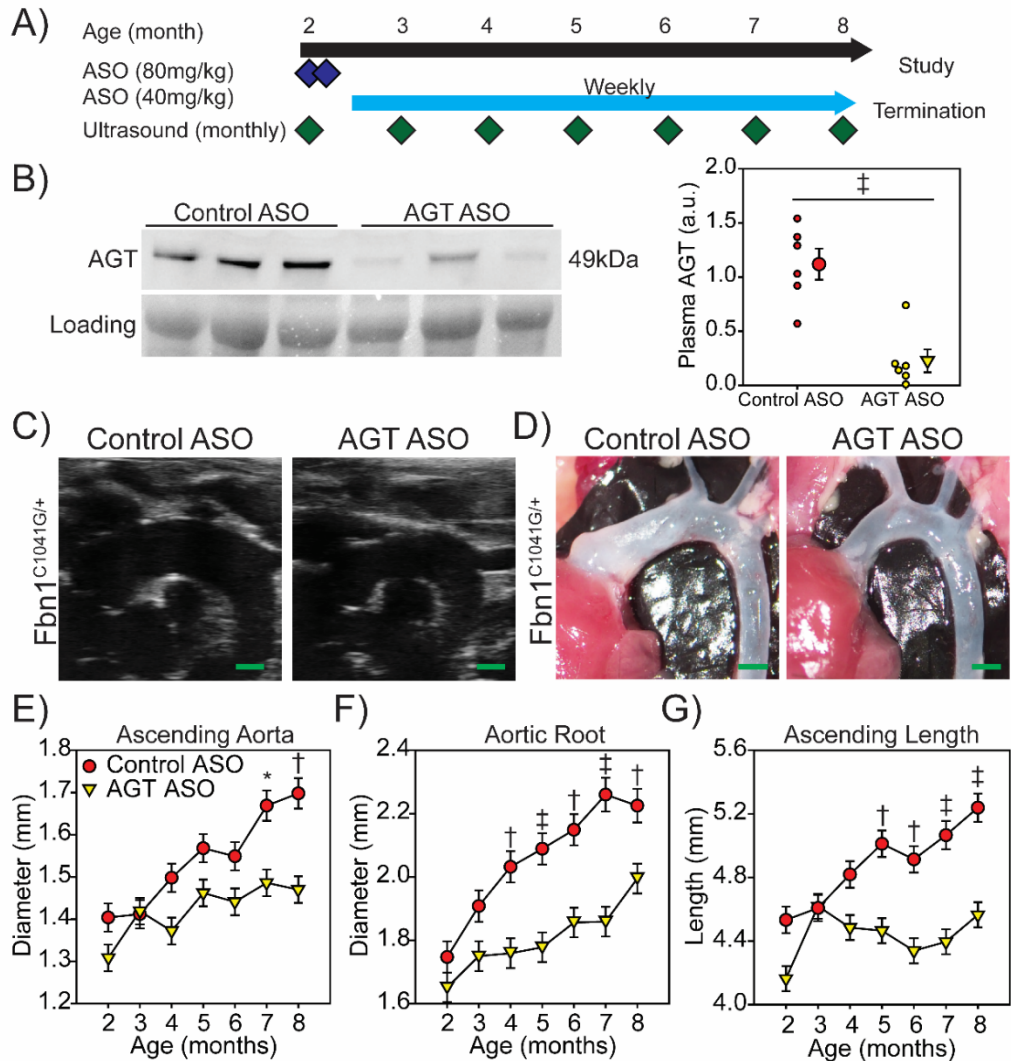


**Figure 3.11 AGT ASOs depleted AGT and attenuated TAA in male  $Fbn1^{C1041G/+}$  mice**

**A)** Study design and administration schedule of ASOs in male  $Fbn1^{C1041G/+}$  mice. A loading dose of control ASO or AGT ASO (80 mg/kg) was administered day 1 and 4 of study. Maintenance doses of control ASO or AGT ASO (40 mg/kg) was administered every 7 days. **B)** Western blot of plasma AGT and total plasma protein in 8 month old male  $Fbn1^{C1041G/+}$  mice administered either control ASO or AGT ASOs. Blot represents one of two experiments. ‡  $p < 0.001$ ;  $n = 6$ /group. Representative **C)** ultrasound and **D)** *in situ* images of aortas from 8 month old  $Fbn1^{C1041G/+}$  mice administered either control ASO or AGT ASO. Green bar = 1 mm. Sequential ultrasound measurements of the **E)** ascending aorta, **F)** aortic root, and **G)** aortic length in diastole from 2 months to 8 months of age in male  $Fbn1^{C1041G/+}$  mice dosed with either control ASO or AGT ASO. \*  $p < 0.05$ , †  $p < 0.01$ , ‡  $p < 0.001$ ;  $n = 8-10$ /group.

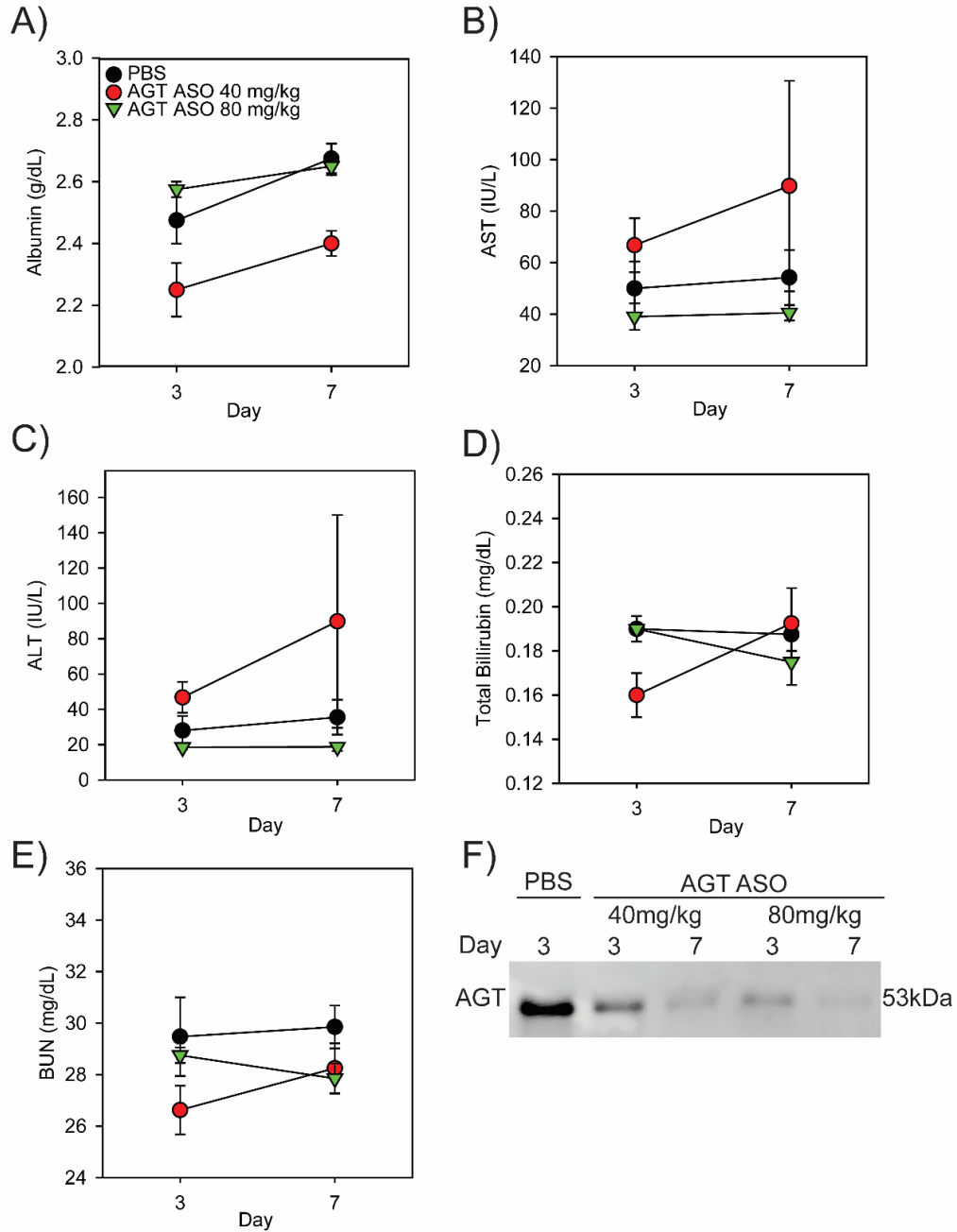


**Figure 3.12 AGT ASOs have low toxicity and effectively reduce circulating AGT**

Plasma concentrations of; **A)** albumin, **B)** alanine transaminase (AST), **C)** aspartate aminotransferase (ALT), **D)** total bilirubin **E)** blood urea nitrogen (BUN) in mice administered either PBS, AGT ASO (40 mg/kg), or AGT ASO (80 mg/kg) at days 1 and 4. Plasma was taken at days 3 and 7. n = 4/group. **F)** Plasma AGT concentrations at days 3 and 7 detected by Western blotting after AGT ASO was administered at days 1 and 4.

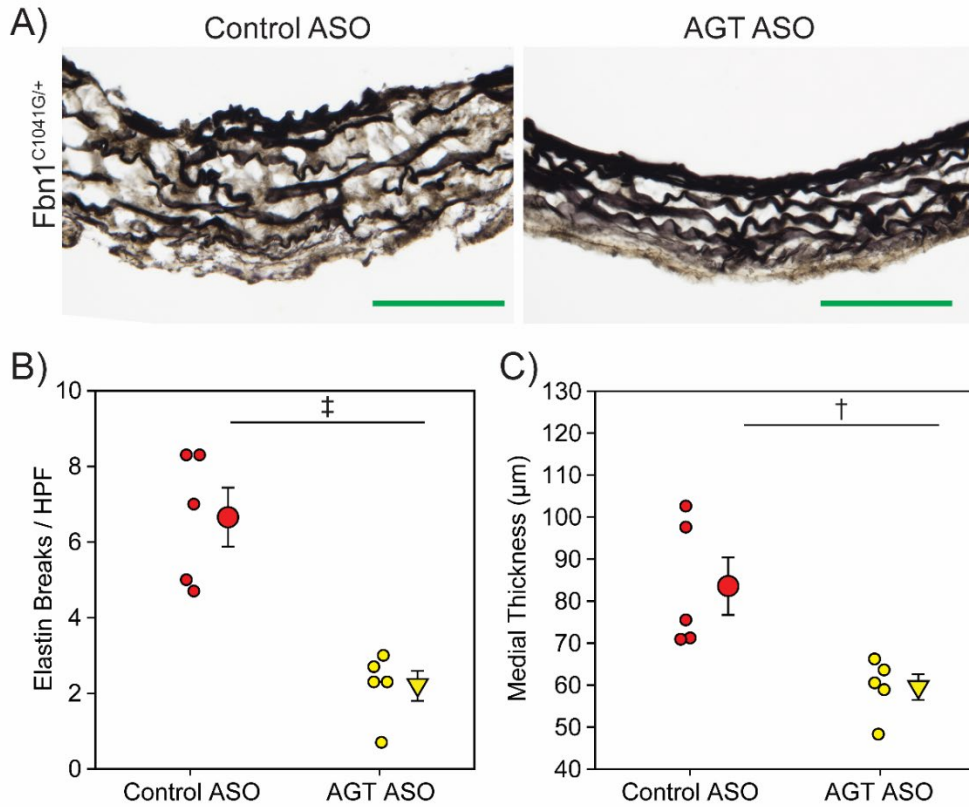


**Figure 3.13 AGT ASOs attenuated medial remodeling in male *Fbn1*<sup>C1041G/+</sup> mice**

**A)** Representative images of Verhoeff's elastin staining in aortic sections from male *Fbn1*<sup>C1041G/+</sup> mice administered either control ASO or AGT ASO for 6 months. Green bar = 100  $\mu$ m. **B)** Number of breaks per high powered field detected in aortic sections. **C)** Medial thickness as measured by the distance between the inner elastic lamina and external elastic lamina in aortic sections. †  $p < 0.01$ , ‡  $p < 0.001$ ;  $n = 5$ /group.

## CHAPTER 4. ENDOGENOUS SEX HORMONE REMOVAL ATTENUATES ACQUIRED THORACIC AORTIC ANEURYSMS

This chapter is based on a publication in preparation titled “Endogenous Sex Hormone Removal Attenuates Acquired Thoracic Aortic Aneurysms” detailing findings that endogenous sex hormone removal attenuates spontaneous but not syndromic thoracic aortic aneurysms.

### 4.1 Synopsis

#### Objective:

Thoracic aortic aneurysm (TAA) of various etiologies have been shown to be sexually dimorphic. In general, sexually mature females have higher levels of circulating estrogens and males have higher levels of circulating androgens. These endogenous sex hormones may remodel tissue. Here, we investigate the impact of removing endogenous sex hormones on TAA development in the angiotensin II (AngII)-infused mouse model of acquired TAA and the fibrillin-1 hypomorphic (FBN1<sup>mgR/mgR</sup>) mouse model of syndromic TAA.

#### Approach and Results:

In situ aortic diameter measurements demonstrated that both male AngII-infused and FBN1<sup>mgR/mgR</sup> mice exhibited increased aortic dimensions compared to their female counterparts. Ovariectomy in female and orchietomy in male mice was employed to remove endogenous estrogen and testosterone, respectively. In AngII-infused females, ovariectomy exacerbated ascending aortic dilation. In AngII-infused males, orchietomy abrogated aortic root and ascending aortic dilation. Gonadectomy failed to modulate established TAA in FBN1<sup>mgR/mgR</sup> mice. AngII-induced ascending aortic elastin fragmentation was exacerbated in ovariectomized females and attenuated in orchietomized males. There was no effect of gonadectomy on FBN1<sup>mgR/mgR</sup> mice with established TAA. Furthermore, expression of  $\alpha$ -smooth muscle actin in the aortic media were altered by removal of endogenous sex hormones.

#### Conclusions:

AngII-induced TAA in mice was exacerbated by ovariectomy of female mice and ameliorated by orchietomy of male mice. This effect was not seen in female or male mice with established TAA. These data indicate that endogenous estrogens are protective against and endogenous androgens are detrimental to the development of TAA but may have limited effect on reversing established, syndromic TAA.

## 4.2 Introduction

Previous observational studies in patients with Marfan syndrome demonstrated that males displayed greater aortic dilation and were more likely to require aortic repair compared to their female counterparts.(157) However, observational studies in human TAAs reveal that female patients have worse outcomes associated with increased aortic stiffness. (158) It is unclear how sexual dimorphism in TAA occurs and why females resist TAA while males are susceptible to TAA. However, females generally have higher concentrations of circulating estrogens and males generally have higher concentrations of circulating androgens. In fact, changes in 17 $\beta$ -estradiol during pregnancy impact Marfan syndrome associated TAA.(56) Thus differences in sex hormones may contribute to sexual dimorphism of TAAs.

To study both acquired and syndromic TAA, we utilized two models with divergent etiologies. First described by our group, the AngII infusion mouse model is a widely used model of acquired TAA.(37) TAA in this mouse model occurs through the action of AngII on AT1a receptors.(28) The FBN1<sup>mgR/mgR</sup> Marfan syndrome mouse model aggressively develops TAA early in the perinatal period and exhibits death by aortic rupture. (12) Previous work in LDL receptor<sup>-/-</sup> x AngII-induced abdominal aortic aneurysms revealed that having a female sex chromosome complement and exposure to endogenous female sex hormone attenuates initiation, progression, and extent of abdominal aortic aneurysms. (159-161) As both the AngII-induced and FBN1<sup>mgR/mgR</sup> mouse models occur without underlying hypercholesterolemia and hyperlipidemia, it is unclear if removal of endogenous sex hormones affects the thoracic aorta in the same manner as the abdominal aorta.

Based on the literature, we hypothesized that sexual dimorphism exists in mouse models of acquired and syndromic TAA. Furthermore, we hypothesized that female mice were protected from TAA due to their exposure to estrogens and that males were more susceptible to TAA due to their exposure to androgens. Based on our previous work, we hypothesized that these changes were also reflected in degradation or preservation of aortic medial structure. To test these hypotheses, we first measured aortic diameters in male and female mice of both AngII-infused and FBN1<sup>mgR/mgR</sup> mice compared to natural sexual dimorphism in non-TAA, vehicle treated or wild type littermates. We then investigated the effect of removing endogenous sex hormones, before sexual maturity, on TAA development and progression. In addition to measuring aortic dilatation, we also characterized the medial structure of the aorta to determine if removing endogenous sex hormones directly impacted aortic tissue structure and function by preserving elastin structure and vascular smooth muscle cell contractile phenotype.

### 4.3 Methods

#### *Mice*

Female and male C57BL/6J (stock #000664) mice were obtained from The Jackson Laboratory (Bar Harbor, ME). FBN1<sup>mgR/mgR</sup> mice (stock #005704) were obtained from The Jackson Laboratory (Bar Harbor, ME) and bred in house. Female and male FBN1<sup>mgR/mgR</sup> mice and their wild type littermates were generated by F1 cross of female and male FBN1<sup>mgR/+</sup> mice. To induce acquired TAA, C57BL/6J mice were infused with 1000ng/kg/min AngII (Bachem H-1705, Lot 1046885) for 28 days by osmotic minipump (Alzet 1004, Lot 10217-08). Mice were housed up to 5/cage and maintained on a 14:10 light:dark cycle. Mice were fed Teklad Irradiated Global 18% Protein Rodent Diet # 2918 ad libidum and allowed ad libidum access to water via a Lixit system. Bedding was provided by P.J. Murphy (Coarse SaniChip) and changed weekly during the study. Shreddable cotton pads were provided as enrichment. The room temperature was set at 22°C throughout the study. The room was also set at 50% humidity. All mice survived to end of study. All protocols were approved by the University of Kentucky IACUC.

#### *Gonadectomy*

Gonadectomies were performed at 6 weeks of age in AngII TAA studies and 8 weeks of age in FBN1<sup>mgR/mgR</sup> mice according to established protocols.(159, 161) Mice were allowed to recover for two weeks before AngII infusion. Post termination, female uteri and male seminiferous vesicles were dissected free and preserved in 10% formalin. Remaining gonads were weighed.

#### *Ultrasound measurements*

Mice were anesthetized and maintained at a heart rate of 450-550 beats per minute. Ultrasound images were captured using a Vevo 3100 system with a 40 MHz transducer according to published protocols.(34, 134) Images captured were standardized according to two anatomical landmarks: the innominate artery branch point and aortic valves. The largest luminal ascending aortic diameter between the sinotubular junction and the innominate artery were measured in mid-systole and end-diastole by two blinded, independent observers.

#### *Histology*

The three ascending aortas per group, as determined by the group median aortic diameter, were selected and fresh frozen sections were generated. Tissue sections (10 µm) were generated from the aortic root to the aortic arch at 100 µm intervals. The section corresponding to the region of largest dilation between the sinotubular junction and the arch were analyzed. Briefly, elastin was visualized by Verhoeff elastin staining under 20x magnification. Three images per section were taken. Fragmentation was defined as the presence of discernable

breaks of continuous elastin lamina. Elastin breaks per high powered field were counted. Medial thickening was measured using NIS-Elements AR software (Nikon). Measurements were verified by an independent investigator who was blinded to the sample group. To detect  $\alpha$ -smooth muscle actin, slides were fixed with acetone for 15 minutes at room temperature; blocked with non-immune goat serum (15 $\mu$ L/mL, sigma G9023); incubated with anti  $\alpha$ -smooth muscle actin (10 $\mu$ g/mL, abcam #ab5694) for 15 minutes at 40°C; incubated with biotinylated goat anti rabbit IgG (2  $\mu$ g/mL, vector #BA1000) for 15 minutes at 40°C; developed with AEC (Vector #PK6100 and #SK4205).

### Statistics

Mice were randomized to sham or gonadectomy and to saline or AngII pump. FBN1<sup>mgR/mgR</sup> mice were randomly housed with their wild type littermates. Primary data were assessed and then verified by an independent observer blinded to group. Statistical analyses were performed using SigmaPlot. Equal variance and normality of data determined whether parametric, non-linear transformation followed by parametric, or non-parametric tests were used. Two-way ANOVA was performed and Holm-Sidak post-hoc test was used. Data are represented as individual data points, mean  $\pm$  SEM, or median with interquartile range as appropriate.

## 4.4 Results

### *Sexual dimorphism is observed in both AngII-induced and FBN1<sup>mgR/mgR</sup> mouse models of thoracic aortic aneurysms.*

We first noticed sexual dimorphism in our thoracic aortic aneurysm mouse models due to an inability to elicit severe aortic dilation in female mice. Thus, we investigated the aortic phenotype of female and male littermates to quantify the degree of sexual dimorphism in our TAA mouse models.

To determine if sexual dimorphism existed in an acquired model of TAA, we infused AngII into male and female C57BL/6J mice for 28 days. At the end of 28 days, we dissected the aortas in situ and measured the dimensions of the ascending aorta. (**Figure 4.1**). Male mice exhibited greater thoracic aortic dilation after AngII infusion compared to their female littermates. (Female = 1.42  $\pm$  0.04 mm, male = 1.70  $\pm$  0.05 mm;  $p < 0.001$ ) Interestingly, saline infused mice did not exhibit sexual dimorphism. (Female = 1.22  $\pm$  0.04 mm, male = 1.35  $\pm$  0.04 mm;  $p = 0.052$ ). During this study, 1/11 male AngII-infused mice expired due to aortic rupture. Cause of death verified by necropsy; all others survived to study termination. (**Figure 4.1**)

Next, to determine if sexual dimorphism existed in a syndromic model of TAA, we generated female and male FBN1<sup>mgR/mgR</sup> littermates and measured their ascending aortic dimension at 120 days. (**Figure 4.1**). Survivors were terminated and ex vivo aortic diameters were measured. Male FBN1<sup>mgR/mgR</sup> mice exhibited

greater thoracic aortic dilation compared to their female littermates. (Female =  $1.54 \pm 0.09$  mm, male =  $1.97 \pm 0.08$  mm;  $p = 0.008$ ) Wild type mice did not exhibit sexual dimorphism. (Female =  $1.18 \pm 0.09$  mm, male =  $1.15 \pm 0.07$  mm;  $p = 0.81$ ) (**Figure 4.1**) 6/21 male FBN1<sup>mgR/mgR</sup> mice and 3/18 female FBN1<sup>mgR/mgR</sup> mice died due to TAA rupture. (**Figure 4.1**)

*Removal of endogenous sex hormones modulates AngII induced acquired thoracic aortic aneurysm model.*

As endogenous sex hormones play a role in aortic remodeling, we investigated the effect of sex hormone removal in the AngII-induced acquired thoracic aortic aneurysm model. We performed gonadectomy of male and female C57BL/6J at 8 weeks of age, allowed two weeks to recover, then induced TAA by AngII-infusion for 28 days. (**Figure 4.2**) Ovariectomy of female mice and orchietomy of male mice reduced levels of endogenous sex hormones, leading to secondary sex organ atrophy. (**Figure 4.3**) We then used high frequency ultrasound to measure the ascending aorta and aortic root dimensions in vivo of female and male mice. (**Figure 4.2**) Confounding features such as blood pressure and body weight did not correlate with aortic diameters in either female or male mice infused with AngII. (**Figure 4.4 and 4.5**)

Gonadectomy exacerbated TAA in female mice and attenuated TAA in male mice. Female mice infused with AngII and subjected to sham surgery showed significant dilation after 4 weeks of AngII (Ascending aorta: Sham Saline =  $1.16 \pm 0.03$  mm versus Sham AngII =  $1.30 \pm 0.03$  mm;  $p = 0.004$ ), demonstrating that TAA was established. However, dilation was increased in ovariectomized female mice (Ascending aorta: OVX Saline =  $1.23 \pm 0.03$  mm versus OVX AngII =  $1.42 \pm 0.03$  mm;  $p < 0.001$ ). Ovariectomy of AngII infused female mice exacerbated ascending aortic dilation ( $p = 0.007$ ). (**Figure 4.2**) Male mice subject to sham surgery were also susceptible to ascending aortic dilation after AngII infusion and showed significant dilation after 4 weeks of AngII (Ascending aorta: Sham Saline =  $1.27 \pm 0.04$  mm versus Sham AngII =  $1.53 \pm 0.04$  mm;  $p < 0.001$ ). However, ascending aortic dilation was not seen in orchietomized males infused with AngII (Ascending aorta: ORCH Saline =  $1.27 \pm 0.04$  mm versus ORCH AngII =  $1.36 \pm 0.04$  mm;  $p = 0.12$ ). Orchietomized males infused with AngII demonstrated attenuated ascending aortic dilation ( $p = 0.004$ ). (**Figure 4.2**)

Interestingly, both sham and ovariectomized female mice infused with AngII exhibited aortic root dilation (Sham Saline =  $1.43 \pm 0.03$  mm versus Sham AngII =  $1.52 \pm 0.03$  mm;  $p < 0.05$ ; OVX Saline =  $1.43 \pm 0.04$  mm versus OVX AngII =  $1.59 \pm 0.04$  mm;  $p = 0.004$ ). However, ovariectomy did not exacerbate aortic root dilation. (**Figure 4.2**) Conversely, orchietomy attenuated aortic root dilation in male AngII infused mice (Aortic root: ORCH Saline =  $1.40 \pm 0.05$  mm versus ORCH AngII =  $1.54 \pm 0.05$  mm;  $p = 0.07$ ). (**Figure 4.2**) During the course of study, one orchietomized male mice implanted with a miniosmotic pump



delivering AngII died due to rupture of the abdominal aorta and was excluded from analysis of thoracic aortic aneurysms according to pre-specified exclusion criteria.

#### *Removal of endogenous sex hormones in FBN1<sup>mgR/mgR</sup> mice*

To determine if gonadectomy affects syndromic TAA, we performed gonadectomy of female and male FBN1<sup>mgR/mgR</sup> mice. Gonadectomies were performed at 8 weeks of age, before sexual maturity but after TAA was established. Aortic dimensions were measured 4 weeks later by high frequency ultrasound. (**Figure 4.6**)

Ovariectomy did not exacerbate ascending aortic dilation in female FBN1<sup>mgR/mgR</sup> mice (Sham = 1.92 IQR 0.41 mm, OVX = 2.13 IQR 0.38 mm;  $p = 1.0$ ). Orchiectomy did not attenuate aortic dilation in male FBN1<sup>mgR/mgR</sup> mice (Sham = 2.40 IQR 0.40 mm, ORCH = 2.12 IQR 0.63 mm;  $p = 1.0$ ). (**Figure 4.6**) Similarly, aortic root dimensions were not altered by gonadectomy in female (Sham = 2.41 IQR 0.28 mm, OVX = 2.13 IQR 0.37 mm;  $p = 1.0$ ) or male (Sham = 2.44 IQR 0.21 mm, ORCH = 2.50 IQR 0.68 mm;  $p = 1.0$ ) FBN1<sup>mgR/mgR</sup> mice. (**Figure 4.6**) During the course of study, one sham operated female FBN1<sup>mgR/mgR</sup> mouse died of TAA rupture and two orchiectomized female FBN1<sup>mgR/mgR</sup> mice died with no evidence of TAA rupture. Additionally, one male sham operated and one male orchiectomized FBN1<sup>mgR/mgR</sup> mouse showed evidence of TAA rupture. These mice were excluded from analysis of in vivo thoracic aortic diameters by ultrasound according to pre-specified analysis criteria.

#### *Gonadectomy modulates AngII-induced medial remodeling.*

TAA is associated with loss of extracellular matrix structure. To determine if gonadectomy modulates remodeling of the extracellular matrix in the ascending aorta during TAA, we sectioned and stained ascending aortas for elastin.

First, we measured fragmentation of the elastic lamina in female and male AngII infused mice. (**Figure 4.7**) Female mice subject to sham surgery did not exhibit increased elastin fragmentation after AngII infusion (Sham Saline =  $0.6 \pm 0.5$  breaks/HPF, Sham AngII =  $1.6 \pm 0.5$  breaks/HPF;  $p = 0.2$ ). However, female mice subject to OVX exhibited increased elastin fragmentation after AngII infusion (OVX Saline =  $0.4 \pm 0.5$  breaks/HPF, OVX AngII =  $3.0 \pm 0.5$  breaks/HPF;  $p = 0.009$ ). (**Figure 4.7**) Male mice subject to sham surgery exhibited increased elastin fragmentation after AngII infusion (Sham Saline =  $0.7 \pm 0.7$  breaks/HPF, Sham AngII =  $4.7 \pm 0.7$  breaks/HPF;  $p = 0.003$ ). Male mice subject to ORCH did not exhibit increased elastin fragmentation after AngII infusion (ORCH Saline =  $0.1 \pm 0.7$  breaks/HPF, ORCH AngII =  $1.7 \pm 0.7$  breaks/HPF;  $p = 0.1$ ). AngII induced elastin fragmentation in male mice was attenuated by orchiectomy ( $p = 0.02$ ). (**Figure 4.7**)

Next, we measured fragmentation of the elastic lamina in female and male FBN1<sup>mgR/mgR</sup> mice. (**Figure 4.7**) OVX and ORCH did not have a significant effect

on elastin fragmentation in female (Sham =  $5.8 \pm 1.0$  breaks/HPF, OVX =  $6.4 \pm 1.0$  breaks/HPF;  $p = 0.63$ ) and male (Sham =  $9.1 \pm 0.9$  breaks/HPF, ORCH =  $7.4 \pm 0.9$  breaks/HPF;  $p = 0.24$ ) FBN1<sup>mgR/mgR</sup> mice. (**Figure 4.7**)

TAA is associated with vascular smooth muscle cell dysfunction and loss of contractile phenotype. Staining was concurrently performed with negative controls to demonstrate specificity. (**Figure 4.8**) To determine if gonadectomy altered cellular residents of the aortic media, ascending aortic sections were stained for  $\alpha$ -smooth muscle actin to detect contractile smooth muscle cells. (**Figure 4.9**)

#### 4.5 Discussion

These findings give strong evidence that removal of endogenous sex hormones can modulate AngII-induced acquired TAA. This study suggests that estrogens are protective against development of acquired thoracic aortic aneurysms and androgens exacerbate acquired thoracic aortic aneurysms. However, the effect of sex hormones may be limited in established, syndromic TAAs.

Divergent results seen in the AngII-infused model of acquired TAA and the FBN1<sup>mgR/mgR</sup> model of syndromic TAA can be explained by the differences in TAA pathogenesis. Because we detected sexual dimorphism in both models, gonadectomies were performed at 8 weeks of age in both TAA models to attenuate exposure to sex hormones following sexual maturity. The AngII-infusion mouse model develops TAA in normolipidemic conditions and independent of blood pressure changes.(28, 37) Aortic pathology can be detected as early as 3 days after AngII-infusion but do not start unless AngII is infused. However, gonadectomies were performed before AngII was infused and before TAA developed. Thus, both initial and progressive TAA was affected. Conversely, FBN1<sup>mgR/mgR</sup> mice exhibit rapid dilation and death by aortic rupture early in life. We chose this model due to its rapid TAA development. By 8 weeks of age, approximately 10% of male FBN1<sup>mgR/mgR</sup> mice expired due to TAA rupture. Gonadectomies were performed at a timepoint when FBN1<sup>mgR/mgR</sup> mice normally exhibited TAA. Thus, sex hormone removal would only impact progressive TAA with minimal impact on dilation occurring before 8 weeks of age. The severity of TAA coupled with a short follow-up period in FBN1<sup>mgR/mgR</sup> mice limits interpretation of the effect of sex hormones in syndromic TAA. To address these limitations, future experiments should investigate the effect of gonadectomy in the milder FBN1 C1041G/+ or GT8/+ models to allow measurement over a longer course.(11, 52)

While this study revealed that gonadectomy alters acquired TAA, the aortic targets of sex hormones are unknown. One possibility is that removal of endogenous sex hormones directly alters the renin angiotensin system. However, this study did not test components of the renin angiotensin system.

This is due to a lack of validated reagents able to detect components of the renin angiotensin system such as tissue angiotensin receptor levels.(162, 163) In fact, several custom anti-angiotensin receptor antibodies generated by our group failed to show specificity. (118) Another possibility is that sex hormone removal impacts renin angiotensin system independent processes. A study of the effects of gonadectomy in AngII and hyperlipidemia induced abdominal aortic aneurysms revealed a myriad of changes in the aortic tissue.(161) However, it is unclear which of these targets contribute to the disease process or are merely correlative. Future studies may make use of transcriptomic or proteomic techniques to elucidate differentially regulated genes. Ultimately, we do not advocate gonadectomy of male patients with TAA. However, future research may reveal the molecular mechanism on how estrogens protect against TAA and androgens exacerbate TAA. We hope that this will lead to effective therapies for patients of both sexes.

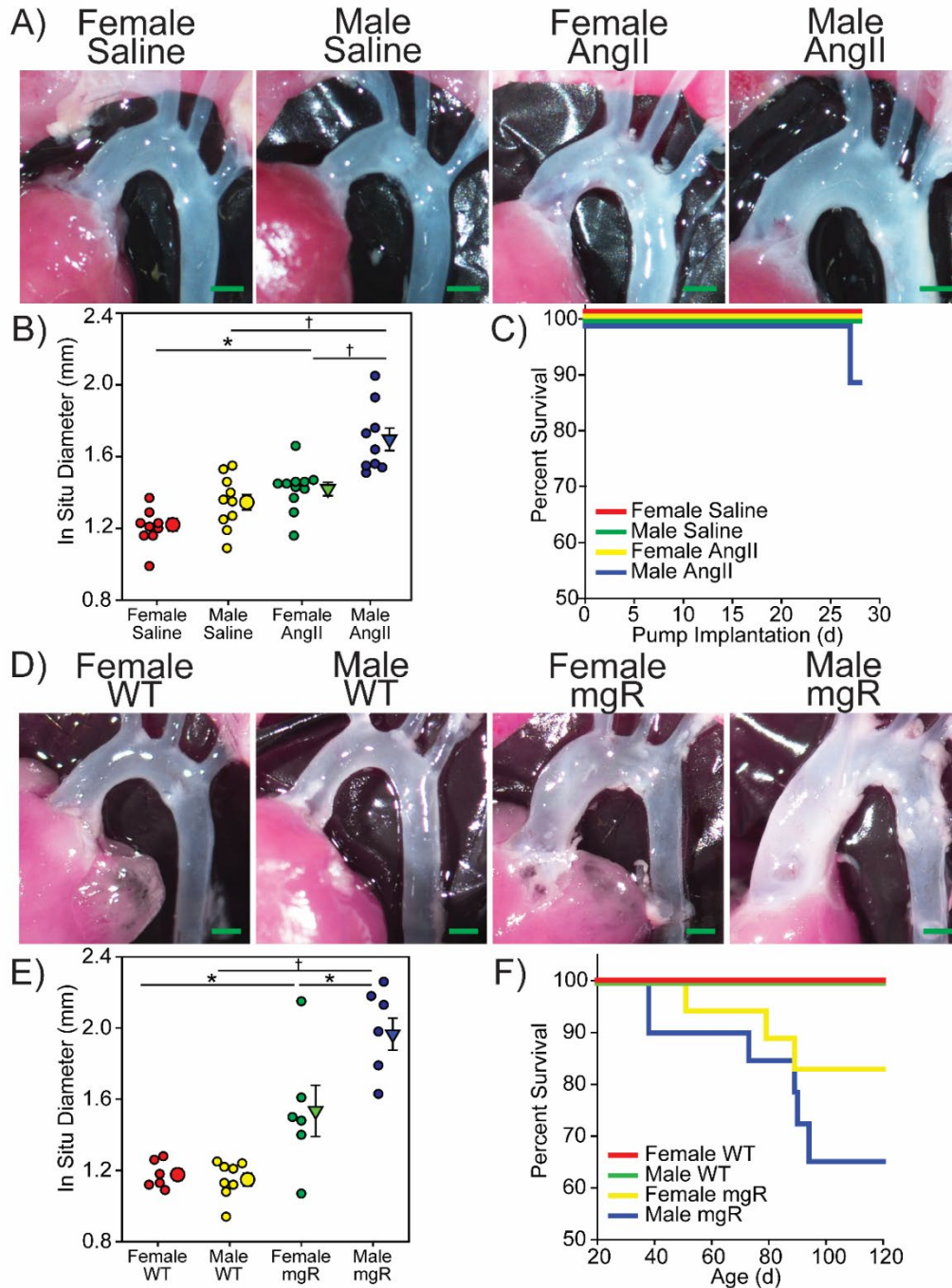


**Figure 4.1 Sexual dimorphism occurs in both acquired and syndromic mouse models of thoracic aortic aneurysms**

**A)** Representative images of in situ ascending aortas from female and male mice infused with either saline or AngII for 28 days. Green bar = 1 mm. **B)** In situ dimensions of ascending aortas from female and male mice infused with either saline or AngII for 28 days.  $n = 9-10/\text{group}$ .  $*p < 0.01$ ,  $\dagger p < 0.001$ . **C)** Survival curves of female and male mice infused with either saline or AngII for 28 days. 1/11 male mice infused with AngII died due to TAA rupture at day 27. **D)** Representative images of in situ ascending aortas from female and male

FBN1<sup>mgR/mgR</sup> mice at 16 weeks of age. Green bar = 1 mm. **E)** In situ dimensions of ascending aortas from female and male FBN1<sup>mgR/mgR</sup> mice at 16 weeks of age. n = 6-8/group. **F)** Survival curves of female and male FBN1<sup>mgR/mgR</sup> mice at 16 weeks of age aggregated from four separate cohorts. n = 16-21/group. \*p<0.01, †p<0.001.

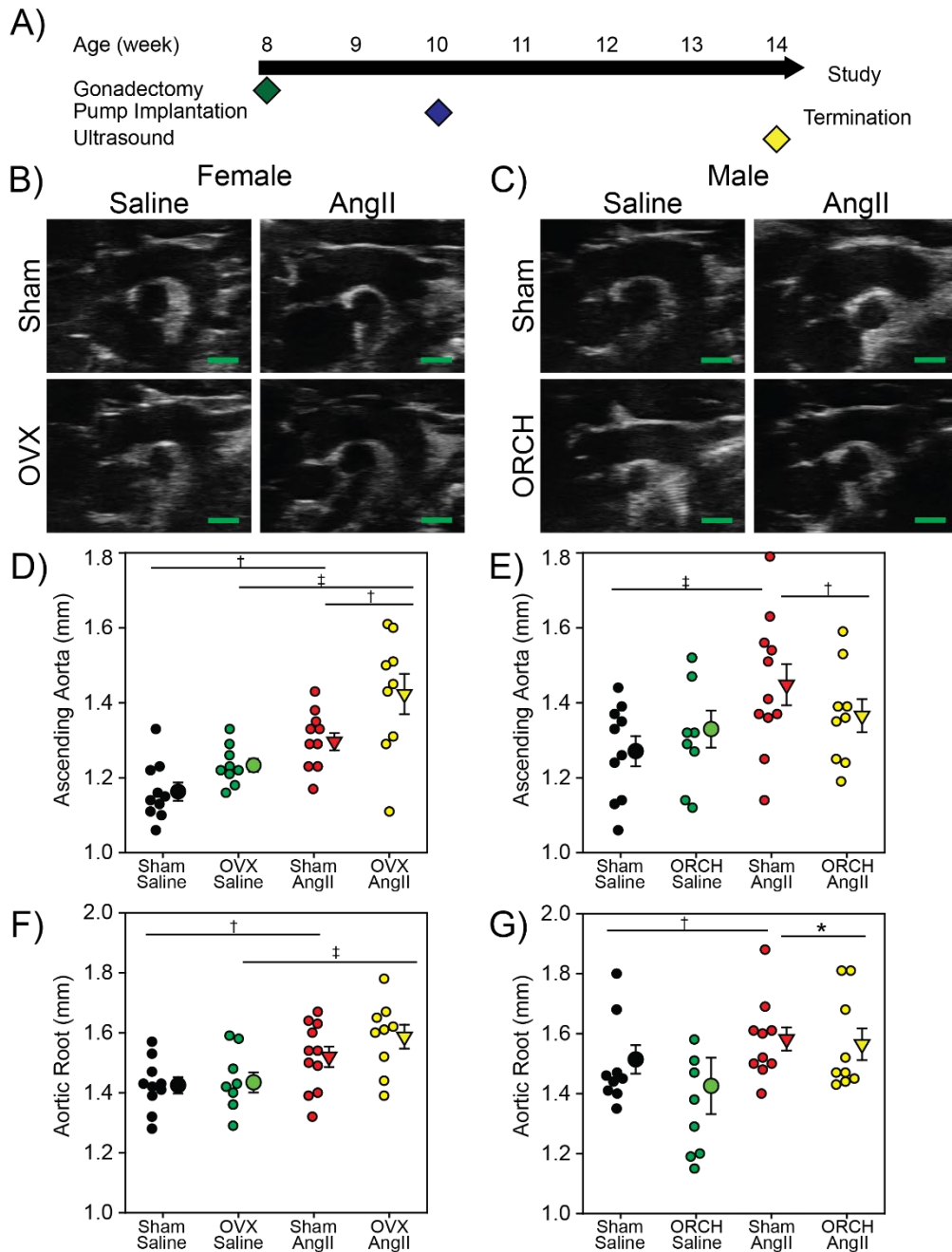


**Figure 4.2 Gonadectomy modulated ascending aortic and aortic root dimensions in AngII-infused female and male mice**

**A)** Study design to investigate sex hormone removal on AngII-induced model of acquired TAA. Representative diastolic ultrasound images of **B)** female and **C)** male mice subjected to castration or sham surgery and implanted with miniosmotic pump delivering saline or AngII. Green bar = 1 mm. Ascending aortic diameters measured by ultrasound in **D)** female and **E)** male mice. Aortic root diameters measured by ultrasound in **F)** female and **G)** male mice. n = 8-11/group. \*p<0.05 †p<0.01 ‡p<0.001.

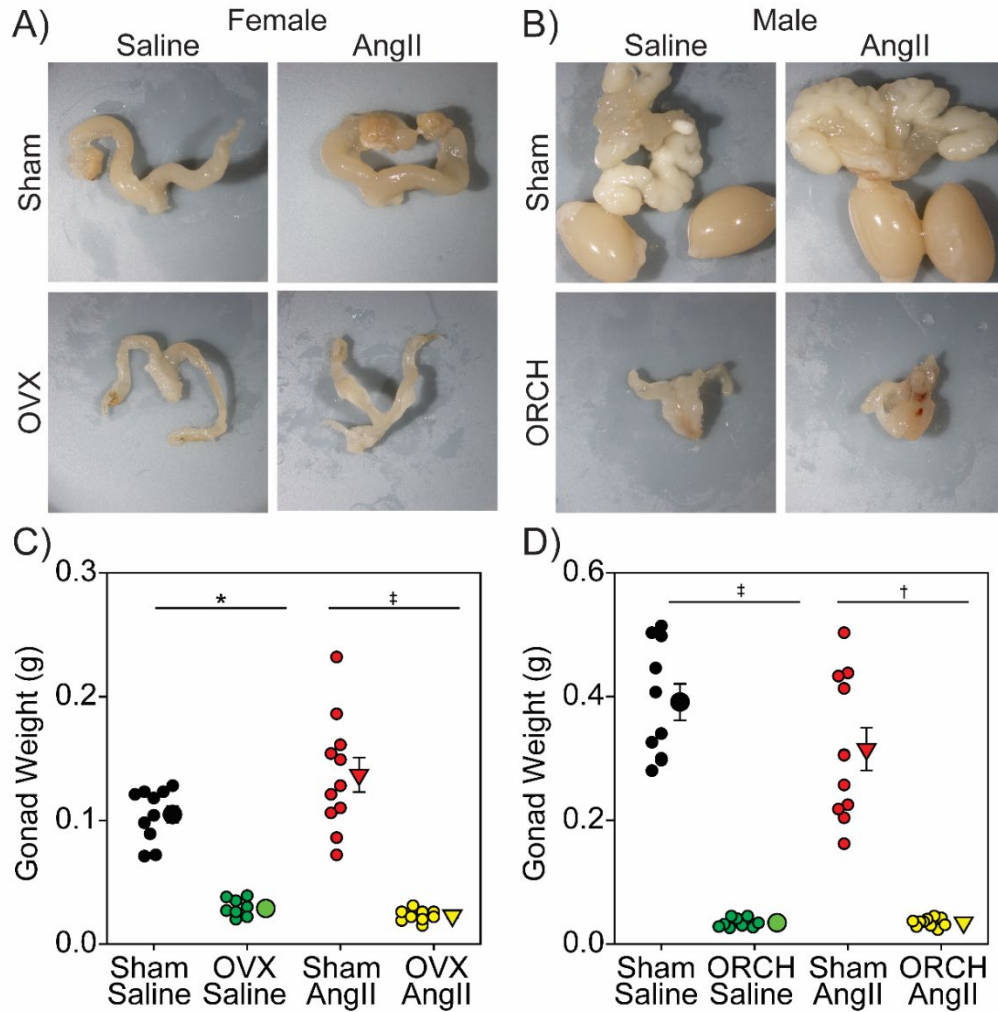


**Figure 4.3 Atrophy of sex responsive organs after gonadectomy of female and male AngII-infused mice**

Representative images of **A)** uteri from female mice after sham or ovariectomy and **B)** testes and seminal vesicles from male mice after sham or orchiectomy. Gonad weight of **C)** female and **D)** male mice after gonadectomy and 28 day infusion of either saline or AngII. n = 8-11/group. \*p<0.05 †p<0.01 ‡p<0.001.

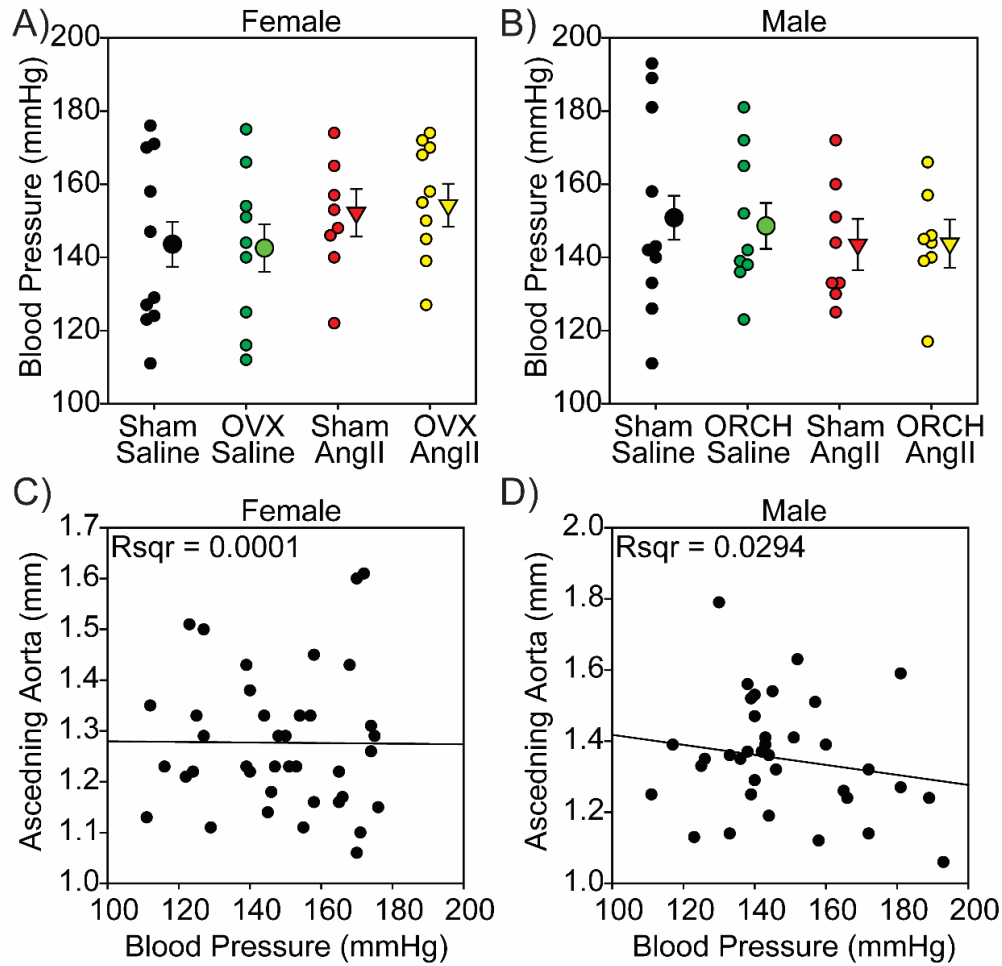


**Figure 4.4 Systolic blood pressure was not altered by gonadectomy and did not correlate with aortic diameter**

Systolic blood pressure was not significantly different between groups in **A)** female or **B)** male mice. Systolic blood pressure was not significantly correlated with aortic diameter in **C)** female or **D)** male mice. n = 8-11/group



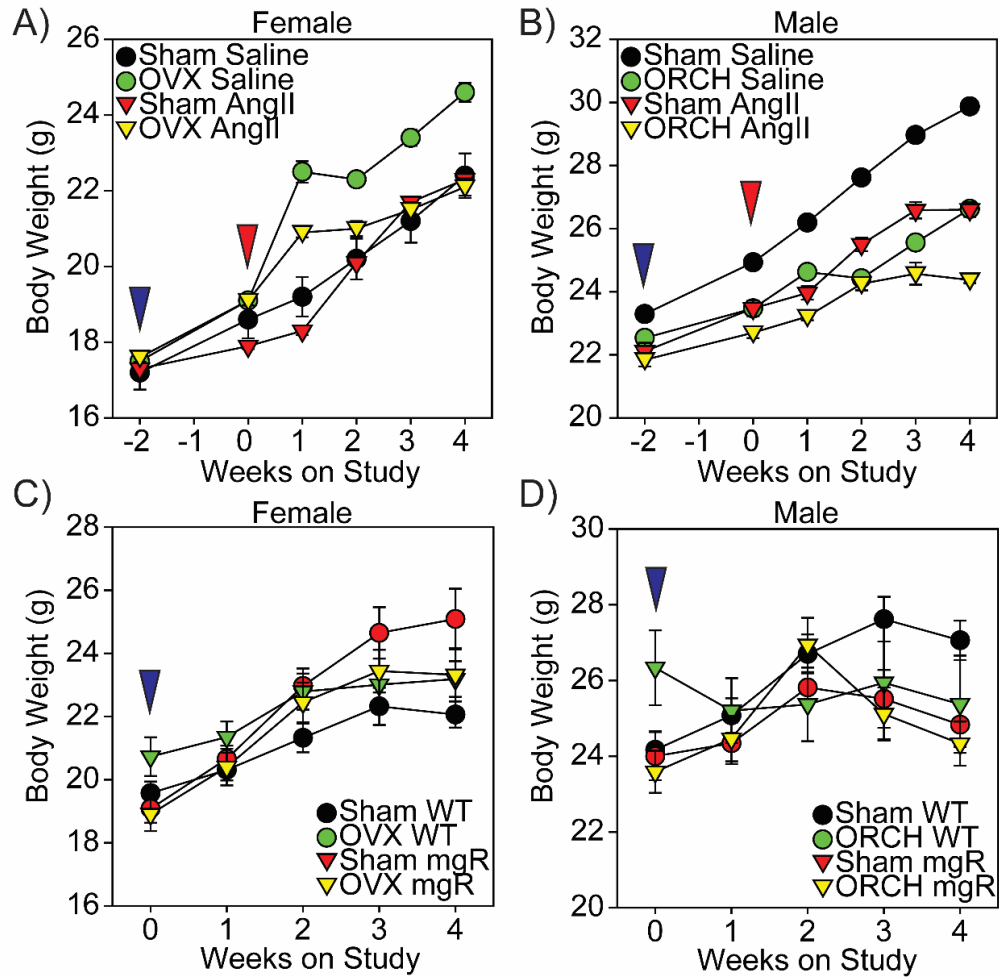


**Figure 4.5 Body weight of mice was not altered by gonadectomy**  
 Body weights of **A)** female and **B)** male AngII-infused mice and their wildtype littermates subject to sham or gonadectomy were not significantly different between groups at the end of study. Gonadectomy was performed 2 weeks prior to study (blue arrow), pump implantation (red arrow). Body weights of **C)** female and **D)** male  $FBN1^{mgR/mgR}$  mice subject to sham or gonadectomy were not significantly different between groups at the end of study.

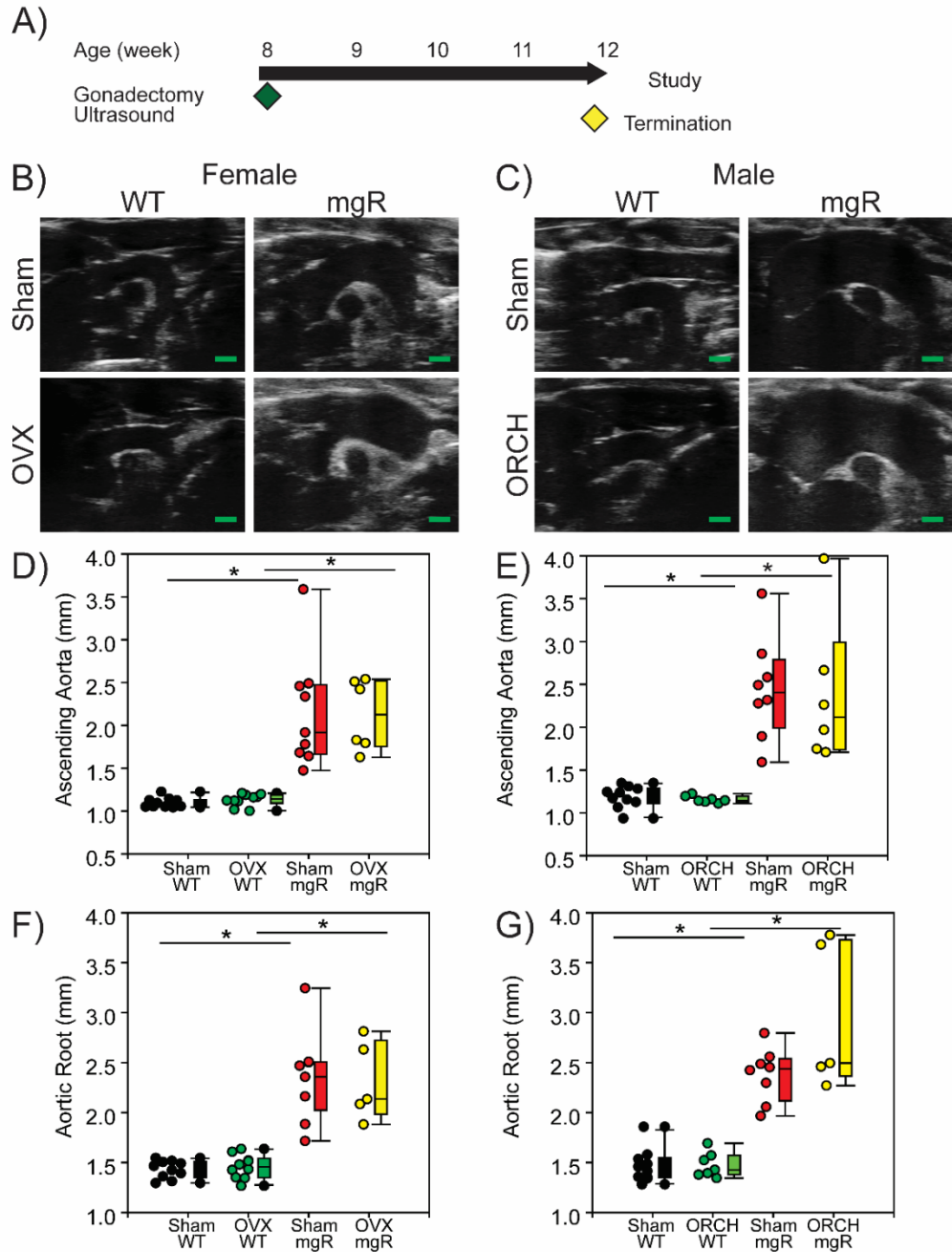


**Figure 4.6 Gonadectomy did not alter aortic dilation after 4 weeks in  $FBN1^{mgR/mgR}$  mice**

**A)** Study design to investigate sex hormone removal on  $FBN1^{mgR/mgR}$  model of syndromic TAA. Representative diastolic ultrasound images of **B)** female and **C)** male  $FBN1^{mgR/mgR}$  mice subjected to castration or sham surgery. Ascending aortic diameters measured by ultrasound in **D)** female and **E)** male mice. Aortic root diameters measured by ultrasound in **F)** female and **G)** male mice.  $n = 4-8$  / group.  $*p < 0.001$ .

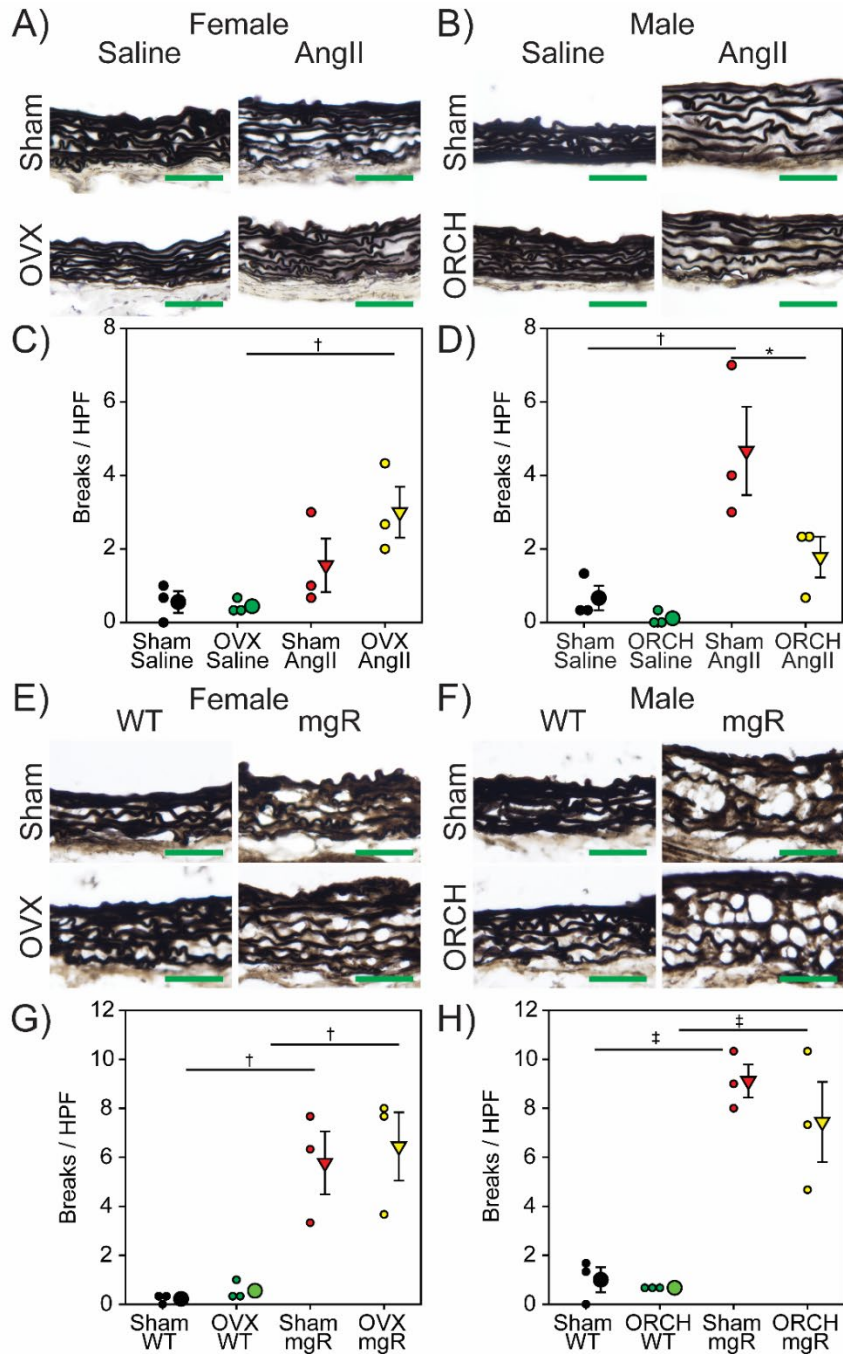


**Figure 4.7 Gonadectomy modulated elastin fragmentation in ascending aorta of male and female mice**

Representative images of ascending aortic sections from **A)** female and **B)** male AngII-infused mice stained with Verhoeff elastin stain demonstrating aortic elastin lamina structure and medial thickness. Quantification of number of elastin breaks per high powered field in **C)** female and **D)** male AngII-infused mice.  $n = 3$  mice/group. \* $p < 0.05$ , † $p < 0.01$ . Representative images of ascending aortic sections from **E)** female and **F)** male  $FBN1^{mgR/mgR}$  mice stained with Verhoeff

elastin stain demonstrating aortic elastin lamina structure and medial thickness. Quantification of number of elastin breaks per high powered field in **G)** female and **H)** male FBN1<sup>mg<sup>R</sup>/mg<sup>R</sup></sup> mice. n = 3 mice/group. †p<0.01, ‡p<0.001.

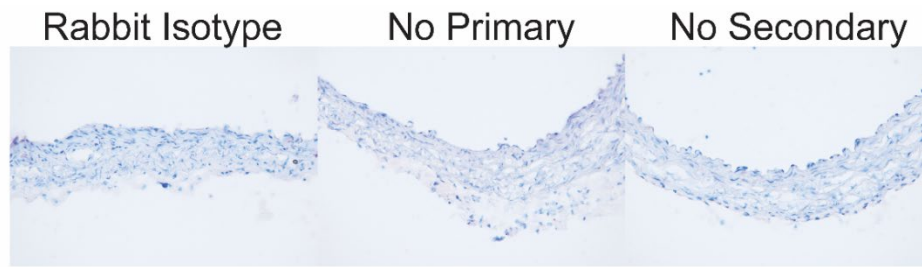


**Figure 4.8 Controls for  $\alpha$ -smooth muscle actin immunostaining**

Negative controls for  $\alpha$ -smooth muscle actin include preimmune IgG (Rabbit IgG, Sigma, I8140), no primary, and no secondary control performed concurrently.

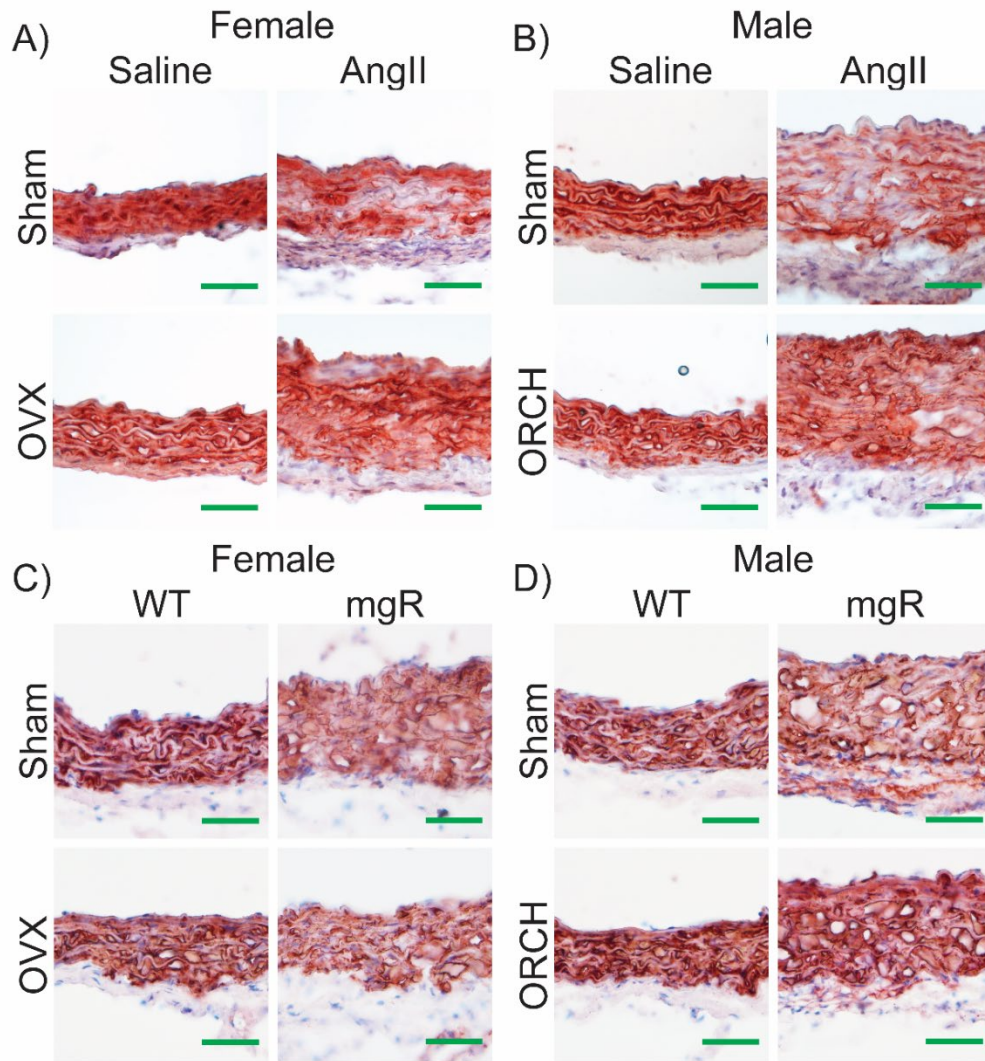


**Figure 4.9 Gonadectomy modulates aortic medial expression of contractile smooth muscle markers in ascending aorta of AngII-infused male mice**  
 Staining of  $\alpha$ -smooth muscle actin in the ascending aorta of **A)** female and **B)** male mice demonstrated that AngII infusion led to areas of medial smooth muscle loss. This was not altered by ovariectomy of female mice and attenuated by orchietomy of male mice. Staining of  $\alpha$ -smooth muscle actin in the ascending aorta of **C)** female and **D)** male  $FBN1^{mgR/mgR}$  mice shows no difference after gonadectomy in females or males.

## CHAPTER 5. S100A4-CRE MEDIATED EXCISION OF AT1A RECEPTORS ATTENUATES SPONTANEOUS BUT NOT SYNDROMIC AORTIC ANEURYSMS IN MICE

This chapter is based on a publication in process titled “S100A4-Cre Mediated Excision of AT1a Receptors Attenuates AngII-induced but not FBN1<sup>C1041G/+</sup> Associated Aortic Aneurysms” detailing findings of the effect of fibroblast specific deletion of AT1aR on aortopathies.

### 5.1 Synopsis

#### Objective:

Thoracic aortic aneurysms (TAA) and aortopathies can have either spontaneous or syndromic etiologies. In general, inhibition of the angiotensin II (AngII) receptor type 1a (AT1aR) attenuates TAA of various etiologies. While this implies that AT1aR stimulation is responsible for TAA, the cell type where AT1aR become stimulated in TAA formation is unknown. Here, we generated fibroblast specific deletion of AT1aR and measured TAA development in an AngII-induced mouse model of spontaneous TAA and in the Fbn1<sup>C1041G/+</sup> mouse model of syndromic TAA.

#### Approach and Results:

Fibroblast specific deletion of AT1aR was accomplished by breeding mice expressing *Cre* under control of the S100A4 promoter (S100A4-*Cre*) to AT1a receptor floxed mice. Lineage tracing experiments demonstrated that S100A4-*Cre* was active in fibroblast rich organs and the aorta but not fibroblast poor organs. Aortic cross sections from S100A4-*Cre* +/0 ROSA26-LacZ mice infused with either saline or AngII demonstrated that AngII infusion increased the number of LacZ traced cells in aortic media. LDL receptor -/- mice with depletion of AT1a receptors was used to assess spontaneous TAA and atherosclerosis. Eight week old, male, littermates were fed a fat-enriched diet for 1 week before and during AngII infusion for 28 days. AngII-induced expansion of ascending aorta area and abdominal aortic width were attenuated significantly in *Cre*+/0 mice. However, there was no significant difference in AngII-augmented atherosclerosis. S100A4-*Cre* driven deletion of AT1aR failed to modulate ascending aorta and aortic root dilation in Fbn1<sup>C1041G/+</sup> mice.

#### Conclusions:

Fibroblast specific deletion of AT1aR had divergent effects on spontaneous and syndromic TAA. Additionally, AT1aR deletion failed to attenuate atherosclerosis. This indicates that the action of AT1aR in TAA development is heterogenous in aortopathies of different etiologies.

## 5.2 Introduction

Fibroblasts are a prominent cell type in the adventitia that have been proposed to be active participants in aortic aneurysms and atherosclerosis. During aneurysm formation, adventitial thickening and inflammation are key histological hallmarks seen in disease. (17, 100) Fibroblasts may play a key role in aortic remodeling during aortopathy.

Based on our own data as well as other publications, genetic targeting of AT1 receptors, or pharmacological inhibition by administration of an antagonist, losartan, ablated development of AngII-induced aortic aneurysms and atherosclerosis as well as TAA in male  $Fbn1^{C1041G/+}$  mice. (64) In male  $Fbn1^{C1041G/+}$  mice, AT1aR is activated in a ligand dependent manner during TAA development. However, the site of action of AT1aR is unknown. Previous studies deleted AT1a receptors in specific cellular subpopulations of the aortic vessel wall using AT1a receptor floxed mice. Subpopulations tested include smooth muscle residents of the aortic media and endothelial cell residents of the aortic intima. Unexpectedly, deletion of AT1a receptors in smooth muscle cells had no effect on AngII-induced aortic pathologies or atherosclerosis. (118, 132, 164) AT1a receptors deleted in endothelial cells have resulted in none or minimal effects on aortic aneurysms and atherosclerosis. (118) In addition to AngII-infusion models, deletion of AT1a receptors in smooth muscle and endothelium also had minimal effects on aortic aneurysms in the genetic fibrillin1 hypomorphic models of the disease. (75) This model had been previously shown to respond to pharmacologic AT1 receptor inhibition.(74) Therefore, despite the profound effects of global AT1a receptor deletion and inhibition on vascular diseases, the cell type stimulated by AngII necessary to promote these diseases has not been identified.

Therefore, to determine the cell type responsible for AT1aR induced aortopathies, we tested the hypothesis that fibroblast specific deletion of AT1aR attenuated both spontaneous and syndromic aortopathy. First we determined the specificity of the S100A4-Cre through lineage tracing in fibroblast rich and fibroblast poor organs. Interestingly, we observed that the traced population in the aorta expanded after AngII infusion. Next, we observed that S100A4-Cre mediated AT1a receptor deletion attenuated AngII-induced TAA and AAA but did not attenuate atherosclerosis. Finally, we observed that S100A4-Cre mediated AT1a receptor deletion failed to attenuated TAA in  $Fbn1^{C1041G/+}$  mice. This indicates that the site of action of AT1aR in aortopathies are heterogenous and specific to each disease process.

## 5.3 Methods

### Mice



AT1a receptor floxed mice were developed by InGenious Targeting, Inc. (Ronkonkoma, NY) using a C57BL/6 embryonic stem cell line and are now available at The Jackson Laboratory (C57BL/6N - *Agtr1a*<sup>tm1Uky/J</sup>; stock # 016211). S100A4-Cre [BALB/c-Tg(S100a4-cre)1Egn/YunkJ; stock #: 012641] to induce fibroblast-specific deletion, ROSA26-LacZ [B6.129S4-Gt(ROSA)26Sor<sup>tm1Sor/J</sup>; stock # 003474] for lineage tracing, and LDL receptor -/- (B6;129S7-*Ldlr*<sup>tm1Her/J</sup>; stock # 002077) mice for inducing hypercholesterolemia, and *Fbn1*<sup>C1041G/+</sup> (stock #012885) mice were purchased from The Jackson Laboratory (Bar Harbor, ME). Mice were bred by the following breeding harems: male S100A4-Cre hemizygous (+/0) x AT1a receptor floxed x LDL receptor -/- to female AT1a receptor floxed x LDL receptor -/- mice; male S100A4-Cre to female ROSA26-LacZ; male S100A4-Cre hemizygous (+/0) x AT1a receptor floxed x female AT1a receptor floxed x *Fbn1*<sup>C1041G/+</sup> mice.

Mice were housed in ventilated cages with negative air pressure (Allentown Inc.; Allentown, NJ). Drinking water filtered by reverse osmosis and normal mouse diet (Global 18% protein rodent diet; Diet # 2918; Harlan Teklad; Madison, WI) were provided ad libitum. Rooms were set with light/dark cycles (14 hr, 10 hr), and temperature (20-23°C) and humidity (50-60%) controlled.

The studies followed the recommendations of The Guide for the Care and Use of Laboratory Animals (National Institutes of Health). All procedures were approved by the University of Kentucky's Institutional Animal Care and Use Committee (Protocol # 2006-0009). Necropsies were performed on mice within 12 hours of death.

#### Detection of $\beta$ -galactosidase expression during S100A4-Cre excision

Male S100A4-Cre +/0 x ROSA26 mice were infused with saline or AngII (1,000 ng/kg/min; N=3-6/group) for 28 days. After termination and exsanguination, aortas were flushed with saline and then perfused with low melting point agarose containing green dye by introducing a 23 gauge needle attached to a 1 ml syringe filled with the agarose into the ventricle of the heart. For sections of ascending aorta, the upper fourth of the heart was left on the aorta and the aorta was severed 3 mm distal to the common carotid. The descending aorta sections started 3 mm below the common carotid. The abdominal aortic sections started 3 mm above the right renal branch. These three regions of aorta were placed in OCT, frozen and sectioned on a cryostat. Tissue sections were arranged serially on sets of 10 slides with 9 sections per slide. Twenty to thirty slides were required to completely section the ascending and abdominal regions of interest. To detect S100A4-Cre positive cells, one slide from each series of 10 slides (9 sections/slide; 2-3 slides) was fixed in paraformaldehyde (4%) for 10 min at 4°C, and stained for  $\beta$ -galactosidase using X-gal protocol above. Then the sections were stained with eosin and coverslipped. Blue stained cells were counted in all 9 sections per slide of each mouse.

#### AngII Induced Aneurysm induction

Male mice (8-10 weeks old) were fed a diet enriched in saturated fat containing milk fat (21% wt/wt) and cholesterol (0.2% wt/wt) for 12 weeks (Diet# TD.88137; Harlan Teklad; Indianapolis, IN). Male mice were used due to their greater susceptibility to AngII-induced aneurysms formation. (160, 161) After 1 week of feeding, mini-osmotic pumps (Model #2004; Durect Corp; Cupertino, CA) infusing either saline or AngII (1,000 ng/kg/min; Cat # H-1705; Bachem; Torrance, CA) were implanted subcutaneously on the right flank of mice. (165) The continuous infusion lasted 28 days.

#### Atherosclerosis induction

Male and female mice (8-10 weeks old) were fed the saturated fat enriched diet listed above for 5 weeks.

#### Quantification of TAA, AAA, and atherosclerosis

Mice were terminated by an overdose of ketamine/xylazine mixture (90 mg, 10 mg/kg, respectively). After exsanguination via cardiac puncture, the right atrium of the heart was cut to allow perfusate drainage. Then aortas were perfused with saline, dissected free, and placed in 10% neutral buffered formalin overnight. Twenty-four hours later, aortas were transferred to saline. Adventitia was removed using a forceps and aortas were cut in half at the diaphragm. Thoracic aortas were opened en face, pinned, and photographed. Atherosclerosis was measured in accord with recent recommendations. Abdominal aortas were pinned and photographed. Abdominal aortic diameter, ascending aortic area, and atherosclerotic lesion area were measured using ImagePro Plus software (Media Cybernetics, Inc.; Bethesda, MD) (166) (17, 167)

#### Statistics

Appropriate statistical analyses were based on numbers of groups compared and parametric characteristics of the data using SigmaPlot (Systat Software Inc.; San Jose, CA). Data are represented as mean  $\pm$  SEM.  $P < 0.05$  was considered statistically significant.

#### 5.4 Results

S100A4-Cre traced cells are abundant in fibroblast rich tissue and are increased in aortas of AngII infused mice.

We demonstrated that S100A4-Cre is active in fibroblast rich tissues but absent in fibroblast poor tissues. (Figure 5.1) However, both the thoracic and abdominal aortas of S100A4-Cre<sup>+/0</sup> x ROSA26-LacZ mice were not uniformly positive. Histologic sections of both ascending and abdominal aortas demonstrated scant positively traced cells in mice infused with saline. However,

this population expanded after AngII infusion. An increased number of  $\beta$ -galactosidase-positive cells after AngII infusion were found in both aortic segments

#### AT1a Receptor Excision by S100A4-Cre Significantly Attenuated AngII-induced Thoracic and Abdominal Aortic Aneurysms But Did Not Protect Against AngII-induced Atherosclerosis

Aortic rupture occurred in 5/28 *Cre* 0/0 and 5/32 *Cre*+0 mice within 5 to 22 days of AngII infusion. There were no deaths in saline-infused mice of either genotype. Location of aortic rupture was mixed; there were 3 thoracic and 2 abdominal aortic ruptures in both groups. As expected, AngII infusion significantly increased aortic arch area compared to saline-infused mice in both genotypes ( $P < 0.001$ ). However, the S100A4-Cre +/0 genotype had a significant reduction in AngII-induced aortic arch dilation compared to 0/0 mice ( $P = 0.003$ ; Figure 5.2). AngII infusion also significantly increased abdominal aortic diameter compared to saline-infused mice in both genotypes ( $P < 0.001$ ). There was a modest but significant decrease of abdominal aortic diameter in *Cre* +/0 mice compared to 0/0 mice ( $P = 0.029$ ). AngII-induced atherosclerotic lesion area was also measured in the arch (Figure 5.2). Saline-infused mice fed a fat-enriched diet for 5 weeks had barely detectable atherosclerotic lesions; while AngII infusion significantly increased atherosclerotic lesion area ( $P < 0.001$ ). Atherosclerotic lesion areas were not different between genotypes.

#### AT1a Receptor Excision by S100A4-Cre Did Not Protect Against TAA in *Fbn1*<sup>C1041G/+</sup> mice

Male and female *Fbn1*<sup>C1041G/+</sup> mice with fibroblast specific deletion of AT1aR were generated. Mice were subject to ultrasound to measure both the aortic root and ascending aorta. (Figure 5.3) Both male and female *Fbn1*<sup>C1041G/+</sup> mice exhibited significant aortic dilation at 6 months of age. However, fibroblast specific deletion of AT1aR failed to attenuate dilation in either segment.

### 5.5 Discussion

Our studies revealed seemingly disparate paradoxes about the role of AT1aR on fibroblasts. S100A4-Cre mediated excision of the AT1a receptor significantly attenuated AngII induced thoracic and abdominal aneurysm formation but not TAA in *Fbn1*<sup>C1041G/+</sup> mice. This occurred despite lifelong deficiency of AT1aR in fibroblasts. The divergent role of AT1aR in spontaneous versus syndromic aneurysms merits investigation. Additionally, rupture incidence was not altered in these studies. Further studies may focus on the differences between aortic dilation and aortic rupture as well as the mechanisms behind how dilation may progress to rupture. Additionally, we have now systematically demonstrated that excision of AT1a receptor within the aortic intima, media, or adventitia fails to attenuate either AngII induced atherosclerosis despite whole

body AT1a receptor being necessary for atherosclerosis formation. Despite the majority of aneurysmal pathology and tissue remodeling affecting the smooth muscle cell rich aortic media, we have now shown that Tie2 and S100A4-*Cre* mediated depletion of AT1a receptors in endothelial cells and fibroblasts can attenuate aneurysm formation whereas SM22-*Cre* mediated depletion cannot. Thus, AT1aR dependent aortopathies rely on activation of AT1a receptors in different cell types.

Surprisingly, cross-sections revealed that most  $\beta$ -galactosidase positive cells were located in the media rather than the adventitial region of the aorta in both saline and AngII-infused mice. The S100A4 promoter may encompass fibroblasts actively remodeling in disease rather than quiescent fibroblasts in the aorta. The S100A4 promoter was identified by comparative transcript analysis of fibroblasts from different micro environments and other cell types and termed fibroblast specific protein-1 (FSP1). (168) Recently, its specificity has been questioned. Kong et al demonstrated that FSP1+ cells increased during myocardial infarction, and >30% of these cells were identified as hematopoietic or endothelial cells. (169) Rather than a marker for fibroblasts, FSP1 may be a driver of fibrosis itself and deletion of AT1a receptor in actively remodeling tissues -- rather than resident adventitial fibroblasts -- may be responsible for protection against thoracic and abdominal aortic aneurysms. While we have previously demonstrated S100A4-*Cre* mediated AT1a receptor deletion reduced AT1a receptor mRNA, detection of AT1a receptor protein levels at this time has been hampered by lack of specific AT1a receptor antibodies. This may also signify that protection afforded by S100A4-*Cre* mediated AT1a receptor deletion corresponds to the degree of AT1a receptor depletion within the whole aorta rather than a cell-specific effect.

Future experiments should address alternate hypotheses and sites of AT1aR action in aortopathies. Equally interesting may be the source of renin angiotensin components, and whether components such as renin and angiotensinogen derive from aortic tissue or from major body sources such as the juxtaglomerular cells or liver respectively. Disparate cell types within the aorta may have synergistic action through the AT1aR via autocrine/paracrine signaling. Additionally, activation of extra-aortic AT1a receptors seems necessary for atherosclerosis formation while activation of vascular AT1a receptors contributes to aneurysm formation. In both cases, more research is needed to address the exact cell types and signaling networks responsible for both atherosclerosis and aneurysm formation. Future experiments in aneurysm formation should address the crosstalk between endothelial and adventitial AT1a receptor activation and medial aortic remodeling. Future experiments investigating the role of renin angiotensin signaling in atherosclerosis should focus on AngII-responsive extra-aortic tissues and organs such as the brain and kidney.

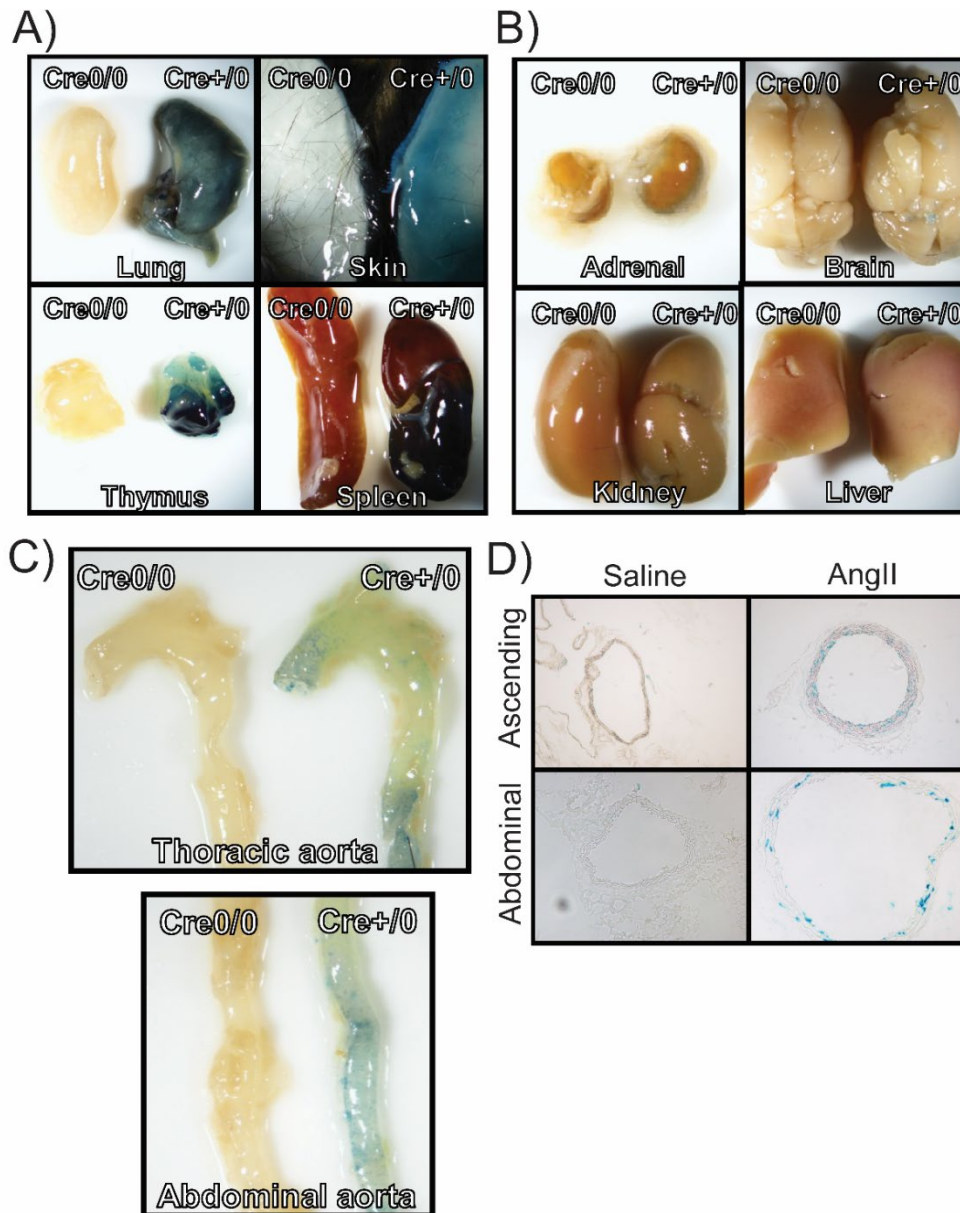


**Figure 5.1 S100A4-Cre traced cells were preferentially enriched in fibroblast rich tissues**

$\beta$ -galactosidase activity (depicted by blue color) by S100A4-Cre mediated excision of ROSA26 in selected whole organs from S100A4-Cre 0/0 x Rosa26-LacZ (left side of each panel) and S100A4-Cre +/0 x Rosa26-LacZ (right side of each panel) in **A)** fibroblast-rich tissue **B)** non-fibrotic tissue and the **C)** thoracic and abdominal aortas. Cre transgene is identified as +/0. **D)** Representative sections from series of ascending and abdominal aortas from S100A4-Cre x ROSA26-LacZ mice infused with saline. Stained with  $\beta$ -galactosidase activity and imaged at 200x magnification. AngII infusion changed distribution of lineage traced cells in the ascending and abdominal aortas.

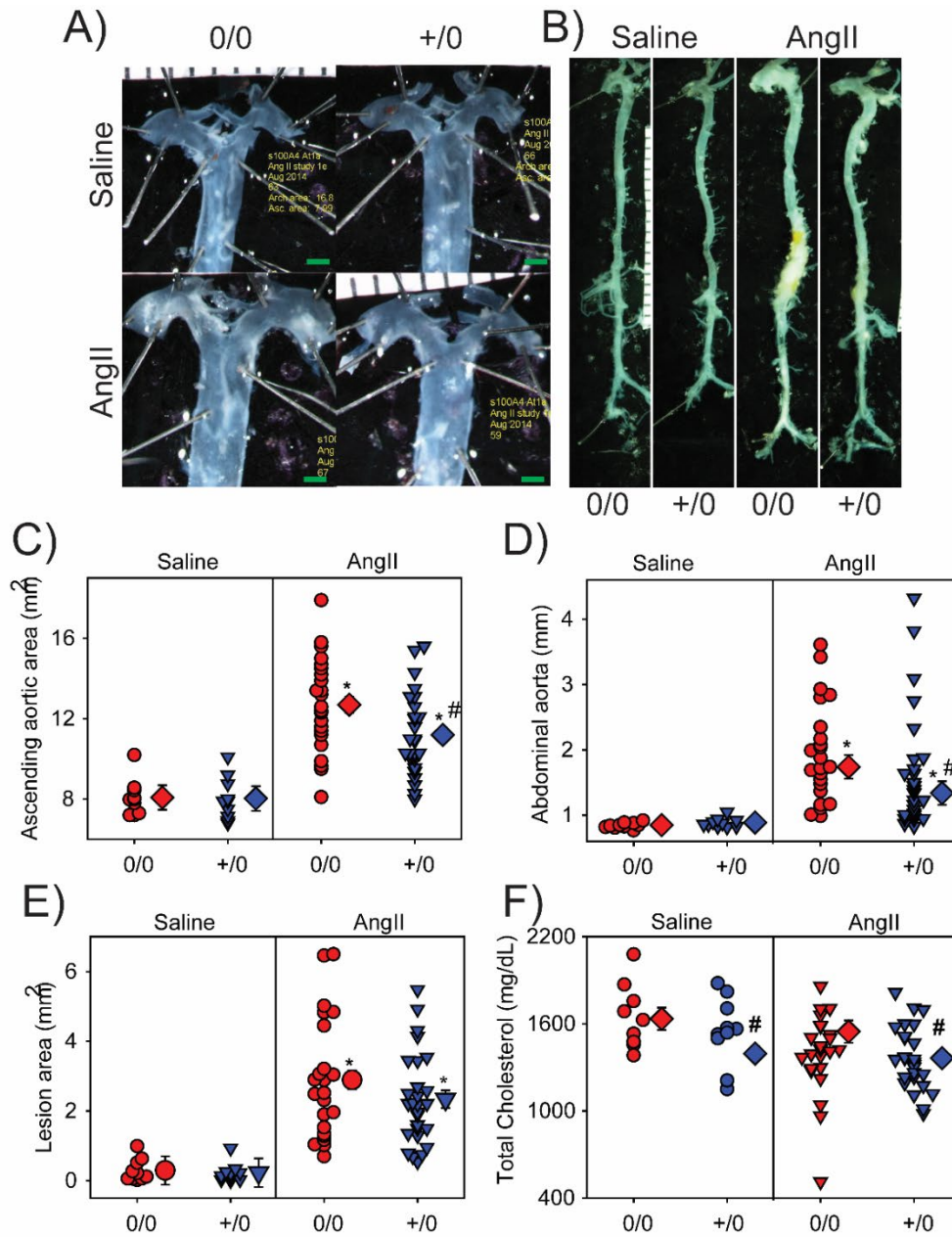


**Figure 5.2 AT1a receptor deletion attenuated AngII-induced TAA and AAA but not AngII-exacerbated atherosclerosis**

Representative images of **A)** enface ascending aortas and **B)** ex vivo aortas from fibroblast specific AT1aR deficient x LDL receptor  $-/-$  mice infused with either saline or AngII. S100A4-Cre mediated excision of AT1a receptors reduced aortic dilation in **C)** ascending **D)** and abdominal aortas of AngII-infused male LDL receptor  $-/-$  mice, but had no effect on **E)** AngII-augmented atherosclerosis despite reductions in **F)** total plasma cholesterol. For **C)**: \* denotes  $P < 0.001$  comparing saline versus AngII within genotypes by Holm-Sidak. # denotes  $P = 0.007$  comparing AngII infused 0/0 versus +/0 by Holm-Sidak. For **D)**: \* denotes  $P < 0.001$  when comparing infusions within 0/0 genotype

by Holm-Sidak. # denotes  $P=0.029$  comparing AngII infused 0/0 vs +/0 by Student's t-test. For **E)** \* denotes  $P<0.001$  for saline versus AngII infusion within Cre 0/0 and +/0 by Holm-Sidak. For **F)** # denotes  $P<0.05$  comparing AngII infused 0/0 vs +/0

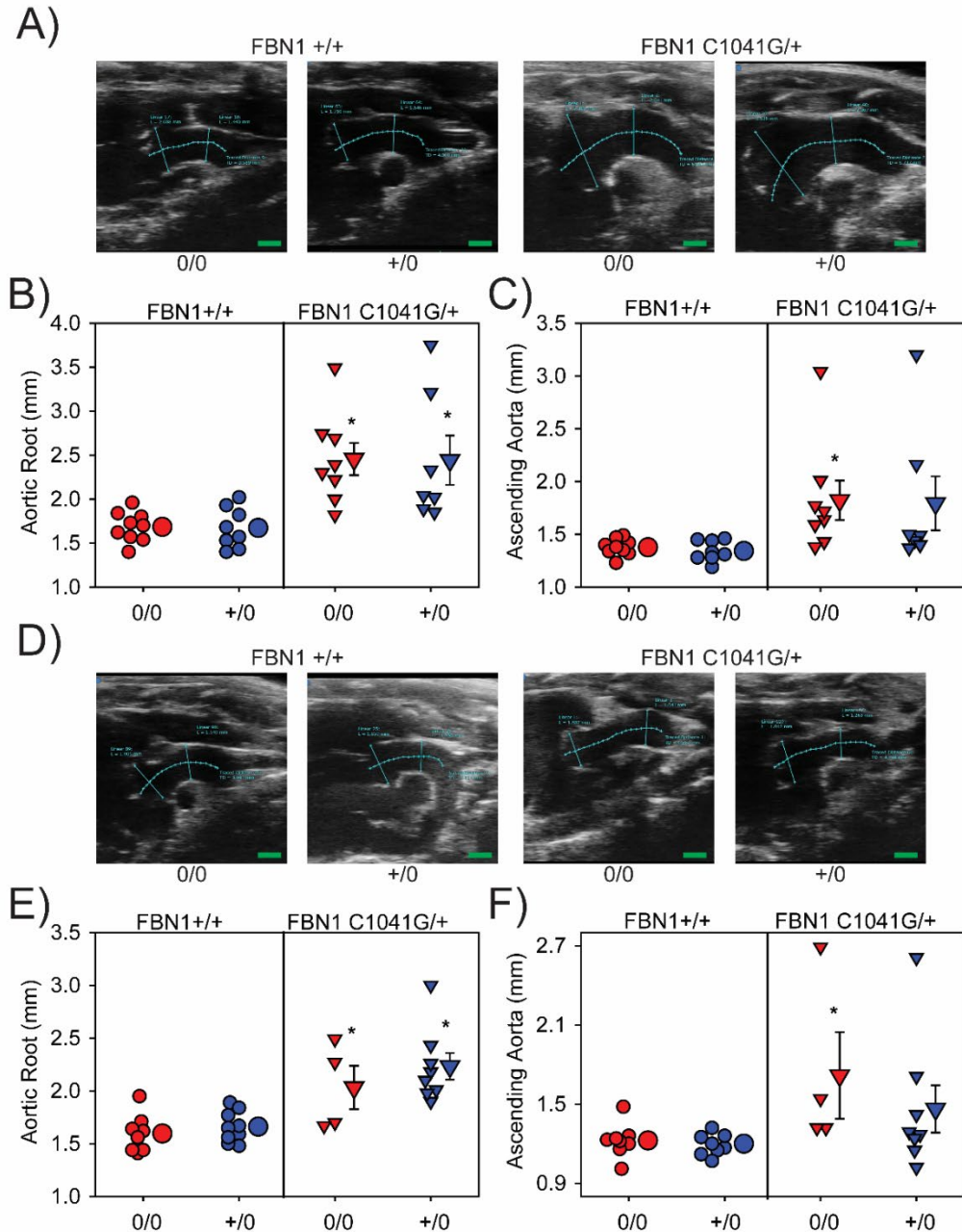


**Figure 5.3 Fibroblast specific AT1aR deletion failed to modulate TAA in Fbn1<sup>C1041G/+</sup> mice**

Representative ultrasound images in **A)** male and **D)** female mice with fibroblast specific deletion of AT1aR. S100A4-Cre driven deletion failed to attenuate **B,E)** aortic root and **C, F)** ascending aortic dilation. \* p < 0.05 when comparing Fbn1<sup>+/+</sup> vs. Fbn1<sup>C1041G/+</sup>.



## CHAPTER 6. DISCUSSION AND FUTURE DIRECTIONS

The overarching goal of these projects was to elucidate factors that were responsible for and can modulate development of Marfan syndrome associated thoracic aortic aneurysms. In accomplishing this goal, we not only developed and validated new methods but also defined the contributions of the AngII-AT1aR axis, sex hormones, and AT1aR on fibroblast to pathogenesis.

### 6.1 Key Methods

To trace the development of TAA sequentially, we needed a non-invasive, in-vivo method of assessing the ascending aorta over the course of the study. We utilized high frequency ultrasound as it had key advantages over other techniques of assessing the ascending aorta. Overall, strengths of ultrasound include low cost and rapid data acquisition compared to more resource intensive imaging modalities such as computed tomography (CT) and magnetic resonance imaging that have been used in studies of aortopathies. (134, 137, 170, 171) No contrast agent is needed for imaging small vessels and imaging data can be acquired much more rapidly with less resources. Additionally, data analysis for three-dimensional (3D) computed tomography and magnetic resonance imaging modalities is much more labor intensive. Despite these advantages, ultrasound has key limitations. Accurately imaging and measuring eccentric aortic dilation is difficult in two-dimensional (2D) ultrasonography. In fact, techniques such as phase contrast X-ray tomographic microscopy and contrast enhanced micro-CT have been proposed as a gold standard for 3D imaging of murine aortas because they are able to detect eccentric dilation. The trans-thoracic ultrasound acquisition and analysis protocol used in this study operates under the assumption that the maximum point of the aorta is imaged and that the aorta expands concentrically with the cardiac cycle. In the aneurysmal state, the dilation is eccentric. In fact, ulceration, dilation, and rupture preferentially occur along the greater curvature. (17) The point of greatest dilation may not occur perpendicular to the aortic valves and innominate artery where this study measures the ascending aorta. Therefore, 3D modalities are useful to elucidate small effect sizes while less accurate 2D methods may be sufficient if effects sizes are large. Advent of 3D ultrasound reconstruction may play a key role by utilizing the advantages of both techniques by decreasing acquisition times. In the lieu of 3D imaging modalities, ex vivo measurements may be valuable in illustrating aortic eccentricity in mice but is not feasible in longitudinal studies. While we did not assess if non-invasive 3D imaging modalities are indeed superior or more accurate, those interested in performing aortic imaging studies should balance the resource requirements against the desired accuracy and precision of the data.

To overcome the limitations of ultrasound, we additionally performed aortic histology to determine if our interventions directly impacted the ascending aorta. This allowed direct measurement of changes to the structure of aortic tissue but are also subject to limitations. We observed that aortas from Marfan syndrome mice exhibit extensive elastin fragmentation and fibrosis, suggesting a loss of elasticity and increase in stiffness. (12, 124) This is consistent with observations made in aneurysmal tissue from AngII-induced TAAs. (37) However, key limitations of histologic assessment of the aorta include the section of aorta measured and the subjective nature of measurement. The American Heart Association recommends that aortopathy studies keep consistent the region of aorta analyzed within a study. (33) As we measured aortic dilation at the area of maximal expansion, this means that histologic sections should be taken at area of maximal expansion as well. This is logistically difficult. While care was taken to quantify elastin fragmentation in the aortic section of largest dilation, aortic sections still are a two-dimensional representation of a tortuous three-dimensional structure. Additionally, assessment of elastin fragmentation and degree of staining was performed by human observers blinded to group assignment. While randomization and blinding reduce bias, use of human observers reduce both the resolution and throughput of measurements. Indeed, it is possible to train an agnostic computer program or artificial intelligence program to perform any measurement of image data in an unbiased manner. However, this would require not only development and deployment of this resource but also training data. Because of the small sample sizes and raw data, it would be difficult to generate both a training and test set of data. By including raw data available in our publications, we may enable future researchers to use our data as a training set for their experiments. Ultimately, these measurements do not stand alone but rather complement measurements from other modalities; we are confident in our observations due to the correlation and agreement of multiple modalities for measuring TAA severity.

## 6.2 Role of AngII-AT1aR axis in Marfan syndrome

We determined that inhibition of the AngII-AT1aR axis, by either pharmacologic depletion of the unique precursor of angiotensin ligands or genetic deletion of the main AT1 isoform in the aorta, attenuated TAA in the male *Fbn1<sup>C1041G/+</sup>* mice. Previous studies claimed that the protective effects of losartan in TAA stem from its pleiotropic or non-AT1aR dependent effects. Sellers et al claimed that losartan, an AT1aR blocker, had divergent effects on Marfan syndrome associated TAA compared to AT1aR deletion. (86) Specifically, losartan attenuated TAA through preservation of endothelial function in an AT1aR independent manner through an alternative VEGFR2/eNOS pathway. Other studies suggested that losartan's protective effect may be due to tumor growth factor  $\beta$  inhibition or AngII receptor type 2 hyperstimulation. (64, 83)

However, our data indicated that blockade of the AngII-AT1aR axis is sufficient to attenuate Marfan syndrome associated TAA. Consistent with our observations, a recently published study in the severe  $Fbn1^{mgR/mgR}$  model indicated that deletion of endothelial AT1aR reduced death by TAA rupture.(75)

Additionally, the contribution of angiotensin receptor ligands was unclear. Neither ACE inhibitors nor angiotensinogen knockout were efficacious in attenuating dilated cardiomyopathy in the  $Fbn1^{mgR/mgR}$  mouse model.(74) Unfortunately, use of either modality in aortopathy research is difficult due to pleotropic effects of ACE inhibitors on the kinin-kallikren system and cardio-renal developmental defects of AGT knockout.(155) Therefore, we used a systemic, post-natal inhibition of AGT synthesis via AGT ASO to deplete AGT.(149) This resulted in sustained AGT depletion and corresponded to reduction in Marfan syndrome associated TAA in male mice. We concluded that angiotensin receptor ligands are critical in TAA and that depletion of AGT is sufficient to attenuate Marfan syndrome associated TAA. These findings expanded previous understanding of the role of the renin angiotensin system in Marfan syndrome associated TAA and challenged the previous paradigm that non-AT1aR effects modulated TAA. While we do not discount the pleotropic effects of losartan and its metabolites, inhibition of AngII dependent AT1aR stimulation may be a key component in attenuating TAA.

However, the direct link between fibrillin-1 and the renin angiotensin system is not clear. It is unexpected that mutations in an extracellular matrix protein would impact the production of ligands responsible for blood pressure control. Angiotensin ligands are mainly synthesized in the liver, an organ not known to have abundant connective tissue. Thus fibrillin-1 may either act on local synthesis of angiotensin peptides or act on extra-aortic tissues in a yet undefined manner. To establish causal links between these two components, future studies should leverage inducible mutations of fibrillin-1 to trace progressive dysregulation of both the aortic and systemic renin angiotensin system.

### 6.3 Role of endogenous sex hormones in aortopathy

We demonstrated that removal of endogenous sex hormones was able to modulate spontaneous TAA. The AngII infusion mouse model induces thoracic aortic aneurysms in normolipidemic conditions and independent of blood pressure changes. (28, 37) Thoracic aortic aneurysms in AngII induced mice impact the ascending aorta more than the aortic root. While TAAs are characterized as a disease that preferentially impacts the aortic root, our group and others have demonstrated that TAA mouse models also involved the ascending aorta - defined as the segment proximal to the innominate artery. (31, 51, 64) Interestingly, gonadectomies did not affect lengthening of the ascending aorta in AngII infused mice, pointing to marked anisotropy of the ascending aorta. Indeed, this observation is consistent with those in abdominal aortic

aneurysms between male and female mice. Previous work in LDL receptor<sup>-/-</sup> x AngII-induced abdominal aortic aneurysms (AAAs) revealed that having a female sex chromosome complement and exposure to endogenous female sex hormone attenuates initiation, progression, and extent of AAAs. (160, 161, 172)

Conversely, our data suggests that removal of endogenous sex hormones was unable to modulate established TAA in Fbn1<sup>mgR/mgR</sup> mice. The FBN1<sup>mgR/mgR</sup> mice exhibit rapid dilation and death by aortic rupture early in life. Indeed, by 56 days old – when our gonadectomy studies were initiated, approximately 10% of male FBN1<sup>mgR/mgR</sup> mice would have expired due to TAA rupture. This mortality makes working with FBN1<sup>mgR/mgR</sup> mice difficult as interventions would need to have dramatic effect to alleviate already present aortic dilation. Thus, the effect of gonadectomy in modulating TAA in FBN1<sup>mgR/mgR</sup> mice may be masked by both existing TAA and mortality due to TAA rupture. Future experiments should investigate the effect of gonadectomy in the milder FBN1 C1041G/+ or GT8/+ models that do not have marked mortality to allow measurement over a longer course. (11, 52) Before we can make the conclusion that gonadectomy is ineffective in syndromic TAA, we must first establish if it acts on the initiation or progression of TAA.

#### 6.4 Role of AT1aR on fibroblasts in aortopathy

S100A4-Cre mediated deletion of AT1aR on fibroblasts had divergent effects on AngII-induced TAA versus Fbn1<sup>C1041G/+</sup> mediated TAA. While we have discussed the limitations of using S100a4-Cre as a fibroblast specific Cre, the divergent effects on spontaneous and syndromic aortopathies merit discussion. The mechanism by which this occurs is unclear. All components necessary for the deletion of AT1aR were present in germ line cells. However, we make the assumption that deletion of AT1aR was equivalent between C57BL/6J mice and Fbn1<sup>C1041G/+</sup> mice. This may not be true as AngII infusion increases S100A4-Cre traced cells in the aortic media. On future experiment that would allow us to interpret these results would be to lineage trace S100A4-Cre positive cells in the Fbn1<sup>C1041G/+</sup> mice in a lineage tracing experiment.

Initially, the obvious hypothesis was that AT1aR on cells of the aortic wall were responsible for aortopathy. In conjunction with other published studies, AT1aR deletion on all major cell types in the aorta have been performed. Endothelial specific AT1aR deletion has marginal effect on TAA. Smooth muscle specific AT1aR has no effect. Fibroblast specific deletion has partial effect on AngII induced aortopathies and no effect of syndromic TAA. Thus, the cell type where AT1aR is stimulated is still unknown. Altogether, there are two alternate hypotheses. First, it is possible that extra-aortic AT1aR is responsible for aortopathies. Indeed, promising results show that renal specific AT1aR deletion modulates atherosclerosis through yet undefined means. Additionally, the base assumption that a single cell type is responsible for TAA becomes increasingly

untenable. While breeding multiple cell lineage specific deletions in a single animal requires novel mouse models and heroic efforts, new targeted gene editing technologies and pharmacologic agents may allow a combination of cell specific knockdowns. For example, it is now possible to target antisense oligonucleotides to both the liver and the kidney independently. The responsible cell(s) type for TAA will eventually be discovered.

## 6.5 Future directions

Several avenues of promising research stem from the studies outlined here. The overarching goals should remain increasing understanding of and developing therapies for Marfan syndrome associated TAA.

It is unclear whether the contribution of disparate systems, such as the renin angiotensin system and endogenous sex hormones, to Marfan syndrome associated TAA occur in isolation or have cross talk. The renin angiotensin system effects some functions through regulation of aldosterone, a mineralocorticoid hormone. While its main function is to regulate salt and water balance as well as blood pressure, pleiotropic effects on endogenous sex hormones is less well known. Conversely, it is known that circulating sex hormone levels regulate liver protein synthesis. As angiotensinogen in the plasma is mainly synthesized by the liver, it is unknown if gonadectomy alters the renin angiotensin system in a manner that would affect aortopathies. Finally, as both the renin angiotensin system and sex hormones have many downstream effectors, it is unclear where these pathways intersect. Future studies may leverage unbiased multi-omics to uncover these interaction networks. The goal of those studies should focus on common up or downstream regulators that can be pharmacologically targeted.

Future mouse studies should also aim to resolve controversy and divergent effects seen between spontaneous and syndromic TAA. Differences may stem from differences in the timing of initiating events. The aorta develops between embryonic day 14 and postnatal day 21. Many spontaneous TAAs rely on an investigator-initiated administration of a causative agent. This usually occurs much later, at around 8 weeks of age. Absent a vascular insult, the aortas from baseline mice can be considered normal and non-aneurysmal. Indeed, it is rare for C57BL/6J mice to spontaneously develop TAA even at advanced ages. In contrast, syndromic models rely on a germline mutation, and thus the initiating event occurs in utero. The consequences of difference in timing may underly the divergent effects of gonadectomy as this is after sexual maturity. Therefore, inducible models of syndromic TAA, using an inducible Cre-Lox system to mutate or delete causative genes such as *Fbn1*, can be used to control the timing of the vascular insult. Conversely, it may be possible for investigators to initiate administration of TAA causing agents earlier.

It is critical to test observations and paradigms elucidated in mouse studies in a human population. Observations to be tested include the role of the AngII-AT1aR axis on Marfan syndrome associated TAA and the effects of sex on spontaneous and syndromic TAA. We may leverage clinical data by performing a retrospective observational study looking at the association of either pharmacologic agents or sex and TAA and aortic dissection. To study if TAA is also modulated by AT1aR in a ligand dependent manner, we can test the association between ACE inhibitors, ARBs, and aortic phenotypes. To study if sex hormones modulate TAA, we may look at the incidence of TAA and dissection in pre- versus post- menopausal females, males and females currently receiving hormone therapy, or males and females who have received surgical oophorectomy or orchiectomy. However, the populations of these patients may be small thus these studies would have difficulty achieving power. Unfortunately, it is difficult to perform lineage tracing and developmental biology experiments in humans. However, primary cell lines or induced pluripotent stem cells may be leveraged to test AT1aR dependent signaling pathways in humans. Ultimately, the cell type to be tested would depend on the cell type elucidated in mouse studies. Thus, the studies outlined here as well as future studies can be leveraged to generate hypotheses to be tested in humans.

Development of an effective pharmacologic agent hinges on the demonstrating superiority to current standard of care. However, current standard of care varies between institutions and providers. Patients with Marfan syndrome are generally treated with beta-adrenocorticoreceptor blockers and angiotensin receptor blockers. However, evidence for the efficacy of either agent is lacking. Evidence for use of beta-adrenocorticoreceptor blockers is based on one underpowered study that had strong predisposition to bias. (59) Evidence for use of angiotensin receptor blockers is mixed, with several studies of losartan showing minimal effect. (58) The widespread use of either agent means that any new agents would be trialed as an add-on agent to standard of care. Promising agents include AGT-ASOs and – if demonstrated in future experiments – agents that modulate estrogens or androgens or their targets in the aorta.

Ultimately, these avenues of research should be performed concurrently and in an iterative manner. Novel observations in mouse studies can be confirmed in retrospective human data and further refined by developing more specific and targeted pharmacologic agents. Associations seen in humans studies can be tested in the optimized environment using validated mouse models to discover their mechanism of action. Granting agencies and foundations should champion research programs in both areas concurrently. Trainees and faculty should aim to collaborate across disciplines if not receive training in interdisciplinary techniques themselves. Momentum behind this research is building. Marfan syndrome was first described in 1896. The gene responsible, FBN1, was discovered in 1995. The first promising agent in mice and humans was described in 2006. Throughout this timeline, life expectancy in

patients living with Marfan syndrome has increased. It is hoped that the studies outline here provide a platform to continue this momentum.

## REFERENCES

1. Lee B, Godfrey M, Vitale E, Hori H, Mattei MG, Sarfarazi M, Tsipouras P, Ramirez F, Hollister DW. Linkage of Marfan Syndrome and a Phenotypically Related Disorder to Two Different Fibrillin Genes. *Nature*. 1991;352(6333):330-4. Epub 1991/07/25. doi: 10.1038/352330a0. PubMed PMID: 1852206.
2. Loeys BL, Dietz HC, Braverman AC, Callewaert BL, De Backer J, Devereux RB, Hilhorst-Hofstee Y, Jondeau G, Faivre L, Milewicz DM, Pyeritz RE, Sponseller PD, Wordworth P, De Paepe AM. The Revised Ghent Nosology for the Marfan Syndrome. *J Med Genet*. 2010;47(7):476-85. Epub 2010/07/02. doi: 10.1136/jmg.2009.072785. PubMed PMID: 20591885.
3. Holmes KW, Maslen CL, Kindem M, Kroner BL, Song HK, Ravekes W, Dietz HC, Weinsaft JW, Roman MJ, Devereux RB, Pyeritz RE, Bavaria J, Milewski K, Milewicz D, LeMaire SA, Hendershot T, Eagle KA, Tolunay HE, Desvigne-Nickens P, Silberbach M. Gentac Registry Report: Gender Differences among Individuals with Genetically Triggered Thoracic Aortic Aneurysm and Dissection. *American journal of medical genetics Part A*. 2013;161a(4):779-86. Epub 2013/02/28. doi: 10.1002/ajmg.a.35836. PubMed PMID: 23444191; PMCID: PMC3606679.
4. Roman MJ, Devereux RB, Preiss LR, Asch FM, Eagle KA, Holmes KW, LeMaire SA, Maslen CL, Milewicz DM, Morris SA, Prakash SK, Pyeritz RE, Ravekes WJ, Shohet RV, Song HK, Weinsaft JW. Associations of Age and Sex with Marfan Phenotype: The National Heart, Lung, and Blood Institute Gentac (Genetically Triggered Thoracic Aortic Aneurysms and Cardiovascular Conditions) Registry. *Circulation Cardiovascular genetics*. 2017;10(3). Epub 2017/06/11. doi: 10.1161/circgenetics.116.001647. PubMed PMID: 28600386; PMCID: PMC5500868.
5. Siddiqi HK, Luminais SN, Montgomery D, Bossone E, Dietz H, Evangelista A, Isselbacher E, LeMaire S, Manfredini R, Milewicz D, Nienaber CA, Roman M, Sechtem U, Silberbach M, Eagle KA, Pyeritz RE. Chronobiology of Acute Aortic Dissection in the Marfan Syndrome (from the National Registry of Genetically Triggered Thoracic Aortic Aneurysms and Cardiovascular Conditions and the International Registry of Acute Aortic Dissection). *Am J Cardiol*. 2017;119(5):785-9. Epub 2017/01/10. doi: 10.1016/j.amjcard.2016.11.021. PubMed PMID: 28065489.
6. Dietz HC, Pyeritz RE. Mutations in the Human Gene for Fibrillin-1 (Fbn1) in the Marfan Syndrome and Related Disorders. *Hum Mol Genet*. 1995;4 Spec No:1799-809. Epub 1995/01/01. PubMed PMID: 8541880.
7. Perejda AJ, Abraham PA, Carnes WH, Coulson WF, Uitto J. Marfan's Syndrome: Structural, Biochemical, and Mechanical Studies of the Aortic Media. *The Journal of laboratory and clinical medicine*. 1985;106(4):376-83. Epub 1985/10/01. PubMed PMID: 4045295.
8. Abraham PA, Perejda AJ, Carnes WH, Uitto J. Marfan Syndrome. Demonstration of Abnormal Elastin in Aorta. *The Journal of clinical investigation*. 1982;70(6):1245-52. Epub 1982/12/01. PubMed PMID: 7174792; PMCID: PMC370341.



9. Robertson IB, Dias HF, Osuch IH, Lowe ED, Jensen SA, Redfield C, Handford PA. The N-Terminal Region of Fibrillin-1 Mediates a Bipartite Interaction with Ltbp1. *Structure*. 2017. Epub 2017/07/04. doi: 10.1016/j.str.2017.06.003. PubMed PMID: 28669633.
10. Robertson IB, Horiguchi M, Zilberberg L, Dabovic B, Hadjiolova K, Rifkin DB. Latent Tgf-B-Binding Proteins. *Matrix Biol*. 2015;47:44-53. Epub 2015/05/12. doi: 10.1016/j.matbio.2015.05.005. PubMed PMID: 25960419; PMCID: PMC4844006.
11. Judge DP, Biery NJ, Keene DR, Geubtner J, Myers L, Huso DL, Sakai LY, Dietz HC. Evidence for a Critical Contribution of Haploinsufficiency in the Complex Pathogenesis of Marfan Syndrome. *The Journal of clinical investigation*. 2004;114(2):172-81. doi: 10.1172/JCI20641. PubMed PMID: 15254584; PMCID: PMC449744.
12. Pereira L, Lee SY, Gayraud B, Andrikopoulos K, Shapiro SD, Bunton T, Biery NJ, Dietz HC, Sakai LY, Ramirez F. Pathogenetic Sequence for Aneurysm Revealed in Mice Underexpressing Fibrillin-1. *Proc Natl Acad Sci U S A*. 1999;96(7):3819-23. PubMed PMID: 10097121; PMCID: PMC22378.
13. Charbonneau NL, Manalo EC, Tufa SF, Carlson EJ, Carlberg VM, Keene DR, Sakai LY. Fibrillin-1 in the Vasculature: In Vivo Accumulation of Egfp-Tagged Fibrillin-1 in a Knockin Mouse Model. *Anatomical record (Hoboken, NJ : 2007)*. 2019. Epub 2019/06/30. doi: 10.1002/ar.24217. PubMed PMID: 31251835.
14. Cook JR, Smaldone S, Cozzolino C, del Solar M, Lee-Arteaga S, Nistala H, Ramirez F. Generation of Fbn1 Conditional Null Mice Implicates the Extracellular Microfibrils in Osteoprogenitor Recruitment. *Genesis*. 2012;50(8):635-41. Epub 2012/03/01. doi: 10.1002/dvg.22022. PubMed PMID: 22374917; PMCID: PMC3405165.
15. Sawada H, Chen JZ, Wright BC, Sheppard MB, Lu HS, Daugherty A. Heterogeneity of Aortic Smooth Muscle Cells: A Determinant for Regional Characteristics of Thoracic Aortic Aneurysms? *Journal of translational internal medicine*. 2018;6(3):93-6. Epub 2018/11/15. doi: 10.2478/jtim-2018-0023. PubMed PMID: 30425944; PMCID: PMC6231305.
16. Sawada H, Rateri DL, Moorlegghen JJ, Majesky MW, Daugherty A. Smooth Muscle Cells Derived from Second Heart Field and Cardiac Neural Crest Reside in Spatially Distinct Domains in the Media of the Ascending Aorta-Brief Report. *Arterioscler Thromb Vasc Biol*. 2017;37(9):1722-6. Epub 2017/07/01. doi: 10.1161/atvbaha.117.309599. PubMed PMID: 28663257; PMCID: PMC5570666.
17. Rateri DL, Davis FM, Balakrishnan A, Howatt DA, Moorlegghen JJ, O'Connor WN, Charnigo R, Cassis LA, Daugherty A. Angiotensin II Induces Region-Specific Medial Disruption During Evolution of Ascending Aortic Aneurysms. *Am J Pathol*. 2014;184(9):2586-95. doi: 10.1016/j.ajpath.2014.05.014. PubMed PMID: 25038458; PMCID: 25038458.
18. Lin CJ, Staiculescu MC, Hawes JZ, Cocciolone AJ, Hunkins BM, Roth RA, Lin CY, Mecham RP, Wagenseil JE. Heterogeneous Cellular Contributions to Elastic Laminae Formation in Arterial Wall Development. *Circ Res*. 2019;125(11):1006-18. Epub 2019/10/09. doi: 10.1161/CIRCRESAHA.119.315348. PubMed PMID: 31590613.

19. Wagenseil JE, Ciliberto CH, Knutsen RH, Levy MA, Kovacs A, Mecham RP. The Importance of Elastin to Aortic Development in Mice. *Am J Physiol Heart Circ Physiol.* 2010;299(2):H257-64. Epub 2010/05/25. doi: 10.1152/ajpheart.00194.2010. PubMed PMID: 20495146; PMCID: PMC2930379.
20. Le VP, Knutsen RH, Mecham RP, Wagenseil JE. Decreased Aortic Diameter and Compliance Precedes Blood Pressure Increases in Postnatal Development of Elastin-Insufficient Mice. *Am J Physiol Heart Circ Physiol.* 2011;301(1):H221-9. Epub 2011/05/04. doi: 10.1152/ajpheart.00119.2011. PubMed PMID: 21536846; PMCID: PMC3129922.
21. Jiao Y, Li G, Korneva A, Caulk AW, Qin L, Bersi MR, Li Q, Li W, Mecham RP, Humphrey JD, Tellides G. Deficient Circumferential Growth Is the Primary Determinant of Aortic Obstruction Attributable to Partial Elastin Deficiency. *Arterioscler Thromb Vasc Biol.* 2017;37(5):930-41. Epub 2017/03/04. doi: 10.1161/atvbaha.117.309079. PubMed PMID: 28254817; PMCID: PMC5501334.
22. Faury G, Pezet M, Knutsen RH, Boyle WA, Heximer SP, McLean SE, Minkes RK, Blumer KJ, Kovacs A, Kelly DP, Li DY, Starcher B, Mecham RP. Developmental Adaptation of the Mouse Cardiovascular System to Elastin Haploinsufficiency. *The Journal of clinical investigation.* 2003;112(9):1419-28. Epub 2003/11/05. doi: 10.1172/jci19028. PubMed PMID: 14597767; PMCID: PMC228452.
23. Ushiki T. Collagen Fibers, Reticular Fibers and Elastic Fibers. A Comprehensive Understanding from a Morphological Viewpoint. *Archives of histology and cytology.* 2002;65(2):109-26. Epub 2002/08/08. PubMed PMID: 12164335.
24. Schriebl AJ, Zeindlinger G, Pierce DM, Regitnig P, Holzappel GA. Determination of the Layer-Specific Distributed Collagen Fibre Orientations in Human Thoracic and Abdominal Aortas and Common Iliac Arteries. *Journal of the Royal Society, Interface.* 2012;9(71):1275-86. Epub 2011/12/16. doi: 10.1098/rsif.2011.0727. PubMed PMID: 22171063; PMCID: PMC3350738.
25. Wolinsky H, Glagov S. Comparison of Abdominal and Thoracic Aortic Medial Structure in Mammals. Deviation of Man from the Usual Pattern. *Circ Res.* 1969;25(6):677-86. Epub 1969/12/01. PubMed PMID: 5364644.
26. Dagenais F. Anatomy of the Thoracic Aorta and of Its Branches. *Thoracic surgery clinics.* 2011;21(2):219-27, viii. Epub 2011/04/12. doi: 10.1016/j.thorsurg.2010.12.004. PubMed PMID: 21477772.
27. Halloran BG, Davis VA, McManus BM, Lynch TG, Baxter BT. Localization of Aortic Disease Is Associated with Intrinsic Differences in Aortic Structure. *J Surg Res.* 1995;59(1):17-22. Epub 1995/07/01. doi: 10.1006/jsre.1995.1126. PubMed PMID: 7630123.
28. Owens AP, 3rd, Subramanian V, Moorleghen JJ, Guo Z, McNamara CA, Cassis LA, Daugherty A. Angiotensin II Induces a Region-Specific Hyperplasia of the Ascending Aorta through Regulation of Inhibitor of Differentiation 3. *Circ Res.* 2010;106(3):611-9. Epub 2009/12/19. doi: 10.1161/circresaha.109.212837. PubMed PMID: 20019328; PMCID: PMC2825288.
29. Ohtsuka S, Kakihana M, Watanabe H, Sugishita Y. Chronically Decreased Aortic Distensibility Causes Deterioration of Coronary Perfusion During Increased

- Left Ventricular Contraction. *Journal of the American College of Cardiology*. 1994;24(5):1406-14. Epub 1994/11/01. PubMed PMID: 7930267.
30. MacFarlane EG, Parker SJ, Shin JY, Ziegler SG, Creamer TJ, Bagirzadeh R, Bedja D, Chen Y, Calderon JF, Weissler K, Frischmeyer-Guerrero PA, Lindsay ME, Habashi JP, Dietz HC. Lineage-Specific Events Underlie Aortic Root Aneurysm Pathogenesis in Loeys-Dietz Syndrome. *The Journal of clinical investigation*. 2019. Epub 2019/01/08. doi: 10.1172/jci123547. PubMed PMID: 30614814.
31. Koenig SN, LaHaye S, Feller JD, Rowland P, Hor KN, Trask AJ, Janssen PM, Radtke F, Lilly B, Garg V. Notch1 Haploinsufficiency Causes Ascending Aortic Aneurysms in Mice. *JCI insight*. 2017;2(21). Epub 2017/11/03. doi: 10.1172/jci.insight.91353. PubMed PMID: 29093270.
32. Robinet P, Milewicz DM, Cassis LA, Leeper NJ, Lu HS, Smith JD. Consideration of Sex Differences in Design and Reporting of Experimental Arterial Pathology Studies-Statement from Atvb Council. *Arterioscler Thromb Vasc Biol*. 2018;38(2):292-303. Epub 2018/01/06. doi: 10.1161/atvbaha.117.309524. PubMed PMID: 29301789; PMCID: PMC5785439.
33. Daugherty A, Tall AR, Daemen M, Falk E, Fisher EA, Garcia-Cardena G, Lusis AJ, Owens AP, 3rd, Rosenfeld ME, Virmani R. Recommendation on Design, Execution, and Reporting of Animal Atherosclerosis Studies: A Scientific Statement from the American Heart Association. *Arterioscler Thromb Vasc Biol*. 2017;37(9):e131-e57. Epub 2017/07/22. doi: 10.1161/atv.0000000000000062. PubMed PMID: 28729366.
34. Sawada H, Chen JZ, Wright BC, Moorleggen JJ, Lu HS, Daugherty A. Ultrasound Imaging of the Thoracic and Abdominal Aorta in Mice to Determine Aneurysm Dimensions. *J Vis Exp*. 2019;8(145):10.3791/59013. Epub 2019/03/26. doi: 10.3791/59013. PubMed PMID: 30907888; PMCID: PMC6594159.
35. Chen JZ, Sawada H, Moorleggen JJ, Weiland M, Daugherty A, Sheppard MB. Aortic Strain Correlates with Elastin Fragmentation in Fibrillin-1 Hypomorphic Mice. *Circ Rep*. 2019;1(5):199-205. doi: 10.1253/circrep.CR-18-0012. PubMed PMID: 31123721; PMCID: PMC6528667.
36. Hiratzka LF, Bakris GL, Beckman JA, Bersin RM, Carr VF, Casey DE, Jr., Eagle KA, Hermann LK, Isselbacher EM, Kazerooni EA, Kouchoukos NT, Lytle BW, Milewicz DM, Reich DL, Sen S, Shinn JA, Svensson LG, Williams DM, American College of Cardiology Foundation/American Heart Association Task Force on Practice G, American Association for Thoracic S, American College of R, American Stroke A, Society of Cardiovascular A, Society for Cardiovascular A, Interventions, Society of Interventional R, Society of Thoracic S, Society for Vascular M. 2010 Accf/Aha/Aats/Acr/Asa/Sca/Scai/Sir/Sts/Svm Guidelines for the Diagnosis and Management of Patients with Thoracic Aortic Disease: A Report of the American College of Cardiology Foundation/American Heart Association Task Force on Practice Guidelines, American Association for Thoracic Surgery, American College of Radiology, American Stroke Association, Society of Cardiovascular Anesthesiologists, Society for Cardiovascular Angiography and Interventions, Society of Interventional Radiology, Society of Thoracic Surgeons,

- and Society for Vascular Medicine. *Circulation*. 2010;121(13):e266-369. doi: 10.1161/CIR.0b013e3181d4739e. PubMed PMID: 20233780.
37. Daugherty A, Rateri DL, Charo IF, Owens AP, Howatt DA, Cassis LA. Angiotensin II Infusion Promotes Ascending Aortic Aneurysms: Attenuation by Ccr2 Deficiency in Apoe<sup>-/-</sup> Mice. *Clinical science*. 2010;118(11):681-9. doi: 10.1042/CS20090372. PubMed PMID: 20088827; PMCID: PMC2841499.
38. Ren W, Liu Y, Wang X, Jia L, Piao C, Lan F, Du J. Beta-Aminopropionitrile Monofumarate Induces Thoracic Aortic Dissection in C57bl/6 Mice. *Sci Rep*. 2016;6:28149. Epub 2016/06/23. doi: 10.1038/srep28149. PubMed PMID: 27329825; PMCID: PMC4916438.
39. Liu S, Xie Z, Daugherty A, Cassis LA, Pearson KJ, Gong MC, Guo Z. Mineralocorticoid Receptor Agonists Induce Mouse Aortic Aneurysm Formation and Rupture in the Presence of High Salt. *Arterioscler Thromb Vasc Biol*. 2013;33(7):1568-79. doi: 10.1161/ATVBAHA.112.300820. PubMed PMID: 23661677; PMCID: PMC3707291.
40. Aoyama T, Francke U, Dietz HC, Furthmayr H. Quantitative Differences in Biosynthesis and Extracellular Deposition of Fibrillin in Cultured Fibroblasts Distinguish Five Groups of Marfan Syndrome Patients and Suggest Distinct Pathogenetic Mechanisms. *The Journal of clinical investigation*. 1994;94(1):130-7. doi: 10.1172/JCI117298. PubMed PMID: 8040255; PMCID: PMC296290.
41. Guo DC, Regalado ES, Gong L, Duan X, Santos-Cortez RL, Arnaud P, Ren Z, Cai B, Hostetler EM, Moran R, Liang D, Estrera A, Safi HJ, University of Washington Center for Mendelian G, Leal SM, Bamshad MJ, Shendure J, Nickerson DA, Jondeau G, Boileau C, Milewicz DM. Lox Mutations Predispose to Thoracic Aortic Aneurysms and Dissections. *Circ Res*. 2016;118(6):928-34. doi: 10.1161/CIRCRESAHA.115.307130. PubMed PMID: 26838787; PMCID: PMC4839295.
42. Guo DC, Regalado ES, Pinard A, Chen J, Lee K, Rigelsky C, Zilberberg L, Hostetler EM, Aldred M, Wallace SE, Prakash SK, Leal SM, Bamshad MJ, Nickerson DA, Natowicz M, Rifkin DB, Milewicz DM. Ltbp3 Pathogenic Variants Predispose Individuals to Thoracic Aortic Aneurysms and Dissections. *Am J Hum Genet*. 2018;102(4):706-12. Epub 2018/04/07. doi: 10.1016/j.ajhg.2018.03.002. PubMed PMID: 29625025; PMCID: PMC5985335.
43. Loeyls BL, Schwarze U, Holm T, Callewaert BL, Thomas GH, Pannu H, De Backer JF, Oswald GL, Symoens S, Manouvrier S, Roberts AE, Faravelli F, Greco MA, Pyeritz RE, Milewicz DM, Coucke PJ, Cameron DE, Braverman AC, Byers PH, De Paepe AM, Dietz HC. Aneurysm Syndromes Caused by Mutations in the Tgf-Beta Receptor. *N Engl J Med*. 2006;355(8):788-98. doi: 10.1056/NEJMoa055695. PubMed PMID: 16928994.
44. Jondeau G, Ropers J, Regalado E, Braverman A, Evangelista A, Teixido G, De Backer J, Muino-Mosquera L, Naudion S, Zordan C, Morisaki T, Morisaki H, Von Kodolitsch Y, Dupuis-Girod S, Morris SA, Jeremy R, Odent S, Ades LC, Bakshi M, Holman K, LeMaire S, Milleron O, Langeois M, Spentchian M, Aubart M, Boileau C, Pyeritz R, Milewicz DM. International Registry of Patients Carrying Tgfb1 or Tgfb2 Mutations: Results of the Montalcino Aortic Consortium.

- Circulation Cardiovascular genetics. 2016. Epub 2016/11/24. doi: 10.1161/circgenetics.116.001485. PubMed PMID: 27879313.
45. Bowen CJ, Calderon Giadrosic JF, Burger Z, Rykiel G, Davis EC, Helmers MR, Benke K, Gallo MacFarlane E, Dietz HC. Targetable Cellular Signaling Events Mediate Vascular Pathology in Vascular Ehlers-Danlos Syndrome. *The Journal of clinical investigation*. 2020;130(2):686-98. Epub 2019/10/23. doi: 10.1172/jci130730. PubMed PMID: 31639107; PMCID: PMC6994142.
46. Kuang SQ, Medina-Martinez O, Guo DC, Gong L, Regalado ES, Reynolds CL, Boileau C, Jondeau G, Prakash SK, Kwartler CS, Zhu LY, Peters AM, Duan XY, Bamshad MJ, Shendure J, Nickerson DA, Santos-Cortez RL, Dong X, Leal SM, Majesky MW, Swindell EC, Jamrich M, Milewicz DM. Foxe3 Mutations Predispose to Thoracic Aortic Aneurysms and Dissections. *The Journal of clinical investigation*. 2016;126(3):948-61. doi: 10.1172/JCI83778. PubMed PMID: 26854927; PMCID: PMC4767350.
47. Milewicz DM, Ostergaard JR, Ala-Kokko LM, Khan N, Grange DK, Mendoza-Londono R, Bradley TJ, Olney AH, Ades L, Maher JF, Guo D, Buja LM, Kim D, Hyland JC, Regalado ES. De Novo Acta2 Mutation Causes a Novel Syndrome of Multisystemic Smooth Muscle Dysfunction. *American journal of medical genetics Part A*. 2010;152a(10):2437-43. Epub 2010/08/25. doi: 10.1002/ajmg.a.33657. PubMed PMID: 20734336; PMCID: PMC3573757.
48. Milewicz DM, Prakash SK, Ramirez F. Therapeutics Targeting Drivers of Thoracic Aortic Aneurysms and Acute Aortic Dissections: Insights from Predisposing Genes and Mouse Models. *Annual review of medicine*. 2017;68:51-67. Epub 2017/01/19. doi: 10.1146/annurev-med-100415-022956. PubMed PMID: 28099082.
49. Wallace SE, Regalado ES, Gong L, Janda AL, Guo DC, Russo CF, Kulmacz RJ, Hanna N, Jondeau G, Boileau C, Arnaud P, Lee K, Leal SM, Hannuksela M, Carlberg B, Johnston T, Antolik C, Hostetler EM, Colombo R, Milewicz DM. Mylk Pathogenic Variants Aortic Disease Presentation, Pregnancy Risk, and Characterization of Pathogenic Missense Variants. *Genetics in medicine : official journal of the American College of Medical Genetics*. 2018. Epub 2018/06/22. doi: 10.1038/s41436-018-0038-0. PubMed PMID: 29925964.
50. Bellini C, Bersi MR, Caulk AW, Ferruzzi J, Milewicz DM, Ramirez F, Rifkin DB, Tellides G, Yanagisawa H, Humphrey JD. Comparison of 10 Murine Models Reveals a Distinct Biomechanical Phenotype in Thoracic Aortic Aneurysms. *Journal of the Royal Society, Interface*. 2017;14(130). Epub 2017/05/12. doi: 10.1098/rsif.2016.1036. PubMed PMID: 28490606.
51. Pereira L, Andrikopoulos K, Tian J, Lee SY, Keene DR, Ono R, Reinhardt DP, Sakai LY, Biery NJ, Bunton T, Dietz HC, Ramirez F. Targetting of the Gene Encoding Fibrillin-1 Recapitulates the Vascular Aspect of Marfan Syndrome. *Nature genetics*. 1997;17(2):218-22. Epub 1997/11/05. doi: 10.1038/ng1097-218. PubMed PMID: 9326947.
52. Charbonneau NL, Carlson EJ, Tufa S, Sengle G, Manalo EC, Carlberg VM, Ramirez F, Keene DR, Sakai LY. In Vivo Studies of Mutant Fibrillin-1 Microfibrils. *J Biol Chem*. 2010;285(32):24943-55. Epub 2010/06/10. doi: 10.1074/jbc.M110.130021. PubMed PMID: 20529844; PMCID: PMC2915730.

53. Angelov SN, Hu JH, Wei H, Airhart N, Shi M, Dichek DA. Tgf-Beta (Transforming Growth Factor-Beta) Signaling Protects the Thoracic and Abdominal Aorta from Angiotensin II-Induced Pathology by Distinct Mechanisms. *Arterioscler Thromb Vasc Biol.* 2017. Epub 2017/07/22. doi: 10.1161/atvbaha.117.309401. PubMed PMID: 28729364.
54. Hu JH, Wei H, Jaffe M, Airhart N, Du L, Angelov SN, Yan J, Allen JK, Kang I, Wight TN, Fox K, Smith A, Enstrom R, Dichek DA. Postnatal Deletion of the Type II Transforming Growth Factor-Beta Receptor in Smooth Muscle Cells Causes Severe Aortopathy in Mice. *Arterioscler Thromb Vasc Biol.* 2015;35(12):2647-56. doi: 10.1161/ATVBAHA.115.306573. PubMed PMID: 26494233; PMCID: PMC4743752.
55. Wei H, Hu JH, Angelov SN, Fox K, Yan J, Enstrom R, Smith A, Dichek DA. Aortopathy in a Mouse Model of Marfan Syndrome Is Not Mediated by Altered Transforming Growth Factor Beta Signaling. *J Am Heart Assoc.* 2017;6(1). Epub 2017/01/26. doi: 10.1161/jaha.116.004968. PubMed PMID: 28119285.
56. Renard M, Muino-Mosquera L, Manalo EC, Tufa S, Carlson EJ, Keene DR, De Backer J, Sakai LY. Sex, Pregnancy and Aortic Disease in Marfan Syndrome. *PLoS one.* 2017;12(7):e0181166. Epub 2017/07/15. doi: 10.1371/journal.pone.0181166. PubMed PMID: 28708846.
57. Hofmann Bowman MA, Eagle KA, Milewicz DM. Update on Clinical Trials of Losartan with and without Beta-Blockers to Block Aneurysm Growth in Patients with Marfan Syndrome: A Review. *JAMA cardiology.* 2019. Epub 2019/05/09. doi: 10.1001/jamacardio.2019.1176. PubMed PMID: 31066871.
58. Milewicz DM, Ramirez F. Therapies for Thoracic Aortic Aneurysms and Acute Aortic Dissections. *Arterioscler Thromb Vasc Biol.* 2019;Atvbaha118310956. Epub 2019/01/18. doi: 10.1161/atvbaha.118.310956. PubMed PMID: 30651002.
59. Koo HK, Lawrence KA, Musini VM. Beta-Blockers for Preventing Aortic Dissection in Marfan Syndrome. *The Cochrane database of systematic reviews.* 2017;11:Cd011103. Epub 2017/11/08. doi: 10.1002/14651858.CD011103.pub2. PubMed PMID: 29110304.
60. Groenink M, den Hartog AW, Franken R, Radonic T, de Waard V, Timmermans J, Scholte AJ, van den Berg MP, Spijkerboer AM, Marquering HA, Zwinderman AH, Mulder BJ. Losartan Reduces Aortic Dilatation Rate in Adults with Marfan Syndrome: A Randomized Controlled Trial. *Eur Heart J.* 2013;34(45):3491-500. doi: 10.1093/eurheartj/eh334. PubMed PMID: 23999449.
61. Lacro RV, Dietz HC, Sleeper LA, Yetman AT, Bradley TJ, Colan SD, Pearson GD, Tierney ESS, Levine JC, Atz AM, Benson DW, Braverman AC, Chen S, De Backer J, Gelb BD, Grossfeld PD, Klein GL, Lai WW, Liou A, Loeys BL, Markham LW, Olson AK, Paridon SM, Pemberton VL, Pierpont ME, Pyeritz RE, Radojewski E, Roman MJ, Sharkey AM, Stylianou MP, Wechsler SB, Young LT, Mahony L. Atenolol Versus Losartan in Children and Young Adults with Marfan's Syndrome. *N Engl J Med.* 2014;371(22):2061-71. doi: 10.1056/NEJMoa1404731.
62. Milleron O, Arnoult F, Ropers J, Aegerter P, Detaint D, Delorme G, Attias D, Tubach F, Dupuis-Girod S, Plauchu H, Barthelet M, Sassolas F, Pangaud N, Naudion S, Thomas-Chabaneix J, Dulac Y, Edouard T, Wolf JE, Faivre L, Odent

- S, Basquin A, Habib G, Collignon P, Boileau C, Jondeau G. Marfan Sartan: A Randomized, Double-Blind, Placebo-Controlled Trial. *Eur Heart J*. 2015;36(32):2160-6. doi: 10.1093/eurheartj/ehv151. PubMed PMID: 25935877.
63. Mullen M, Jin XY, Child A, Stuart AG, Dodd M, Aragon-Martin JA, Gaze D, Kiotsekoglou A, Yuan L, Hu J, Foley C, Van Dyck L, Knight R, Clayton T, Swan L, Thomson JDR, Erdem G, Crossman D, Flather M, Investigators A. Irbesartan in Marfan Syndrome (Aims): A Double-Blind, Placebo-Controlled Randomised Trial. *Lancet*. 2020;394(10216):2263-70. Epub 2019/12/15. doi: 10.1016/S0140-6736(19)32518-8. PubMed PMID: 31836196; PMCID: PMC6934233.
64. Habashi JP, Judge DP, Holm TM, Cohn RD, Loeys BL, Cooper TK, Myers L, Klein EC, Liu G, Calvi C, Podowski M, Neptune ER, Halushka MK, Bedja D, Gabrielson K, Rifkin DB, Carta L, Ramirez F, Huso DL, Dietz HC. Losartan, an At1 Antagonist, Prevents Aortic Aneurysm in a Mouse Model of Marfan Syndrome. *Science*. 2006;312(5770):117-21. doi: 10.1126/science.1124287. PubMed PMID: 16601194; PMCID: PMC1482474.
65. Doyle JJ, Doyle AJ, Wilson NK, Habashi JP, Bedja D, Whitworth RE, Lindsay ME, Schoenhoff F, Myers L, Huso N, Bachir S, Squires O, Rusholme B, Ehsan H, Huso D, Thomas CJ, Caulfield MJ, Van Eyk JE, Judge DP, Dietz HC, Gen TACRC, Consortium ML. A Deleterious Gene-by-Environment Interaction Imposed by Calcium Channel Blockers in Marfan Syndrome. *Elife*. 2015;4. doi: 10.7554/eLife.08648. PubMed PMID: 26506064; PMCID: PMC4621743.
66. Frankel WC, Trautner BW, Spiegelman A, Grigoryan L, LeMaire SA. Patients at Risk for Aortic Rupture Often Exposed to Fluoroquinolones During Hospitalization. *Antimicrobial agents and chemotherapy*. 2018. Epub 2018/11/28. doi: 10.1128/aac.01712-18. PubMed PMID: 30478167.
67. Wu C, Lu H, Cassis LA, Daugherty A. Molecular and Pathophysiological Features of Angiotensinogen: A Mini Review. *North American journal of medicine & science*. 2011;4(4):183-90. PubMed PMID: 22389749; PMCID: PMC3291105.
68. Lu H, Wu C, Howatt DA, Balakrishnan A, Moorlegheh JJ, Chen X, Zhao M, Graham MJ, Mullick AE, Crooke RM, Feldman DL, Cassis LA, Vander Kooi CW, Daugherty A. Angiotensinogen Exerts Effects Independent of Angiotensin II. *Arterioscler Thromb Vasc Biol*. 2016;36(2):256-65. doi: 10.1161/ATVBAHA.115.306740. PubMed PMID: 26681751; PMCID: PMC4732917.
69. Gaidarov I, Adams J, Frazer J, Anthony T, Chen X, Gatlin J, Semple G, Unett DJ. Angiotensin (1-7) Does Not Interact Directly with Mas1, but Can Potentially Antagonize Signaling from the At1 Receptor. *Cellular signalling*. 2018;50:9-24. Epub 2018/06/22. doi: 10.1016/j.cellsig.2018.06.007. PubMed PMID: 29928987.
70. Poduri A, Owens AP, 3rd, Howatt DA, Moorlegheh JJ, Balakrishnan A, Cassis LA, Daugherty A. Regional Variation in Aortic At1b Receptor mRNA Abundance Is Associated with Contractility but Unrelated to Atherosclerosis and Aortic Aneurysms. *PloS one*. 2012;7(10):e48462. Epub 2012/11/03. doi: 10.1371/journal.pone.0048462. PubMed PMID: 23119030; PMCID: PMC3485205.
71. Daugherty A, Rateri DL, Howatt DA, Charnigo R, Cassis LA. Pd123319 Augments Angiotensin II-Induced Abdominal Aortic Aneurysms through an At2

- Receptor-Independent Mechanism. *PLoS one*. 2013;8(4):e61849. Epub 2013/04/18. doi: 10.1371/journal.pone.0061849. PubMed PMID: 23593499; PMCID: PMC3625148.
72. Cassis LA, Rateri DL, Lu H, Daugherty A. Bone Marrow Transplantation Reveals That Recipient At1a Receptors Are Required to Initiate Angiotensin II-Induced Atherosclerosis and Aneurysms. *Arterioscler Thromb Vasc Biol*. 2007;27(2):380-6. doi: 10.1161/01.ATV.0000254680.71485.92. PubMed PMID: 17158350.
73. Cavanaugh NB, Qian L, Westergaard NM, Kutschke WJ, Born EJ, Turek JW. A Novel Murine Model of Marfan Syndrome Accelerates Aortopathy and Cardiomyopathy. *Ann Thorac Surg*. 2017;104(2):657-65. Epub 2017/03/30. doi: 10.1016/j.athoracsur.2016.10.077. PubMed PMID: 28347539; PMCID: PMC5705055.
74. Cook JR, Clayton NP, Carta L, Galatioto J, Chiu E, Smaldone S, Nelson CA, Cheng SH, Wentworth BM, Ramirez F. Dimorphic Effects of Transforming Growth Factor-Beta Signaling During Aortic Aneurysm Progression in Mice Suggest a Combinatorial Therapy for Marfan Syndrome. *Arterioscler Thromb Vasc Biol*. 2015;35(4):911-7. doi: 10.1161/ATVBAHA.114.305150. PubMed PMID: 25614286; PMCID: PMC4376614.
75. Galatioto J, Caescu CI, Hansen J, Cook JR, Miramontes I, Iyengar R, Ramirez F. Cell Type-Specific Contributions of the Angiotensin II Type 1a Receptor to Aorta Homeostasis and Aneurysmal Disease-Brief Report. *Arterioscler Thromb Vasc Biol*. 2018;38(3):588-91. Epub 2018/01/27. doi: 10.1161/ATVBAHA.117.310609. PubMed PMID: 29371244; PMCID: PMC5823778.
76. Yang HH, Kim JM, Chum E, van Breemen C, Chung AW. Long-Term Effects of Losartan on Structure and Function of the Thoracic Aorta in a Mouse Model of Marfan Syndrome. *British journal of pharmacology*. 2009;158(6):1503-12. doi: 10.1111/j.1476-5381.2009.00443.x. PubMed PMID: 19814725; PMCID: PMC2795217.
77. Lee JJ, Galatioto J, Rao S, Ramirez F, Costa KD. Losartan Attenuates Degradation of Aorta and Lung Tissue Micromechanics in a Mouse Model of Severe Marfan Syndrome. *Ann Biomed Eng*. 2016;44(10):2994-3006. doi: 10.1007/s10439-016-1616-4. PubMed PMID: 27090893.
78. Nistala H, Lee-Arteaga S, Carta L, Cook JR, Smaldone S, Siciliano G, Rifkin AN, Dietz HC, Rifkin DB, Ramirez F. Differential Effects of Alendronate and Losartan Therapy on Osteopenia and Aortic Aneurysm in Mice with Severe Marfan Syndrome. *Hum Mol Genet*. 2010;19(24):4790-8. doi: 10.1093/hmg/ddq409. PubMed PMID: 20871099; PMCID: PMC2989889.
79. Huang J, Davis EC, Chapman SL, Budatha M, Marmorstein LY, Word RA, Yanagisawa H. Fibulin-4 Deficiency Results in Ascending Aortic Aneurysms: A Potential Link between Abnormal Smooth Muscle Cell Phenotype and Aneurysm Progression. *Circ Res*. 2010;106(3):583-92. Epub 2009/12/19. doi: 10.1161/circresaha.109.207852. PubMed PMID: 20019329; PMCID: PMC2826613.



80. Li W, Li Q, Jiao Y, Qin L, Ali R, Zhou J, Ferruzzi J, Kim RW, Geirsson A, Dietz HC, Offermanns S, Humphrey JD, Tellides G. Tgfbr2 Disruption in Postnatal Smooth Muscle Impairs Aortic Wall Homeostasis. *The Journal of clinical investigation*. 2014;124(2):755-67. doi: 10.1172/JCI69942. PubMed PMID: 24401272; PMCID: PMC3904608.
81. Gallo EM, Loch DC, Habashi JP, Calderon JF, Chen Y, Bedja D, van Erp C, Gerber EE, Parker SJ, Sauls K, Judge DP, Cooke SK, Lindsay ME, Rouf R, Myers L, ap Rhys CM, Kent KC, Norris RA, Huso DL, Dietz HC. Angiotensin li-Dependent Tgf-Beta Signaling Contributes to Loeys-Dietz Syndrome Vascular Pathogenesis. *The Journal of clinical investigation*. 2014;124(1):448-60. doi: 10.1172/JCI69666. PubMed PMID: 24355923; PMCID: PMC3871227.
82. Triggle DJ. Angiotensin li Receptor Antagonism: Losartan - Sites and Mechanisms of Action. *Clin Ther*. 1995;17(6):1005-30. PubMed PMID: 8750395.
83. Habashi JP, Doyle JJ, Holm TM, Aziz H, Schoenhoff F, Bedja D, Chen Y, Modiri AN, Judge DP, Dietz HC. Angiotensin li Type 2 Receptor Signaling Attenuates Aortic Aneurysm in Mice through Erk Antagonism. *Science*. 2011;332(6027):361-5. doi: 10.1126/science.1192152. PubMed PMID: 21493863; PMCID: PMC3097422.
84. Wan Y, Wallinder C, Plouffe B, Beaudry H, Mahalingam AK, Wu X, Johansson B, Holm M, Botoros M, Karlen A, Pettersson A, Nyberg F, Fandriks L, Gallo-Payet N, Hallberg A, Alterman M. Design, Synthesis, and Biological Evaluation of the First Selective Nonpeptide At2 Receptor Agonist. *Journal of medicinal chemistry*. 2004;47(24):5995-6008. Epub 2004/11/13. doi: 10.1021/jm049715t. PubMed PMID: 15537354.
85. Lange C, Sommerfeld M, Namsolleck P, Kintscher U, Unger T, Kaschina E. At<Sub>2</Sub>R (Angiotensin At2 Receptor) Agonist, Compound 21, Prevents Abdominal Aortic Aneurysm Progression in the Rat. *Hypertension*. 2018. doi: 10.1161/hypertensionaha.118.11168.
86. Sellers SL, Milad N, Chan R, Mielnik M, Jermilova U, Huang PL, de Crom R, Hirota JA, Hogg JC, Sandor GG, Van Breemen C, Esfandiarei M, Seidman MA, Bernatchez P. Inhibition of Marfan Syndrome Aortic Root Dilation by Losartan: Role of Angiotensin li Receptor Type 1-Independent Activation of Endothelial Function. *Am J Pathol*. 2018;188(3):574-85. Epub 2018/02/13. doi: 10.1016/j.ajpath.2017.11.006. PubMed PMID: 29433732.
87. Chen X, Lu H, Zhao M, Tashiro K, Cassis LA, Daugherty A. Contributions of Leukocyte Angiotensin-Converting Enzyme to Development of Atherosclerosis. *Arterioscler Thromb Vasc Biol*. 2013;33(9):2075-80. doi: 10.1161/atvbaha.113.301777. PubMed PMID: 23846498; PMCID: 23846498.
88. Chen X, Howatt DA, Balakrishnan A, Moorlegheh JJ, Wu C, Cassis LA, Daugherty A, Lu H. Angiotensin-Converting Enzyme in Smooth Muscle Cells Promotes Atherosclerosis-Brief Report. *Arterioscler Thromb Vasc Biol*. 2016;36(6):1085-9. Epub 2016/04/09. doi: 10.1161/atvbaha.115.307038. PubMed PMID: 27055902; PMCID: PMC4882263.
89. Zou Y, Akazawa H, Qin Y, Sano M, Takano H, Minamino T, Makita N, Iwanaga K, Zhu W, Kudoh S, Toko H, Tamura K, Kihara M, Nagai T, Fukamizu A, Umemura S, Iiri T, Fujita T, Komuro I. Mechanical Stress Activates Angiotensin li

- Type 1 Receptor without the Involvement of Angiotensin II. *Nat Cell Biol.* 2004;6(6):499-506. doi: 10.1038/ncb1137. PubMed PMID: 15146194.
90. Sadoshima J, Xu Y, Slayter HS, Izumo S. Autocrine Release of Angiotensin II Mediates Stretch-Induced Hypertrophy of Cardiac Myocytes in Vitro. *Cell.* 1993;75(5):977-84. PubMed PMID: 8252633.
91. Li Q, Muragaki Y, Hatamura I, Ueno H, Ooshima A. Stretch-Induced Collagen Synthesis in Cultured Smooth Muscle Cells from Rabbit Aortic Media and a Possible Involvement of Angiotensin II and Transforming Growth Factor-Beta. *J Vasc Res.* 1998;35(2):93-103. Epub 1998/05/20. doi: 10.1159/000025570. PubMed PMID: 9588872.
92. Cook JR, Carta L, Benard L, Chemaly ER, Chiu E, Rao SK, Hampton TG, Yurchenco P, Gen TACRC, Costa KD, Hajjar RJ, Ramirez F. Abnormal Muscle Mechanosignaling Triggers Cardiomyopathy in Mice with Marfan Syndrome. *The Journal of clinical investigation.* 2014;124(3):1329-39. doi: 10.1172/JCI71059. PubMed PMID: 24531548; PMCID: PMC3934180.
93. Yetman AT, Bornemeier RA, McCrindle BW. Usefulness of Enalapril Versus Propranolol or Atenolol for Prevention of Aortic Dilatation in Patients with the Marfan Syndrome. *The American Journal of Cardiology.* 2005;95(9):1125-7. doi: <https://doi.org/10.1016/j.amjcard.2005.01.032>.
94. Sweeting MJ, Thompson SG, Brown LC, Greenhalgh RM, Powell JT. Use of Angiotensin Converting Enzyme Inhibitors Is Associated with Increased Growth Rate of Abdominal Aortic Aneurysms. *J Vasc Surg.* 2010;52(1):1-4. doi: 10.1016/j.jvs.2010.02.264. PubMed PMID: 20494541.
95. Hackam DG, Thiruchelvam D, Redelmeier DA. Angiotensin-Converting Enzyme Inhibitors and Aortic Rupture: A Population-Based Case-Control Study. *Lancet.* 2006;368(9536):659-65. doi: 10.1016/S0140-6736(06)69250-7. PubMed PMID: 16920471.
96. Bicknell CD, Kiru G, Falaschetti E, Powell JT, Poulter NR, Collaborators A. An Evaluation of the Effect of an Angiotensin-Converting Enzyme Inhibitor on the Growth Rate of Small Abdominal Aortic Aneurysms: A Randomized Placebo-Controlled Trial (Aardvark). *Eur Heart J.* 2016. doi: 10.1093/eurheartj/ehw257. PubMed PMID: 27371719.
97. Katwa LC, Ratajska A, Cleutjens JP, Sun Y, Zhou G, Lee SJ, Weber KT. Angiotensin Converting Enzyme and Kininase-II-Like Activities in Cultured Valvular Interstitial Cells of the Rat Heart. *Cardiovasc Res.* 1995;29(1):57-64. Epub 1995/01/01. PubMed PMID: 7895240.
98. Regoli D, Gobeil F. Kallikrein-Kinin System as the Dominant Mechanism to Counteract Hyperactive Renin-Angiotensin System. *Canadian journal of physiology and pharmacology.* 2017;95(10):1117-24. Epub 2017/04/07. doi: 10.1139/cjpp-2016-0619. PubMed PMID: 28384411.
99. Gohlke P, Pees C, Unger T. AT2 Receptor Stimulation Increases Aortic Cyclic Gmp in SHRSP by a Kinin-Dependent Mechanism. *Hypertension.* 1998;31(1 Pt 2):349-55. Epub 1998/02/07. PubMed PMID: 9453327.
100. Poduri A, Rateri DL, Howatt DA, Balakrishnan A, Moorleggen JJ, Cassis LA, Daugherty A. Fibroblast Angiotensin II Type 1a Receptors Contribute to Angiotensin II-Induced Medial Hyperplasia in the Ascending Aorta. *Arterioscler*

- Thromb Vasc Biol. 2015;35(9):1995-2002. doi: 10.1161/ATVBAHA.115.305995. PubMed PMID: 26160957; PMCID: PMC4552596.
101. Trask TM, Trask BC, Ritty TM, Abrams WR, Rosenbloom J, Mecham RP. Interaction of Tropoelastin with the Amino-Terminal Domains of Fibrillin-1 and Fibrillin-2 Suggests a Role for the Fibrillins in Elastic Fiber Assembly. *J Biol Chem.* 2000;275(32):24400-6. Epub 2000/05/29. doi: 10.1074/jbc.M003665200. PubMed PMID: 10825173.
102. Reinhardt DP, Keene DR, Corson GM, Poschl E, Bachinger HP, Gambée JE, Sakai LY. Fibrillin-1: Organization in Microfibrils and Structural Properties. *J Mol Biol.* 1996;258(1):104-16. doi: 10.1006/jmbi.1996.0237. PubMed PMID: 8613981.
103. Reinhardt DP, Gambée JE, Ono RN, Bachinger HP, Sakai LY. Initial Steps in Assembly of Microfibrils. Formation of Disulfide-Cross-Linked Multimers Containing Fibrillin-1. *J Biol Chem.* 2000;275(3):2205-10. Epub 2000/01/15. doi: 10.1074/jbc.275.3.2205. PubMed PMID: 10636927.
104. Schrijver I, Liu W, Brenn T, Furthmayr H, Francke U. Cysteine Substitutions in Epidermal Growth Factor-Like Domains of Fibrillin-1: Distinct Effects on Biochemical and Clinical Phenotypes. *Am J Hum Genet.* 1999;65(4):1007-20. Epub 1999/09/16. doi: 10.1086/302582. PubMed PMID: 10486319; PMCID: PMC1288233.
105. Zeyer KA, Zhang RM, Kumra H, Hassan A, Reinhardt DP. The Fibrillin-1 Rgd Integrin Binding Site Regulates Gene Expression and Cell Function through Micrnas. *J Mol Biol.* 2018. Epub 2018/12/01. doi: 10.1016/j.jmb.2018.11.021. PubMed PMID: 30500337.
106. Urban Z, Riazzi S, Seidl TL, Katahira J, Smoot LB, Chitayat D, Boyd CD, Hinek A. Connection between Elastin Haploinsufficiency and Increased Cell Proliferation in Patients with Supravalvular Aortic Stenosis and Williams-Beuren Syndrome. *Am J Hum Genet.* 2002;71(1):30-44. Epub 2002/05/23. doi: 10.1086/341035. PubMed PMID: 12016585; PMCID: PMC384991.
107. Li DY, Brooke B, Davis EC, Mecham RP, Sorensen LK, Boak BB, Eichwald E, Keating MT. Elastin Is an Essential Determinant of Arterial Morphogenesis. *Nature.* 1998;393(6682):276-80. Epub 1998/06/02. doi: 10.1038/30522. PubMed PMID: 9607766.
108. Carta L, Pereira L, Arteaga-Solis E, Lee-Arteaga SY, Lenart B, Starcher B, Merkel CA, Sukoyan M, Kerkis A, Hazeki N, Keene DR, Sakai LY, Ramirez F. Fibrillins 1 and 2 Perform Partially Overlapping Functions During Aortic Development. *J Biol Chem.* 2006;281(12):8016-23. Epub 2006/01/13. doi: 10.1074/jbc.M511599200. PubMed PMID: 16407178; PMCID: PMC3052983.
109. Kostka G, Giltay R, Bloch W, Addicks K, Timpl R, Fässler R, Chu M-L. Perinatal Lethality and Endothelial Cell Abnormalities in Several Vessel Compartments of Fibulin-1-Deficient Mice. *Molecular and Cellular Biology.* 2001;21(20):7025-34. doi: 10.1128/mcb.21.20.7025-7034.2001.
110. Sicot FX, Tsuda T, Markova D, Klement JF, Arita M, Zhang RZ, Pan TC, Mecham RP, Birk DE, Chu ML. Fibulin-2 Is Dispensable for Mouse Development and Elastic Fiber Formation. *Mol Cell Biol.* 2008;28(3):1061-7. Epub 2007/12/12. doi: 10.1128/mcb.01876-07. PubMed PMID: 18070922; PMCID: PMC2223402.

111. McLaughlin PJ, Bakall B, Choi J, Liu Z, Sasaki T, Davis EC, Marmorstein AD, Marmorstein LY. Lack of Fibulin-3 Causes Early Aging and Herniation, but Not Macular Degeneration in Mice. *Hum Mol Genet.* 2007;16(24):3059-70. Epub 2007/09/18. doi: 10.1093/hmg/ddm264. PubMed PMID: 17872905.
112. Horiguchi M, Inoue T, Ohbayashi T, Hirai M, Noda K, Marmorstein LY, Yabe D, Takagi K, Akama TO, Kita T, Kimura T, Nakamura T. Fibulin-4 Conducts Proper Elastogenesis Via Interaction with Cross-Linking Enzyme Lysyl Oxidase. *Proc Natl Acad Sci U S A.* 2009;106(45):19029-34. Epub 2009/10/27. doi: 10.1073/pnas.0908268106. PubMed PMID: 19855011; PMCID: PMC2776456.
113. McLaughlin PJ, Chen Q, Horiguchi M, Starcher BC, Stanton JB, Broekelmann TJ, Marmorstein AD, McKay B, Mecham R, Nakamura T, Marmorstein LY. Targeted Disruption of Fibulin-4 Abolishes Elastogenesis and Causes Perinatal Lethality in Mice. *Mol Cell Biol.* 2006;26(5):1700-9. Epub 2006/02/16. doi: 10.1128/mcb.26.5.1700-1709.2006. PubMed PMID: 16478991; PMCID: PMC1430262.
114. Nakamura T, Lozano PR, Ikeda Y, Iwanaga Y, Hinek A, Minamisawa S, Cheng CF, Kobuke K, Dalton N, Takada Y, Tashiro K, Ross J, Jr., Honjo T, Chien KR. Fibulin-5/Dance Is Essential for Elastogenesis in Vivo. *Nature.* 2002;415(6868):171-5. Epub 2002/01/24. doi: 10.1038/415171a. PubMed PMID: 11805835.
115. Zanetti M, Braghetta P, Sabatelli P, Mura I, Doliana R, Colombatti A, Volpin D, Bonaldo P, Bressan GM. Emilin-1 Deficiency Induces Elastogenesis and Vascular Cell Defects. *Mol Cell Biol.* 2004;24(2):638-50. Epub 2004/01/01. PubMed PMID: 14701737; PMCID: PMC343785.
116. Doliana R, Bot S, Mungiguerra G, Canton A, Cilli SP, Colombatti A. Isolation and Characterization of Emilin-2, a New Component of the Growing Emilins Family and a Member of the Emi Domain-Containing Superfamily. *J Biol Chem.* 2001;276(15):12003-11. Epub 2001/03/30. doi: 10.1074/jbc.M011591200. PubMed PMID: 11278945.
117. Schiavinato A, Becker AK, Zanetti M, Corallo D, Milanetto M, Bizzotto D, Bressan G, Guljelmovic M, Paulsson M, Wagener R, Braghetta P, Bonaldo P. Emilin-3, Peculiar Member of Elastin Microfibril Interface-Located Protein (Emilin) Family, Has Distinct Expression Pattern, Forms Oligomeric Assemblies, and Serves as Transforming Growth Factor Beta (Tgf-Beta) Antagonist. *J Biol Chem.* 2012;287(14):11498-515. Epub 2012/02/16. doi: 10.1074/jbc.M111.303578. PubMed PMID: 22334695; PMCID: PMC3322879.
118. Rateri DL, Moorleghen JJ, Balakrishnan A, Owens AP, 3rd, Howatt DA, Subramanian V, Poduri A, Charnigo R, Cassis LA, Daugherty A. Endothelial Cell-Specific Deficiency of Ang II Type 1a Receptors Attenuates Ang II-Induced Ascending Aortic Aneurysms in Ldl Receptor-/- Mice. *Circ Res.* 2011;108(5):574-81. doi: 10.1161/CIRCRESAHA.110.222844. PubMed PMID: 21252156; PMCID: PMC3076204.
119. Kuang SQ, Geng L, Prakash SK, Cao JM, Guo S, Villamizar C, Kwartler CS, Peters AM, Brasier AR, Milewicz DM. Aortic Remodeling after Transverse Aortic Constriction in Mice Is Attenuated with At1 Receptor Blockade. *Arterioscler*

- Thromb Vasc Biol. 2013;33(9):2172-9. doi: 10.1161/ATVBAHA.113.301624. PubMed PMID: 23868934.
120. Ramnath NW, Hawinkels LJ, van Heijningen PM, te Riet L, Paauwe M, Vermeij M, Danser AH, Kanaar R, ten Dijke P, Essers J. Fibulin-4 Deficiency Increases Tgf-Beta Signalling in Aortic Smooth Muscle Cells Due to Elevated Tgf-Beta2 Levels. *Sci Rep.* 2015;5:16872. doi: 10.1038/srep16872. PubMed PMID: 26607280; PMCID: PMC4660353.
121. Akazawa Y, Motoki N, Tada A, Yamazaki S, Hachiya A, Matsuzaki S, Kamiya M, Nakamura T, Kosho T, Inaba Y. Decreased Aortic Elasticity in Children with Marfan Syndrome or Loeys-Dietz Syndrome. *Circulation journal : official journal of the Japanese Circulation Society.* 2016;80(11):2369-75. Epub 2016/10/28. doi: 10.1253/circj.CJ-16-0739. PubMed PMID: 27733734.
122. Chen J, Peters A, Papke CL, Villamizar C, Ringuette LJ, Cao J, Wang S, Ma S, Gong L, Byanova KL, Xiong J, Zhu MX, Madonna R, Kee P, Geng YJ, Brasier AR, Davis EC, Prakash S, Kwartler CS, Milewicz DM. Loss of Smooth Muscle Alpha-Actin Leads to Nf-Kappab-Dependent Increased Sensitivity to Angiotensin li in Smooth Muscle Cells and Aortic Enlargement. *Circ Res.* 2017;120(12):1903-15. Epub 2017/05/04. doi: 10.1161/circresaha.117.310563. PubMed PMID: 28461455; PMCID: PMC5518614.
123. Xiong W, Meisinger T, Knispel R, Worth JM, Baxter BT. Mmp-2 Regulates Erk1/2 Phosphorylation and Aortic Dilatation in Marfan Syndrome. *Circ Res.* 2012;110(12):e92-e101. doi: 10.1161/CIRCRESAHA.112.268268. PubMed PMID: 22550139; PMCID: PMC4162309.
124. Marque V, Kieffer P, Gayraud B, Lartaud-Idjouadiene I, Ramirez F, Atkinson J. Aortic Wall Mechanics and Composition in a Transgenic Mouse Model of Marfan Syndrome. *Arterioscler Thromb Vasc Biol.* 2001;21(7):1184-9. PubMed PMID: 11451749.
125. Howell DW, Popovic N, Metz RP, Wilson E. Regional Changes in Elastic Fiber Organization and Transforming Growth Factor Beta Signaling in Aortas from a Mouse Model of Marfan Syndrome. *Cell Tissue Res.* 2014;358(3):807-19. doi: 10.1007/s00441-014-1993-7. PubMed PMID: 25238995.
126. Ikonomidis JS, Gibson WC, Gardner J, Sweterlitsch S, Thompson RP, Mukherjee R, Spinale FG. A Murine Model of Thoracic Aortic Aneurysms. *J Surg Res.* 2003;115(1):157-63. Epub 2003/10/24. PubMed PMID: 14572787.
127. Ikonomidis JS, Gibson WC, Butler JE, McClister DM, Sweterlitsch SE, Thompson RP, Mukherjee R, Spinale FG. Effects of Deletion of the Tissue Inhibitor of Matrix Metalloproteinases-1 Gene on the Progression of Murine Thoracic Aortic Aneurysms. *Circulation.* 2004;110(11 Suppl 1):Ij268-73. Epub 2004/09/15. doi: 10.1161/01.cir.0000138384.68947.20. PubMed PMID: 15364874.
128. Daugherty A, Rateri D, Hong L, Balakrishnan A. Measuring Blood Pressure in Mice Using Volume Pressure Recording, a Tail-Cuff Method. *J Vis Exp.* 2009(27). Epub 2009/06/03. doi: 10.3791/1291. PubMed PMID: 19488026; PMCID: PMC2794298.
129. Goergen CJ, Barr KN, Huynh DT, Eastham-Anderson JR, Choi G, Hedehus M, Dalman RL, Connolly AJ, Taylor CA, Tsao PS, Greve JM. In Vivo Quantification of Murine Aortic Cyclic Strain, Motion, and Curvature: Implications for Abdominal

- Aortic Aneurysm Growth. *Journal of magnetic resonance imaging : JMRI*. 2010;32(4):847-58. Epub 2010/10/01. doi: 10.1002/jmri.22331. PubMed PMID: 20882615; PMCID: PMC2975391.
130. Preibisch S, Saalfeld S, Tomancak P. Globally Optimal Stitching of Tiled 3d Microscopic Image Acquisitions. *Bioinformatics*. 2009;25(11):1463-5. Epub 2009/04/07. doi: 10.1093/bioinformatics/btp184. PubMed PMID: 19346324; PMCID: PMC2682522.
131. Barisione C, Charnigo R, Howatt DA, Moorlegghen JJ, Rateri DL, Daugherty A. Rapid Dilatation of the Abdominal Aorta During Infusion of Angiotensin II Detected by Noninvasive High-Frequency Ultrasonography. *J Vasc Surg*. 2006;44(2):372-6. Epub 2006/08/08. doi: 10.1016/j.jvs.2006.04.047. PubMed PMID: 16890871.
132. Rateri DL, Moorlegghen JJ, Knight V, Balakrishnan A, Howatt DA, Cassis LA, Daugherty A. Depletion of Endothelial or Smooth Muscle Cell-Specific Angiotensin II Type 1a Receptors Does Not Influence Aortic Aneurysms or Atherosclerosis in LDL Receptor Deficient Mice. *PloS one*. 2012;7(12):e51483. Epub 2012/12/14. doi: 10.1371/journal.pone.0051483. PubMed PMID: 23236507; PMCID: PMC3517567.
133. Plonek T, Berezowski M, Kurcz J, Podgorski P, Sasiadek M, Rylski B, Mysiak A, Jasinski M. The Evaluation of the Aortic Annulus Displacement During Cardiac Cycle Using Magnetic Resonance Imaging. *BMC Cardiovasc Disord*. 2018;18(1):154. Epub 2018/08/02. doi: 10.1186/s12872-018-0891-4. PubMed PMID: 30064358.
134. Trachet B, Fraga-Silva RA, Londono FJ, Swillens A, Stergiopoulos N, Segers P. Performance Comparison of Ultrasound-Based Methods to Assess Aortic Diameter and Stiffness in Normal and Aneurysmal Mice. *PloS one*. 2015;10(5):e0129007. Epub 2015/05/30. doi: 10.1371/journal.pone.0129007. PubMed PMID: 26023786; PMCID: PMC4449181.
135. Haggerty CM, Mattingly AC, Gong MC, Su W, Daugherty A, Fornwalt BK. Telemetric Blood Pressure Assessment in Angiotensin II-Infused ApoE<sup>-/-</sup> Mice: 28 Day Natural History and Comparison to Tail-Cuff Measurements. *PloS one*. 2015;10(6):e0130723. Epub 2015/06/19. doi: 10.1371/journal.pone.0130723. PubMed PMID: 26086817; PMCID: PMC4472759.
136. Favreau JT, Nguyen BT, Gao I, Yu P, Tao M, Schneiderman J, Gaudette GR, Ozaki CK. Murine Ultrasound Imaging for Circumferential Strain Analyses in the Angiotensin II Abdominal Aortic Aneurysm Model. *J Vasc Surg*. 2012;56(2):462-9. Epub 2012/04/17. doi: 10.1016/j.jvs.2012.01.056. PubMed PMID: 22503226; PMCID: PMC3581859.
137. Trachet B, Piersigilli A, Fraga-Silva RA, Aslanidou L, Sordet-Dessimoz J, Astolfo A, Stampanoni MF, Segers P, Stergiopoulos N. Ascending Aortic Aneurysm in Angiotensin II-Infused Mice: Formation, Progression, and the Role of Focal Dissections. *Arterioscler Thromb Vasc Biol*. 2016;36(4):673-81. doi: 10.1161/ATVBAHA.116.307211. PubMed PMID: 26891740.
138. Lee L, Cui JZ, Cua M, Esfandiarei M, Sheng X, Chui WA, Xu MH, Sarunic MV, Beg MF, van Breemen C, Sandor GG, Tibbits GF. Aortic and Cardiac Structure and Function Using High-Resolution Echocardiography and Optical Coherence Tomography in a Mouse Model of Marfan Syndrome. *PloS one*.

- 2016;11(11):e0164778. Epub 2016/11/09. doi: 10.1371/journal.pone.0164778. PubMed PMID: 27824871; PMCID: PMC5100915.
139. Shen M, Lee J, Basu R, Sakamuri SS, Wang X, Fan D, Kassiri Z. Divergent Roles of Matrix Metalloproteinase 2 in Pathogenesis of Thoracic Aortic Aneurysm. *Arterioscler Thromb Vasc Biol.* 2015;35(4):888-98. doi: 10.1161/ATVBAHA.114.305115. PubMed PMID: 25657308.
140. Jiao Y, Li G, Li Q, Ali R, Qin L, Li W, Qyang Y, Greif DM, Geirsson A, Humphrey JD, Tellides G. Mtor (Mechanistic Target of Rapamycin) Inhibition Decreases Mechanosignaling, Collagen Accumulation, and Stiffening of the Thoracic Aorta in Elastin-Deficient Mice. *Arterioscler Thromb Vasc Biol.* 2017;37(9):1657-66. Epub 2017/07/29. doi: 10.1161/atvbaha.117.309653. PubMed PMID: 28751568; PMCID: PMC5574180.
141. Milewicz DM, Dietz HC, Miller DC. Treatment of Aortic Disease in Patients with Marfan Syndrome. *Circulation.* 2005;111(11):e150-7. Epub 2005/03/23. doi: 10.1161/01.Cir.0000155243.70456.F4. PubMed PMID: 15781745.
142. Dietz HC, Cutting CR, Pyeritz RE, Maslen CL, Sakai LY, Corson GM, Puffenberger EG, Hamosh A, Nanthakumar EJ, Curristin SM, Stetten G, Meyers DA, Francomano CA. Marfan Syndrome Caused by a Recurrent De Novo Missense Mutation in the Fibrillin Gene. *Nature.* 1991;352(6333):337-9. Epub 1991/07/25. doi: 10.1038/352337a0. PubMed PMID: 1852208.
143. Brooke BS, Habashi JP, Judge DP, Patel N, Loeys B, Dietz HC, 3rd. Angiotensin II Blockade and Aortic-Root Dilation in Marfan's Syndrome. *N Engl J Med.* 2008;358(26):2787-95. doi: 10.1056/NEJMoa0706585. PubMed PMID: 18579813; PMCID: PMC2692965.
144. Sadoshima J. Novel  $\alpha_1$  Receptor-Independent Functions of Losartan. *Circ Res.* 2002;90(7):754-6. PubMed PMID: 11964366.
145. Yasuda N, Miura S, Akazawa H, Tanaka T, Qin Y, Kiya Y, Imaizumi S, Fujino M, Ito K, Zou Y, Fukuhara S, Kunimoto S, Fukuzaki K, Sato T, Ge J, Mochizuki N, Nakaya H, Saku K, Komuro I. Conformational Switch of Angiotensin II Type 1 Receptor Underlying Mechanical Stress-Induced Activation. *EMBO Rep.* 2008;9(2):179-86. doi: 10.1038/sj.embor.7401157. PubMed PMID: 18202720; PMCID: PMC2246415.
146. Iwasaki H, Yoshimoto T, Sugiyama T, Hirata Y. Activation of Cell Adhesion Kinase Beta by Mechanical Stretch in Vascular Smooth Muscle Cells. *Endocrinology.* 2003;144(6):2304-10. Epub 2003/05/15. doi: 10.1210/en.2002-220939. PubMed PMID: 12746290.
147. Schleifenbaum J, Kassmann M, Szijártó IA, Hercule HC, Tano JY, Weinert S, Heidenreich M, Pathan AR, Anistan YM, Alenina N, Rusch NJ, Bader M, Jentsch TJ, Gollasch M. Stretch-Activation of Angiotensin II Type 1a Receptors Contributes to the Myogenic Response of Mouse Mesenteric and Renal Arteries. *Circ Res.* 2014;115(2):263-72. Epub 2014/05/20. doi: 10.1161/circresaha.115.302882. PubMed PMID: 24838176.
148. Sawada H, Chen JZ, Wright BC, Moorleghen JJ, Lu HS, Daugherty A. Ultrasound Imaging of the Thoracic and Abdominal Aorta in Mice to Determine Aneurysm Dimensions. *J Vis Exp.* 2018;145:e59013. doi: doi:10.3791/59013.

149. Wu CH, Wang Y, Ma M, Mullick AE, Crooke RM, Graham MJ, Daugherty A, Lu HS. Antisense Oligonucleotides Targeting Angiotensinogen: Insights from Animal Studies. *Bioscience reports*. 2019;39(1). Epub 2018/12/12. doi: 10.1042/BSR20180201. PubMed PMID: 30530571; PMCID: PMC6328882.
150. Bhatt AB, Buck JS, Zuflacht JP, Milian J, Kadivar S, Gauvreau K, Singh MN, Creager MA. Distinct Effects of Losartan and Atenolol on Vascular Stiffness in Marfan Syndrome. *Vascular medicine (London, England)*. 2015;20(4):317-25. Epub 2015/03/22. doi: 10.1177/1358863x15569868. PubMed PMID: 25795452.
151. Hibender S, Franken R, van Roomen C, Ter Braake A, van der Made I, Schermer EE, Gunst Q, van den Hoff MJ, Lutgens E, Pinto YM, Groenink M, Zwinderman AH, Mulder BJ, de Vries CJ, de Waard V. Resveratrol Inhibits Aortic Root Dilatation in the Fbn1c1039g/+ Marfan Mouse Model. *Arterioscler Thromb Vasc Biol*. 2016;36(8):1618-26. doi: 10.1161/ATVBAHA.116.307841. PubMed PMID: 27283746.
152. Zhou Y, Dirksen WP, Babu GJ, Periasamy M. Differential Vasoconstrictions Induced by Angiotensin II: Role of AT1 and AT2 Receptors in Isolated C57Bl/6j Mouse Blood Vessels. *Am J Physiol Heart Circ Physiol*. 2003;285(6):H2797-803. Epub 2003/08/09. doi: 10.1152/ajpheart.00466.2003. PubMed PMID: 12907424.
153. Ito M, Oliverio MI, Mannon PJ, Best CF, Maeda N, Smithies O, Coffman TM. Regulation of Blood Pressure by the Type 1a Angiotensin II Receptor Gene. *Proc Natl Acad Sci U S A*. 1995;92(8):3521-5. PubMed PMID: 7724593; PMCID: PMC42199.
154. Mangrum AJ, Gomez RA, Norwood VF. Effects of at(1a) Receptor Deletion on Blood Pressure and Sodium Excretion During Altered Dietary Salt Intake. *American journal of physiology Renal physiology*. 2002;283(3):F447-53. Epub 2002/08/09. doi: 10.1152/ajprenal.00259.2001. PubMed PMID: 12167595.
155. Ding Y, Stec DE, Sigmund CD. Genetic Evidence That Lethality in Angiotensinogen-Deficient Mice Is Due to Loss of Systemic but Not Renal Angiotensinogen. *J Biol Chem*. 2001;276(10):7431-6. Epub 2000/11/30. doi: 10.1074/jbc.M003892200. PubMed PMID: 11096065.
156. Ye F, Wang Y, Wu C, Howatt DA, Wu CH, Balakrishnan A, Mullick AE, Graham MJ, Danser AHJ, Wang J, Daugherty A, Lu HS. Angiotensinogen and Megalin Interactions Contribute to Atherosclerosis-Brief Report. *Arterioscler Thromb Vasc Biol*. 2019;39(2):150-5. Epub 2018/12/21. doi: 10.1161/ATVBAHA.118.311817. PubMed PMID: 30567480; PMCID: PMC6344256.
157. Holmes KW, Maslen CL, Kindem M, Kroner BL, Song HK, Ravekes W, Dietz HC, Weinsaft JW, Roman MJ, Devereux RB, Pyeritz RE, Bavaria J, Milewski K, Milewicz D, LeMaire SA, Hendershot T, Eagle KA, Tolunay HE, Desvigne-Nickens P, Silberbach M, Gen TACRC. Gentac Registry Report: Gender Differences among Individuals with Genetically Triggered Thoracic Aortic Aneurysm and Dissection. *Am J Med Genet A*. 2013;161A(4):779-86. Epub 2013/02/28. doi: 10.1002/ajmg.a.35836. PubMed PMID: 23444191; PMCID: PMC3606679.
158. Roman MJ, Devereux RB, Preiss LR, Asch FM, Eagle KA, Holmes KW, LeMaire SA, Maslen CL, Milewicz DM, Morris SA, Prakash SK, Pyeritz RE, Ravekes WJ, Shohet RV, Song HK, Weinsaft JW, Gen TACI. Associations of Age



and Sex with Marfan Phenotype: The National Heart, Lung, and Blood Institute Gentac (Genetically Triggered Thoracic Aortic Aneurysms and Cardiovascular Conditions) Registry. *Circ Cardiovasc Genet.* 2017;10(3). Epub 2017/06/11. doi: 10.1161/CIRCGENETICS.116.001647. PubMed PMID: 28600386; PMCID: PMC5500868.

159. Thatcher SE, Zhang X, Woody S, Wang Y, Alsiraj Y, Charnigo R, Daugherty A, Cassis LA. Exogenous 17-Beta Estradiol Administration Blunts Progression of Established Angiotensin II-Induced Abdominal Aortic Aneurysms in Female Ovariectomized Mice. *Biol Sex Differ.* 2015;6(1):12. doi: 10.1186/s13293-015-0030-1. PubMed PMID: 26131353; PMCID: PMC4485333.

160. Arnold AP, Cassis LA, Eghbali M, Reue K, Sandberg K. Sex Hormones and Sex Chromosomes Cause Sex Differences in the Development of Cardiovascular Diseases. *Arterioscler Thromb Vasc Biol.* 2017;37(5):746-56. Epub 2017/03/11. doi: 10.1161/atvbaha.116.307301. PubMed PMID: 28279969; PMCID: PMC5437981.

161. Alsiraj Y, Thatcher SE, Blalock E, Fleenor B, Daugherty A, Cassis LA. Sex Chromosome Complement Defines Diffuse Versus Focal Angiotensin II-Induced Aortic Pathology. *Arterioscler Thromb Vasc Biol.* 2018;38(1):143-53. Epub 2017/11/04. doi: 10.1161/atvbaha.117.310035. PubMed PMID: 29097367.

162. Benicky J, Hafko R, Sanchez-Lemus E, Aguilera G, Saavedra JM. Six Commercially Available Angiotensin II AT1 Receptor Antibodies Are Non-Specific. *Cell Mol Neurobiol.* 2012;32(8):1353-65. doi: 10.1007/s10571-012-9862-y. PubMed PMID: 22843099; PMCID: PMC3508356.

163. Herrera M, Sparks MA, Alfonso-Pecchio AR, Harrison-Bernard LM, Coffman TM. Lack of Specificity of Commercial Antibodies Leads to Misidentification of Angiotensin Type 1 Receptor Protein. *Hypertension.* 2013;61(1):253-8. doi: 10.1161/HYPERTENSIONAHA.112.203679. PubMed PMID: 23150519; PMCID: PMC3523722.

164. Sparks MA, Parsons KK, Stegbauer J, Gurley SB, Vivekanandan-Giri A, Fortner CN, Snouwaert J, Raasch EW, Griffiths RC, Haystead TA, Le TH, Pennathur S, Koller B, Coffman TM. Angiotensin II Type 1a Receptors in Vascular Smooth Muscle Cells Do Not Influence Aortic Remodeling in Hypertension. *Hypertension.* 2011;57(3):577-85. Epub 2011/01/19. doi: 10.1161/hypertensionaha.110.165274. PubMed PMID: 21242463; PMCID: PMC3077960.

165. Lu H, Howatt DA, Balakrishnan A, Moorleghen JJ, Rateri DL, Cassis LA, Daugherty A. Subcutaneous Angiotensin II Infusion Using Osmotic Pumps Induces Aortic Aneurysms in Mice. *J Vis Exp.* 2015(103). doi: 10.3791/53191. PubMed PMID: 26436287; PMCID: PMC4692630.

166. Daugherty A, Whitman SC. Quantification of Atherosclerosis in Mice. *Methods Mol Biol.* 2003;209:293-309. Epub 2002/10/03. doi: 10.1385/1-59259-340-2:293. PubMed PMID: 12357958.

167. Daugherty A, Manning MW, Cassis LA. Antagonism of AT2 Receptors Augments Angiotensin II-Induced Abdominal Aortic Aneurysms and Atherosclerosis. *British journal of pharmacology.* 2001;134(4):865-70. Epub

- 2001/10/19. doi: 10.1038/sj.bjp.0704331. PubMed PMID: 11606327; PMCID: PMC1573019.
168. Strutz F, Okada H, Lo CW, Danoff T, Carone RL, Tomaszewski JE, Neilson EG. Identification and Characterization of a Fibroblast Marker: Fsp1. *J Cell Biol.* 1995;130(2):393-405. PubMed PMID: 7615639; PMCID: PMC2199940.
169. Kong P, Christia P, Saxena A, Su Y, Frangogiannis NG. Lack of Specificity of Fibroblast-Specific Protein 1 in Cardiac Remodeling and Fibrosis. *Am J Physiol Heart Circ Physiol.* 2013;305(9):H1363-72. doi: 10.1152/ajpheart.00395.2013. PubMed PMID: 23997102; PMCID: PMC3840245.
170. Logghe G, Trachet B, Aslanidou L, Villaneuva-Perez P, De Backer J, Stergiopoulos N, Stampanoni M, Aoki H, Segers P. Propagation-Based Phase-Contrast Synchrotron Imaging of Aortic Dissection in Mice: From Individual Elastic Lamella to 3d Analysis. *Sci Rep.* 2018;8(1):2223. Epub 2018/02/06. doi: 10.1038/s41598-018-20673-x. PubMed PMID: 29396472; PMCID: PMC5797148.
171. Trachet B, Fraga-Silva RA, Piersigilli A, Tedgui A, Sordet-Dessimoz J, Astolfo A, Van der Donckt C, Modregger P, Stampanoni MF, Segers P, Stergiopoulos N. Dissecting Abdominal Aortic Aneurysm in Ang II-Infused Mice: Suprarenal Branch Ruptures and Apparent Luminal Dilatation. *Cardiovasc Res.* 2015;105(2):213-22. doi: 10.1093/cvr/cvu257. PubMed PMID: 25538157.
172. Thatcher SE, Zhang X, Woody S, Wang Y, Alsiraj Y, Charnigo R, Daugherty A, Cassis LA. Exogenous 17-B Estradiol Administration Blunts Progression of Established Angiotensin II-Induced Abdominal Aortic Aneurysms in Female Ovariectomized Mice. *Biology of Sex Differences.* 2015;6(1):12. doi: 10.1186/s13293-015-0030-1.

VITA

Jeff Zheyang Chen  
University of Kentucky

**Education**

INSTITUTION AND LOCATION	DEGREE ( <i>pending</i> )	START DATE	END DATE ( <i>or expected date</i> )	FIELD OF STUDY
University of California: Los Angeles	BS	09/2009	06/2013	Biochemistry
University of Kentucky	(MD)	06/2014	(06/2022)	Medicine
University of Kentucky	(PhD)	06/2016	(06/2020)	Physiology

**Positions and Employment**

ACTIVITY/ OCCUPATION	START DATE	END DATE	FIELD	INSTITUTION/ COMPANY	SUPERVISOR/ EMPLOYER
Undergraduate Research Assistant	08/2010	06/2013	Pharmacology	UCLA	Daniel Kaufman PhD
Research Assistant	06/2013	06/2014	Pharmacology	UCLA	Daniel Kaufman PhD
Graduate Student	07/2016	Present	Physiology	Univ. of Kentucky	Alan Daugherty PhD DSc

**Other Experience and Professional Memberships**

2018 – Current American Physician Scientist Association: Events Committee  
2019 Program: PSTP Program Luncheon, Policy Panel, and Women in Science Panel  
2020 Program: PSTP Program Luncheon, COVID-19 contingency planning  
2016 – Current American Heart Association, Great Rivers Affiliate: Student Member  
2014 – Current Lexington Medical Society / Kentucky Medical Society: Student Member  
2014 – 2018 American Medical Association: Student Member

**Academic and Professional Honors**

2019 Society for Vascular Surgery: 2019 Vascular Research Initiatives Conference Poster Award  
Awarded for best aortic aneurysms poster presentation. Title: AT1a Receptor Deficiency Attenuates Thoracic Aortic Aneurysm Progression in FBN1<sup>C1041G/+</sup> mice

- 2019 – 2022 University of Kentucky: Graduate Student Incentive Program  
Awarded for receipt of competitive extramural grant funding
- 2018 Burroughs Wellcome Fund Trainee Travel Award  
Awarded to top abstracts at Translational Science 2018. Title:  
Sexual Dimorphism in a Mouse Model of Syndromic Thoracic  
Aortic Aneurysm
- 2016, 2018 University of Kentucky Department of Physiology: Best Student  
Research Blitz and Poster  
Awarded to best presentation among graduate students
- 2017 Saha Cardiovascular Research Center MD/PhD Student Award  
Awarded to MD/PhD Students who show an active interest in  
cardiovascular medicine.
- 2015-2016 University of Kentucky CCTS Professional Student Mentored  
Research Fellowship  
Competitive award for medical students interested in research
- 2009-2012 University of California – Los Angeles: Dean’s Honors List

### **Grants**

NRSA F30

Chen (PI)

09/01/2019-09/01/2022

NHLBI F30HL143943

Title: Mechanisms of Renin Angiotensin Modulation in Thoracic Aortic  
Aneurysms

University of Kentucky CCTS TL1

09/01/2017-8/31/2019

NCATS UL1TR001998

Project title: Renin Angiotensin System in Marfan Syndrome Associated Thoracic  
Aortic Aneurysms

Role: CCTS Trainee; Competitive intramural funding for translational research  
projects

### **Presentations:**

1. **Chen JZ**, Sawada H, Gao Y, Howatt DA, Moorlegghen JJ, Sheppard MB, Daugherty A. 2020 Sexual Dimorphism of AngII Induced Thoracic Aortic Aneurysms. AHA Vascular Disease SFRN, Nashville TN. *Poster*
2. **Chen JZ**, Howatt DA, Lu HS, Daugherty A. 2019 Sexual Dimorphism of Experimental Thoracic Aortic Diseases. Vascular Discovery, Boston MA. *Oral and Poster*.
3. **Chen JZ**, Moorlegghen JJ, Sheppard MB, Daugherty A. 2019 AT1a Receptor Deficiency Attenuates Thoracic Aortic Aneurysm Progression in FBN1 C1041G/+ Mice. Vascular Discovery; Vascular Research Initiatives Conference, Boston MA. *Poster*
4. **Chen JZ**, Sawada H, Moorlegghen JJ, and Daugherty A. 2018. Aortic Dilation and Elasticity in Thoracic Aortic Aneurysm in a Marfan model is Sexually Dimorphic. Vascular Discovery. San Francisco, CA. *Poster*

5. **Chen Z**, Daugherty A, Sheppard MB. 2018. Sexual Dimorphism in a Mouse Model of Syndromic Thoracic Aortic Aneurysm. Translational Science 2018, Washington DC. *Oral and poster*
6. **Chen Z**, Daugherty A, Sheppard MB. 2018. Sexual Dimorphism in a Mouse Model of Syndromic Thoracic Aortic Aneurysm. CCTS Spring Conference, Lexington, KY. *Oral and poster*
7. **Chen Z**, Rateri D, Daugherty A, Sheppard MB. 2017. Sexual Dimorphism in a Marfan Syndrome Mouse Model. American Heart Association Scientific Sessions, Anaheim, CA. *Poster*
8. **Chen Z**, Sawada H, Rateri DL, Daugherty A, Sheppard MB. 2017. Cardiac Cycle Affects Ultrasound Measurements of Ascending Aortic Diameter in a Marfan Syndrome Mouse Model. ATVB/PVD Scientific Sessions. Minneapolis MN. *Poster*
9. **Chen Z**, Sawada H, Rateri DL, Daugherty A, Sheppard MB. 2017. Cardiac Cycle Affects Ultrasound Measurements of Ascending Aortic Diameter in a Marfan Syndrome Mouse Model. ATVB/PVD Scientific Sessions. Minneapolis MN. *Poster*

#### **Bibliography:**

- Chen JZ**, Sawada H, Moorleghen JJ, Weiland M, Daugherty A, Sheppard MB. Aortic strain correlates with elastin fragmentation in fibrillin-1 hypomorphic mice. *Circ Rep*. 2019; 1(5):199-205. DOI:10.1253/circrep.CR-18-0012
- Sawada H, **Chen JZ**, Wright BC, Moorleghen JJ, Lu HS, and Daugherty A. Ultrasound imaging of the thoracic and abdominal aorta in mice to determine aneurysm dimensions. *J Vis Exp*. 2019 Mar 8;(145). doi: 10.3791/59013.
- Shoemaker R, AlSiraj Y, **Chen J**, Cassis L. Pancreatic AT1aR Deficiency Decreases Insulin Secretion in Obese C57BL/6 Mice. *Am J Hypertens*. 2019;32(6):597-604. doi: 10.1093/ajh/hpz042.
- Sawada H, **Chen JZ**, Wright BC, Sheppard MB, Lu HS, Daugherty A. Heterogeneity of aortic smooth muscle cells: A determinant for regional characteristics of thoracic aortic aneurysms? *J Transl Int Med*. 2018;6(3):93-6. Epub 2018/11/15. doi: 10.2478/jtim-2018-0023. PMID: 30425944; PMCID: PMC6231305. *Review*
- Sawada H, Wright BC, **Chen JZ**, Lu HS, Daugherty A. Drebrin - a new player in angiotensin ii-induced aortopathies. *Cardiovasc Res*. 2018. Epub 2018/08/15. doi: 10.1093/cvr/cvy205. PMID: 30107397.
- Wu CH, Mohammadmoradi S, **Chen JZ**, Sawada H, Daugherty A, Lu HS. Renin-angiotensin system and cardiovascular functions. *Arterioscler Thromb Vasc Biol*. 2018;38(7):e108-e16. Epub 2018/06/29. doi: 10.1161/atvbaha.118.311282. PMID: 29950386; PMCID: PMC6039412.
- Daugherty A, **Chen Z**, Sawada H, Rateri DL, Sheppard MB. Transforming growth factor-beta in thoracic aortic aneurysms: Good, bad, or irrelevant? *Journal of the American Heart Association*. 2017;6(1). Epub 2017/01/26. doi: 10.1161/jaha.116.005221. PMID: 28119286.

- Tian J, Dang H, Nguyen AV, **Chen Z**, Kaufman DL. Combined therapy with gaba and proinsulin/alum acts synergistically to restore long-term normoglycemia by modulating t-cell autoimmunity and promoting beta-cell replication in newly diabetic nod mice. *Diabetes*. 2014;63(9):3128-34. doi: 10.2337/db13-1385. PMID: 25146474; PMCID: PMC4141368.
- Tian J, Dang H, **Chen Z**, Guan A, Jin Y, Atkinson MA, Kaufman DL. Gamma-aminobutyric acid regulates both the survival and replication of human beta-cells. *Diabetes*. 2013;62(11):3760-5. doi: 10.2337/db13-0931. PMID: 23995958; PMCID: 3806626.